

JIMMA UNIVERSITY

Jimma Institute of Technology

Faculty of Mechanical Engineering

**Modeling and Simulation of a Semi-Automated *Injera* Baking
Machine: *Injera* Extracting Kinematic Mechanism**

**A Thesis Submitted to the School of Graduate Studies of Jimma
University Institute of Technology in Partial Fulfillment of the
Requirements for the Degree of Masters of**

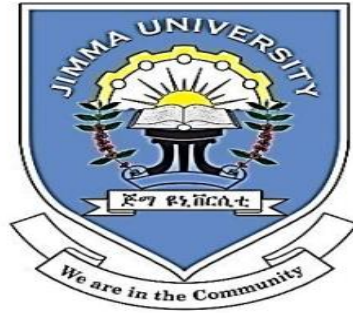
Science

In

Mechanical System Design Engineering

By: Amanuel Abebe T.

July, 2019



JIMMA UNIVERSITY

JIMMA INSTITUTE OF TECHNOLOGY

Faculty of Mechanical Engineering

Mechanical System Design Engineering

**Modeling and Simulation of a Semi-Automated *Injera* Baking
Machine: *Injera* Extracting Kinematic Mechanism**

By

Amanuel Abebe T.

Advisor: Seungwon Youn (PhD)

Co-Advisor: Abiyou Solomon (PhD. Candidate)

*Thesis Submitted to the School of Graduate Studies of
Jimma University in Partial Fulfillment of the Requirements
for the Degree of Master of Science in Mechanical
Engineering (Design of Mechanical System)*

Jimma, Ethiopia

Approval Sheet

Amanuel Abebe T. _____

Researcher Name

Signature

Date

Degree: Masters of Science in Mechanical System Design Engineering

Title: Modeling and Simulation of a Semi-Automated *Injera* Baking Machine:

***Injera* Extracting Kinematic Mechanism**

Examining Committee:

Mr. Yohannis Dabesa (M.Sc.) _____

Chairperson

Signature

Date

Seungwon Youn (PhD.)

Advisor

Signature

Date

Abiyou Solomon (PhD. Candidate)

Co-Advisor

Signature

Date

Prof. Hirpa G. Lemu (PhD.)

External Examiner

Signature

Date

Mr. Yohannis Dabesa (M.Sc.) _____

Internal Examiner

Signature

Date

ABSTRACT

This study presents the kinematic modeling and simulation of an *injera* extracting mechanism of a semi-automated *injera* baking machine. The mechanical structures and mechanisms of *injera* baking machine and extracting mechanism was designed according to the classical existing electrical baking *mitads* integrating with some mechanisms in order to obtain the requested motion. The motion equation of *injera* extracting mechanism was formulated by referring to the motion analysis of scotch yoke mechanism. And for the case of the dynamic behaviors of time sequential events, i.e., opening and closing of pan-lid mechanism and polishing of pan, pouring of dough, *injera* baking machine is used in the simulation.

The simulation of *injera* extracting mechanism was done in rigid multi-body dynamics of ANSYS Version 19.2 software by importing the 3D assembled model from SolidWorks. The motion equation of *injera* baking machine and extracting mechanism is done in PTC Creo Mathcad prime 3.0 in order to check either the ANSYS simulation is approached to the dynamic behaviors or not. In addition, it helps to be clear with the SI-units and to avoid manual calculation errors, to assign the variables once and recall them through all the design in the same document.

In this study, to compare and validate the analysis result of the simulation of the motion, there is no other related literature review is done; due to this, as a reference, considering the kinematic motion behaviors and events with the understanding of the real events of *injera* baking process is very important. Accordingly, the analysis results of simulation of motion is valid corresponding to the effectiveness of the *injera* baking machine consecutive activities.

Keywords: Cam-guide, *Injera*, *injera* extracting, *Mitad*, Modeling, Semi-automated, baking time, Simulation, Scotch yoke mechanism, Pan Lid.

ACKNOWLEDGEMENT

First of all, I would like to express my humility and utmost gratitude to the Mighty God for his everlasting blessings and gifts in my life. The ups and downs of the challenging days have been passed with the help of Him; and all have been for good and taught more. Verily, no success would have been accomplished without his grace and mercy.

Secondly, I would like to express my sincere appreciation and gratitude to Mr. Abiyou Solomon for being my advisor and for his valuable guidance and encouragement during the process of this thesis. The provision of appropriate materials on this thesis that he gave and recommended me made it easy.

Last but certainly not the least, I would like to thank my beloved families and my class mates for their friendly advices, positive attitude buildings and politely treatments by being my side.

<i>Contents</i>	<i>Page</i>
APPROVAL SHEET.....	i
ABSTRACT	ii
ACKNOWLEDGEMENT	iii
CHAPTER I.....	1
INTRODUCTION	1
1.1 Background.....	1
1.2 Statement of the Problem.....	2
1.3 Objectives	3
1.3.1 General Objective.....	3
1.3.2 Specific Objectives.....	3
1.4 Scope of the Study	3
1.5 Limitations of the Study	4
1.6 Significance of the Study.....	4
1.7 Research Methodology	4
1.8 Outline of the Study.....	4
CHAPTER II	6
REVIEW OF LITERATURE	6
2.1 Development of Injera Baking Machine.....	6
2.2 Traditional Injera Baking Method	7
2.3 Electrical Power Consuming Stove Injera Baking Method.....	8
2.4 Solar Power Consuming Stove Injera Baking Method.....	8
2.5 Semi-Automated or Automated Injera Baking Machine	9
CHAPTER III	11
METHOD, MODELING AND SIMULATION OF <i>INJERA</i> EXTRACTING KINEMATIC SYSTEM	11
3.1 Method.....	11
3.2 Definition of the Problem:	12
3.2 Physical Laws and Phenomenon of Injera Baking Process	12
3.3 Setup of Model Specifications of IBM	14
3.4 Semi-Automated Rotary Injera Baking System	15
3.4.1 Terminology.....	17
3.5 Kinematics of IBM Design Process.....	19

3.6 Synthesis and Kinematics of Injera Extracting Mechanism	19
3.6.1 Synthesis of Pan-Lid Linkage Mechanisms	19
3.6.2 Dynamic Determinants of the Operations of the System.....	23
3.7 Synthesis and Kinematics of Injera Extracting Mechanism.....	30
3.7.1 Synthesis of Injera Extracting Mechanism	31
3.7.2 Skeletal Representation	33
3.7.3 Mobility of the System.....	33
3.7.4 Coordinate System.....	34
3.7.5 Instantaneous Center of the Injera Extracting Mechanism.....	34
3.7.6 Characterization of Angles with Link Positions	38
3.7.7 Kinematic and Dynamic Loop-Closure Equation	38
3.7.8 Identification of Input and Output Variables	39
3.7.9 Solve the Loop-Closure Equation.....	39
3.7.9.1 Position Analysis	39
3.7.9.2 Velocity Analysis	40
3.7.9.3 Acceleration Analysis	42
3.8 Working Principles of Injera Extracting Mechanism	42
3.9 Methods to Simulate	43
CHAPTER IV	51
RESULTS AND DISCUSSION.....	51
4.1 Kinematic Simulation of <i>Injera</i> Extracting	51
4.1.1 Position Simulation of <i>Injera</i> Extracting Mechanism	51
4.1.2 Velocity Simulation of <i>Injera</i> Extracting Mechanism	60
4.1.3 Acceleration Analysis of <i>IEM</i>	65
CHAPTER V	68
CONCLUSION AND FUTURE WORK	68
5.1 Conclusion	68
5.2 Recommendation	69
5.3 Future Work.....	70
REFERENCES	71
Appendix I	73
Appendix II.....	74

Appendix IV	92
Appendix V	97

<u>Table of Figures</u>	<u>Page</u>
Figure 1: Literature review on development category of IBM.....	7
Figure 2: Traditional injera baking	7
Figure 3: Solar injera baking process	9
Figure 4: Zelalem injera machine	10
Figure 5: Wassie Mulugeta's injera machine	10
Figure 6: Work flow chart of IEM and IBM modeling and simulation.....	12
Figure 7: Physical cyclic modeling of injera processing in IBM model	13
Figure 8: Semi-automated rotary IBM	17
Figure 9: The cam-guide path curve of pan-lid	19
Figure 10: Opening of cover to x-axis.....	20
Figure 11: Three ports of IBM with cover opening and closing.	20
Figure 12: The translation of cover after dough pouring.....	21
Figure 13: The direction of angular velocity direction to x-axis.....	22
Figure 14: The subcomponent skeletal representation of IBM machine	24
Figure 15: Cover opening and closing mechanism.....	25
Figure 16 DRRD graph of cover opening and closing position vector curve	26
Figure 17: DRRD graph of cover opening and closing curve by Mathcad	27
Figure 18: Optimized cam guided cover opener/closer path curve by Mathcad ..	27
Figure 19: Virtual opening and closing motion path of a SIBM system	28
Figure 20: Trigonometric graph of cover opening and/or closing motion	28
Figure 21: Conventional electric mitad with edge barrier	31
Figure 22: IBM electric flat mitad without edge barrier.....	31
Figure 23: Injera extraction, a) Injera extracting mechanism.....	32

Figure 24: Scotch yoke mechanism with double end-effectors.....	32
Figure 25: Injera extracting mechanism-gripping positions.....	33
Figure 26: Skeletal representation of scotch yoke mechanism with springs	33
Figure 27: Injera extracting mechanism without disk pin as crank	34
Figure 28: Skeleton of Scotch yoke mechanism.....	35
Figure 29: Injera extractor finger (upper finger)	35
Figure 30: Instantaneous center for injera extracting mechanism	36
Figure 31: Location of instantaneous center for injera extracting mechanism.....	37
Figure 32: The corresponding vector diagram.....	38
Figure 33: Velocity and acceleration analysis of injera extracting mechanism ...	42
Figure 34: Injera extracting mechanism	43
Figure 35: Dynamic Simulation Setting of a Semi-automated IBM	46
Figure 36: Identifying the number and types of kinematic joints or constraints ..	47
Figure 37: Adjusting the Systems.....	48
Figure 38: Global coordinates by right selection of the faces of bodies	48
Figure 39: Setting dynamic constraints, their directions and input parameters....	49
Figure 40: Running the kinematic simulation of the mechanism	49
Figure 41: Kinematic simulation or responses of the syste	50
Figure 42: Initial position of IEM.....	53
Figure 43: Kinematic analysis of IEM by PTC Creo Mathcad Prime 3.0.....	53
Figure 44: Total displacement vs time simulation of IEM graph by ANSYS.....	54
Figure 45: Displacement vs time graph of injera extracting mechanism	54
Figure 46: Position analysis of link 2 by ANSYS MBD V19.2	55
Figure 47: Magnitude position analysis of link 2 by ANSYS V19.2	56

Figure 48: 3D position analysis path of link 2 of IEM by ANSYS V19.2.....	56
Figure 49: Link 3 or translational link position analysis by ANSYS	57
Figure 50: Magnitude of kinematic analysis of slider link or link 4	57
Figure 51: Position analysis of the lower finger by PTC Mathcad Prime 3.0	58
Figure 52: Position analysis of lower finger by ANSYS V19.2.....	58
Figure 53: Upper fingers directional position analysis.....	59
Figure 54: One loop lower finger injera grasping and dropping analysis	59
Figure 55: Directional position analysis of lower fingers	60
Figure 56: Position analysis of injera extracting mechanism	60
Figure 57: Total velocity analysis of link 3 and link 4 for 30 seconds.....	62
Figure 58: Total velocity analysis of IEM for 120 seconds.....	62
Figure 59: Velocity analysis of lower finger	63
Figure 60: Assigning the revolute joint constraint of link 2 to the ground.....	64
Figure 61: Angular velocity analysis of link 2 by ANSYS	65
Figure 62: Directional acceleration analysis of injera extracting mechanism	65
Figure 63: Directional acceleration analysis of injera extracting mechanism	66
Figure 64: Acceleration analysis of link 2 by ANSYS V19.2.....	66
Figure 65: Acceleration analysis of link 4.....	66
Figure 66: Kinematics analysis of baking machine integrated with IEM	67
Figure 67: Diameter formulation for the IBM system.....	75
Figure 68: Centerline diameter calculation and demonstration	76
Figure 69: Dimension of pan lid; (a) pan lid (b) Equivalent dimensions	77
Figure 70: Geometric properties of mitad model	78
Figure 71: Location of a mitad on the circular frame for IEM.....	81

Figure 72: IBM 3D Draft.....	84
Figure 73: IBM Subcomponents before operation	84
Figure 74: Rolling cylinder to the x-direction due to friction from the mitad.....	85
Figure 75: Semi-automated injera baking machine	86
Figure 76: Displacement Analysis of one cycle rotation of the IBM.....	93
Figure 77: Total displacement analysis of two cycle rotation of IBM	93
Figure 78: Total displacement analysis of two cycle rotation of IBM frame	93
Figure 79: Position analysis of mitad per two cycle revolution	94
Figure 80: Total Position analysis of cover opening and closing mechanism.....	94
Figure 81: Injera baking machine integrated with injera extracting mechanism..	95
Figure 82: Directional position analysis of the system.....	95
Figure 83: Total position analysis of the system	96
Figure 84: Directional velocity analysis of the integrated (IBM & IEM)	96
Figure 85: Position Analysis of link 2 of IEM integrated with IBM	97

<u>Table List</u>	<u>Page</u>
Table 1: Model specification of IBM	15
Table 2: Tabular value of IC for five links	36
Table 3: Types of joints or constraints in <i>injera</i> extracting mechanism.....	47
Table 4: Subcomponents of semi-automated <i>injera</i> baking machine.....	87
Table 5: Calculation of kinematics of <i>injera</i> baking machine.....	88
Table 6: Kinematic behavior calculation of IEM	89
Table 7: Kinematics boundary condition calculation of IEM and IBM.....	90
Table 9: Cover opening and closing boundary condition magnitude	91
Table 10: Total displacement IBM rotation for the real time event	92

LIST OF ABBREVIATIONS AND ACRONYMS

A	Area
AC	Alternative Current
α_i	Corresponding Angular Acceleration of Links at Specific Joints
atan	arc tan, Trigonometric Identity, tan () Inverse
$\vec{a}(t)$	Acceleration Vector, Directional Acceleration
CAD	Computer Aided Drawing
C_f	Circumference of <i>Mitad</i> Carrier Circular Frame
C_i	Order Number of Pan-Lid
°C	Degree Centigrade
DC	Direct Current
DOF	Degree of Freedom
3D	Three-Dimensional Model
DP	Dough Pouring
DRRD	Dwell Rise Return Dwell
DRDRD	Dwell Rise Dwell Return Dwell
\vec{e}_θ	Angular Unit Vector along the Polar Axis
\vec{e}_r	Radial Unit Vector along the Radial Axis
f	Frequency
hp	Horse Power
\emptyset	Phi, diameter of flywheel disc
i, j	Number of Preceding Joints, Number of Neighboring Joints
$\hat{i}, \hat{j}, \hat{k}$	Vector Coordinates Orientation
IBM	Injera Baking Machine
IC	Instantaneous Center
ICV	Instantaneous Center Velocity
IE	<i>Injera</i> Extraction
IEM	<i>Injera</i> Extracting Mechanism

IP	Input Port
kWh	kilo Watt hour
kW	kilo Watt
MRBD	Multi-Rigid-Body-Dynamics
MBD	Multi-Body-Dynamics
N	Angular Speed in RPM
n	Number of Links
N_p	Number of Sets of <i>Mitads</i>
OP	Output Port, <i>Injera</i> Extractor
PP	Pan Polishing
π	<i>Pi, constant number</i>
R	Radius of <i>Mitad</i> Carrier Circular Frame
RBD	Rigid-Body-Dynamics
r_i	Radial Measure of Each Links
$\vec{r}(t)$	Position Vector
r (t)	Position
RPM	Revolution per Minute
SIBM	Semi-automated <i>Injera</i> Baking Machine
SU	Setup the system
T	Period, Transpose
t	time taken
t_d	Delay time
θ_i	Angle Measure of Links at Specific Joints
X_F	Total Displacement Covered by IEM
V	Volume
v_i	Velocity of Each Links
$\vec{v}(t)$	Velocity Vector
ω_i	Corresponding Angular Velocity of Links at Specific Joints

CHAPTER I

INTRODUCTION

1.1 Background

Injera is the best-known food among the traditional staple foods of Ethiopia. It is baked from *teff*, sorghum, barely, rice, etc. Among these cereals, *teff* is the most popular grain to bake *injera*. Based on the power consumption, *injera* needs averagely 2.5 minutes to 3.5 minutes to be baked enough on the electric used pan. *Injera* baking needs temperatures ranging from 180 °C to 220 °C [1]. The pan is made of molded clay whose diameter varies from 40 cm to 60 cm and thickness 2 to 3 cm.

Baking *injera* is practiced for a long period with the history of Ethiopian people by classical way. In classical *injera* baking method, the pan is arranged on the equal sized three stones. The stones help as supporters of the pan. Among the three stones that are set beneath the pan, the fire wood is used as a fuel.

Nowadays, although, the availabilities of electrical pan, solar pan and biogas pan are on utility, *injera* is baked in classical way by using manual labor. There are few early works on the semi-automated *injera* baking machines that use manual extraction for taking out *injera* from the baking surface.

There are three consecutive activities during *injera* baking. These are sweeping, dough pouring, and *injera* extracting. These activities determine the study variables such as time duration, revolution speed, and number of pans regarding with powers on the system.

Injera baking is a difficult task that takes time and effort with same ritual tasks repeatedly. The released heat when the pan-lid is opened as a form of steam during the moment of taking out *injera* and the same repeatedly task frequently, suffers the health of labors. These activities are weird especially for the massive *injera* production.

This paper deals with the model and simulation of *injera* extracting kinematic mechanism. A semi-automated *injera*-making machine provides safety ensuring

purpose, production rate, less consumption of time, etc. To use a semi-automated *injera* baking machine, it is important to synthesis kinematic and kinetic mechanisms with an appropriate design that bakes *injera* semi-automatically. Accordingly, this study aimed on modeling and simulation of *injera* taking off kinematic mechanisms of massive *injera* baking machine.

However, this thesis deals with the kinematics of the system synthesis, model and simulation of *injera* taking out mechanism. The purpose of kinematic modeling and simulation of *injera* taking out mechanism is for solving the proper time, position, speed, and geometric shape between the rotation of pans and the extracting mechanism relative to the other activities that are mentioned above. There are twelve pans on the circular-frame that revolves per 3 minutes.

1.2 Statement of the Problem

Although *injera* counts a long history as an Ethiopian staple traditional food, its baking process machines and their improvement of standards are not set yet. No adequate researches are done on the semi-automated and fully automated *injera* baking machines except focused on the improvement of *mitad* energy consumption efficiency.

Until now, baking *injera* is practiced manually for big hotels and higher academic institutions as well as households through all the country. Women and young females bake *injera* almost the time in the kitchen, for the purpose of massive production in the hotels, universities, colleges, and wedding ceremonies, etc. It is obvious that *injera* making is much difficult than cooking other meals as its activities are repeatedly and ritual tasks. Manual *injera* baking system affects health and reduces production rate.

Among the three consecutive activities during *injera* baking process, *injera* extracting and dough pouring are difficult. Especially, in manual baking, the releasing of heat in the form of steam and hotness of the *mitads* hocks the nails of fingers of the baker and the edge lip of *injera* needs to be separated well before taken it out, makes the extraction of *injera* a difficult task. Hence, all these problems are the consequences of shortage of an automated or a semi-automated *injera* baking machine or device. In addition, this is the cause of inadequate design, modeling and simulation of *injera*

baking machines has not been done, as *injera* is a staple and wide-spreading traditional food.

It is obvious that *injera* baking is somewhat too difficult to change the conventional following methods to automatic baking method. For example, batter pouring from some diameter approximate to zero diameter and *injera* extraction with barrier-rounded edge of *mitad* etc.

Technology and innovation has risen slightly on the fully automated and semi-automated *injera* baking machines in United States by Ethiopians. The semi-automated *injera* baking that is entitled and patented as “Rotary Baking Systems and Method” [2] has a good initial base with automatic dough pouring, cover closing and well designed in geometry structure. In the rotary baking system and method, extraction of *injera* and opening of cover are done manually.

1.3 Objectives

1.3.1 General Objective

The general objective of this study is modeling and simulation of *injera* extracting kinematic mechanisms; in order to make a semi-automated *injera* baking machine.

1.3.2 Specific Objectives

This study deals specifically with

- Synthesis of *injera* extracting and pan cover opening and closing mechanisms
- Kinematic formulation and analytical analysis
- 3D software physical modeling by SolidWork V2018
- Kinematic modeling and simulation of *injera* extracting and cover opening and closing mechanisms in ANSYS MBRD V19.2

1.4 Scope of the Study

This study focused only on modeling and simulation of *injera* taking out kinematic mechanisms of semi-automated *injera* baking machine. It focused on dynamic system model of the time taken, position, velocity and acceleration vector of *injera* extracting mechanism relative to the rotational angle and motion of pan, dough pouring and opening and closing of cover.

1.5 Limitations of the Study

Based on the specific objectives of this study, lacking of the preceding related literature reviews, insinuation giving materials, immensity of the portion content and bothering with lacking of advisor was some of the challenges among the related limitations during this study.

1.6 Significance of the Study

The advantages of modeling and simulation of semi-automated *injera* taking off kinematic mechanisms are manifold: it reduces the expensive and time-consuming prototype preparation and the number of the tests, the kinematic properties and design parameters of the product will be improved, the production time shortens and the quality standard of products rises.

1.7 Research Methodology

This study is concerned with the synthesis, modeling and simulation of an *injera* extraction kinematic mechanism based on the physical laws and principles observed from the traditional *injera* baking method. Kinematic synthesis, modeling and simulation of an *injera* extraction kinematic mechanism is integrated with scotch yoke mechanism. The equation of motion is derived from dynamic analysis using a uniform circular motion method and polar and radial coordinate's system rigid body dynamics by taking other bodies' motion into relative reference. Further geometric modeling of a IBM mechanism is constructed using SolidWorks V. 2018 software and its kinematic responses are determined in MRBD of ANSYS V. 19.2 Simulator. Based on the mathematical modeling the analytical analysis is solved both numerically and graphically in PTC Creo 6.0 Mathcad Prime 3.0. And the analytical graphical analysis and ANSYS simulation result graphs are compared.

1.8 Outline of the Study

This thesis report has been organized in a manner that is achieved. The entire research work is organized into six chapters: Following the Introduction part in **Chapter 1**, the previous work related to this study: the historical outlook of *injera* baking method and its classification including their reviewed literature reviews in **Chapter 2**. In **Chapter 3** the experience of basic physical laws and principles of an

injera baking processes and its time based sequential operations, the interpretation of the operation is done. The kinematic synthesis, modeling and simulation of the configuration of linkages that form an *injera* extracting kinematic mechanism, its analysis to derive the equation of motion using the closure loop method from the expression of kinematics is discussed. Inclusively, the working principles of *injera* extracting mechanism is discussed. **Chapter 4** deals with result and discussion obtained from motion simulation in Multi-Rigid-Body-Dynamics (MRBD) of the CAD geometry of 3D-physical modeling with the entry of mathematical modeling. The kinematic response is interpreted and discussed from the graph that is extracted from the MRBD in ANSYS V. 19.2. Lastly, **Chapter 5** deals with the overall description of the thesis work conclusion. Moreover, the conclusions of the thesis are summarized and recommendations and future works are given for the future studios. Reference and Appendices are attached at the end of the document.

CHAPTER II

REVIEW OF LITERATURE

In a classic baking, the slim *mirt* with integrated chimney and institutional *mirt*, takes 102 minutes to bake maximum 30 *injer*as of 16 kg dough. For the same weight dough, the conventional three-stone open fire stove baking takes 121 minutes according to Anteneh Gulilat report on “Stove Testing Results” [3].

According to Asfafaw H. Tesfaye, the traditional electric *injera* stove was tested for different ranges and a quality *injera* is baked from in average 130-220°C, 3.5 kWh to 3.9 kWh [4, 5, 6] and the temperature could be reduced averagely from 165 to 100°C during polishing the surface of baking. In addition, one *injera* requires an average of 0.1 kWh and 2.5 minutes to be well cooked.

2.1 Development of *Injera* Baking Machine

This study categorized the development of *injera* baking device studies from time to time for its performances as it is shown in Fig. 1 below. The development of IBM is come from time to time as the following four categories based on its baking method/device and power source they use to bake. Not only this, the time chronicle order is also another factor. The shaded box at the right edge is where this study takes place its study as it is mentioned under general objective.

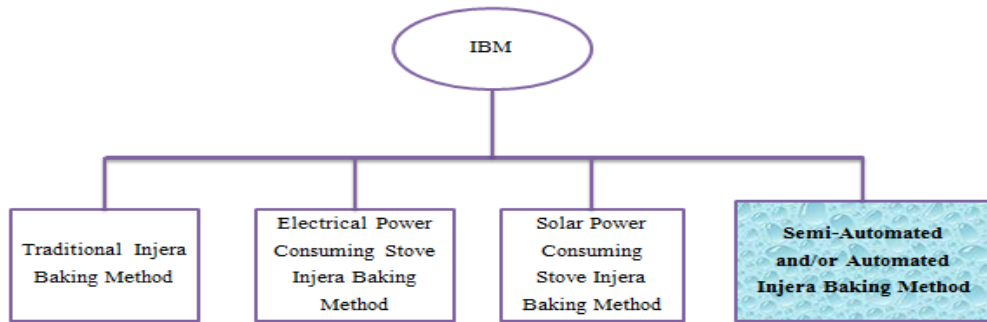


Figure 1: Literature review on development category of *injera* baking machine according to baking power development stages

2.2 Traditional Injera Baking Method

For centuries in Ethiopia, and perhaps even for millennia, women made *injera* through a labor-intensive process that required them to pour the batter or dough onto a hot clay pan or *mitad* one piece at a time, piece after piece, letting it cook for few minutes, removing it, and then beginning the process over all again.

Traditionally, *injera* baking practiced is similar over all the country with a slight difference in pan dimension and stove efficiency. Some researchers indicated the traditional clay stoves, 11-20 mm thickness and 500-600mm diameter, have an estimated efficiency of 5%. Others show the Tigray state *mitad* and *Mirt* Stove, improved stove, has registered an efficiency of 25 % and 35 % respectively [7].



Figure 2: Traditional *injera* baking [8]

2.3 Electrical Power Consuming Stove Injera Baking Method

Recent field tests have shown that improvements in air control and firebox design is currently the most effective and socially acceptable stove design modification. However, their usefulness with regard to saving the resource base from depletion is limited in the face of growing population and urbanization because they use fire wood as the source of energy [9] and this causes health impacts.

Electrical *injera mitads* are growing high alternative in Ethiopia because of its relatively wide in availability of electricity generating hydropower. On other hand, these electrical *mitads* have designs dating back to the 1960's, are highly as well, and are overloading the electricity grid. Consequently, a research and design project called 'Magic *Mitad*' initiated to develop an energy-efficient electric *injera mitad*. Starting with the introduction of a new type of fuel-efficient baking plate a range of research and design experiments were initiated to further optimize the energy-efficiency as well as the baking quality of the Magic *Mitad* [10] but later is recognized as with ununiformed heat distribution.

Gashaw Getenet has developed mathematical models and finite element formulations for baking pan and *injera* during baking. Simulation was done in terms of temperature profile during heat-up and cyclic *injera* baking using MATLAB. Performed simulation for four different electric power sources (1.867 kW, 2.2 kW, 2.5 kW, and 3 kW) using two types of baking pans (clay and ceramic) [5].

2.4 Solar Power Consuming Stove *Injera* Baking Method

According to Asfaw Haile Selassie [7], Conference Paper at Mekelle University communities and external guests, solar *injera* baking *mitad* to social media, the solar *injera* baking shows smooth baking process with very good *injera* quality, which is the same as the quality of *injera* baked on customary *injera* stove as shown below in Fig.3. This system has smooth baking texture similar to the ordinary stove and it used oil seeds to polish it. Unlike oil, oil seeds have the ability to give smooth baking surfaces by filling its irregularities.



Figure 3: Solar *injera* baking process [7]

As it is shown Fig.3 above, even though it is a power save good technology, but the task is routine and performed by labor that affects health from heat during mitad polishing, dough pouring, and taking off *injera*.

2.5 Semi-Automated or Automated *Injera* Baking Machine

Innovation and technology has slowly begun to change in American cities and other abroad places by some Ethiopians. Due to this, it is possible to make *injera* in mass quantities using automated devices that require for less human labor than the traditional way. Among those, since 2002 - June 2006, Zelalem *injera*, with locations in Dallas and Washington, D.C., makes its daily bread with the Zelalem *Injera* Machine; the creation of Dr. Wudneh (“Woody”) Admassu, an Ethiopian- born professor of Chemical engineering at the University of Ladaho [10] is one example.



Figure 4: Zelalem *injera* machine

Since 1999-2008, Wassie Mulugeta has been working for 12 years to make a fundamental development change in the way which *injera* is cooked by Ethiopians; His effort was struggled to build an *injera* machine with a conveyor belt system and that did not work well. So he put the project aside for a while and tackled it again 2006 and 2008, finally, he invented a rotary baking system and method *mitad* for making *injera* which received patent in 2011 as it is shown in Figure 5 below, but so far he has not built one to mass produce *injera* [12] because of capital shortage, the machine is not build.

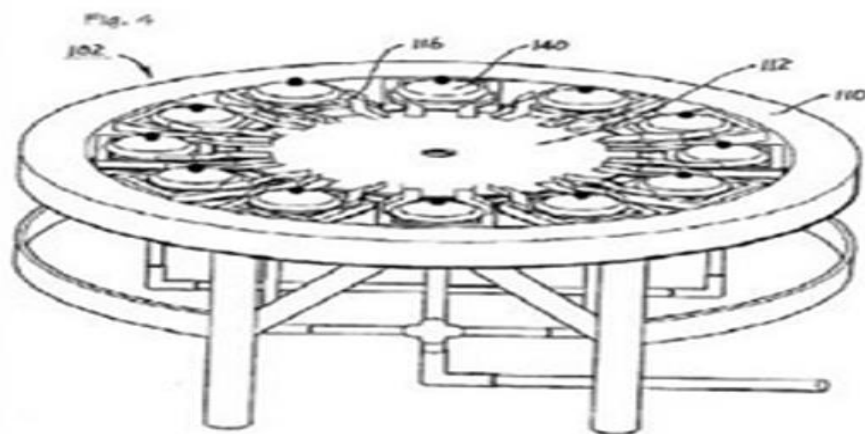


Figure 5: Wassie Mulugeta's *injera* machine [12]

CHAPTER III

METHOD, MODELING AND SIMULATION OF *INJERA* EXTRACTING KINEMATIC SYSTEM

3.1 Method

This study depends on the parameter of the *injera* baking time of electrical power consuming *mitad*. Specifically, Wassie digital *injera* baking *mitad* is typical device for this study purpose. The diameter and thickness of *mitad* in this study is based on the mentioned *mitad* type.

This research concentrated on the model of *injera* extracting system by limiting its scope to system-level. At this level, the other components, and sub-systems of a semi-automated *injera* baking machine are taken into account as a black boxes that interrelate with each other through a distinct interface. It surveys the speed, angular position, velocity, extracting time, and angle of the *injera* extracting mechanism with relative to the other operational mechanisms.

To test whether the set up design specifications of the system met or not, the designers use modeling and simulation by using virtual representation rather than the real physical experiments or prototypes. They are the virtual prototypes to shorten the cycle of design and reduce the cost of design significantly. Simulation enables the designer with instant response on design decisions to improve the design with examinations of better performance alternatives to get an optimum effective system.

The focus of this work is not on the differential equation modeling but further attended on the perspective of modeling and simulation of the necessary particular parameters of *injera* extracting design. Specifically, it explores the time of *injera* taking out mechanism interrelated with the other operational components of the system, speed, velocity, and position and angle arrangement of the components. In detail, in this study, the methodology is given as follows in Fig. 6 below.

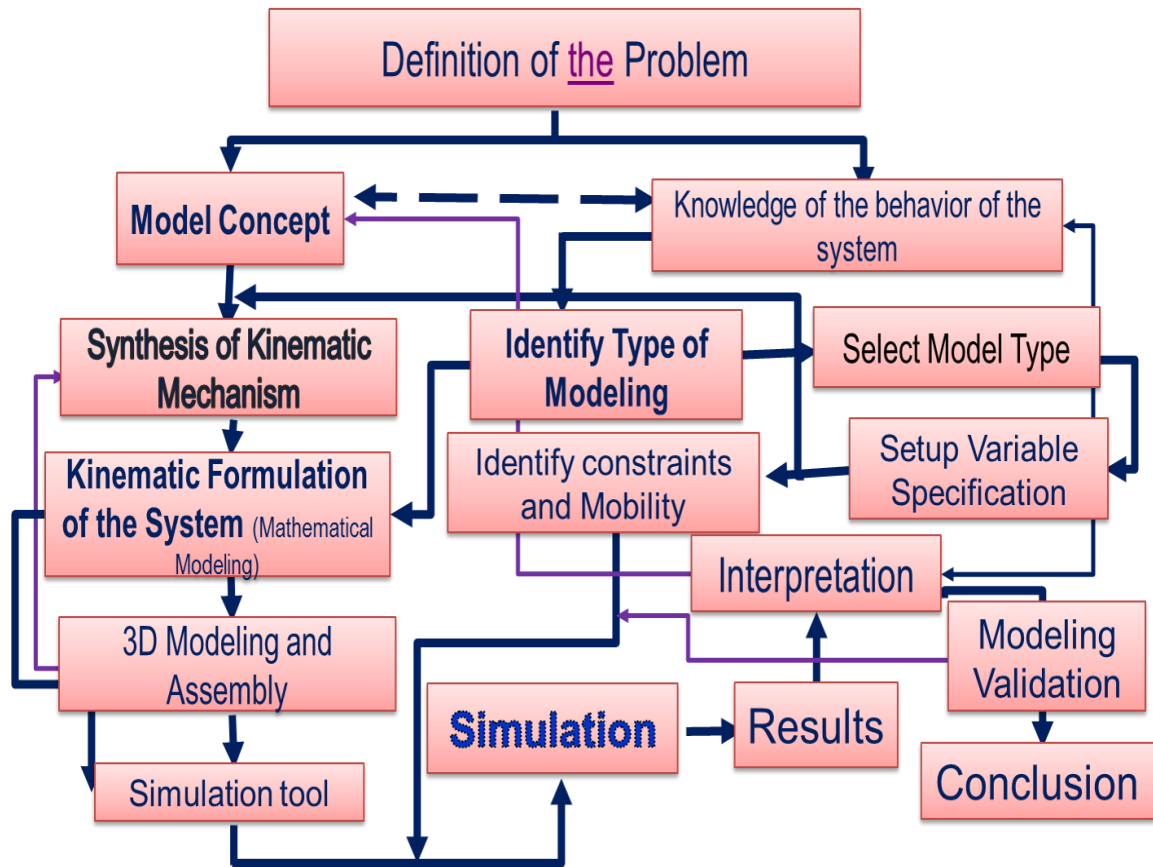


Figure 6: Work flow chart of IEM and IBM modeling and simulation

3.2 Definition of the Problem:

The objective of this study is taking out *injera* automatically from the *mitad*. In addition, putting it properly on the reserved place as a temporary bin within a proper time interval. The system has three ports. i.e., the *mitad* polishing, dough pouring and *injera* extracting ports. The ports are fixed in series connection with equal gap among them. The time interval and speed for these activities between these gaps during the rotary movement of *mitad* assumed as equal.

3.2 Physical Laws and Phenomenon of *Injera* Baking Process

Injera is an Ethiopian pancake, 2 to 3 mm thin, leavened flat and soft bread made from fermented batter of different cereals such as *teff*, sorghum, barley, rice, etc. The quality of a good *injera* is its softness, size, texture, uniform distribution of gas holes or eyes over its top surface, free from being sticky together, marginally sour taste, rollability, etc. The small eyes or gas holes on the top surface of *injera* are due

to its batter fermentation and content of *absit* (the add-in starter ingredient of dough), facility of gas-producing bacteria present in the dough [13], baking process, the baking surface quality and thickness of *mitad*, the geometry of pan cover and its closing time.

It takes averagely 2 to 3.5 minutes to bake *injera* according to the amount of electric or other power consumption. It is baked on the top surface of circular *mitad* whose 40 to 60 cm diameter, 20 to 30 mm thick, 5 to 12 kg and made of clay. *Injera* has 330 to 500 gram weight [14].

In classic baking, the dough pouring onto the baking surface follows circular path motion from the outer diameter to inner that approaches to zero diameters. The dough is poured manually by using a jug like tool. The elevation of pouring of dough above the baking surface and the rotational speed of hand determines the thickness of *injera*. After the pouring of dough, the cover is closed after 5 to 10 seconds approximately. This study models the activities as follows in Figure 7 below.

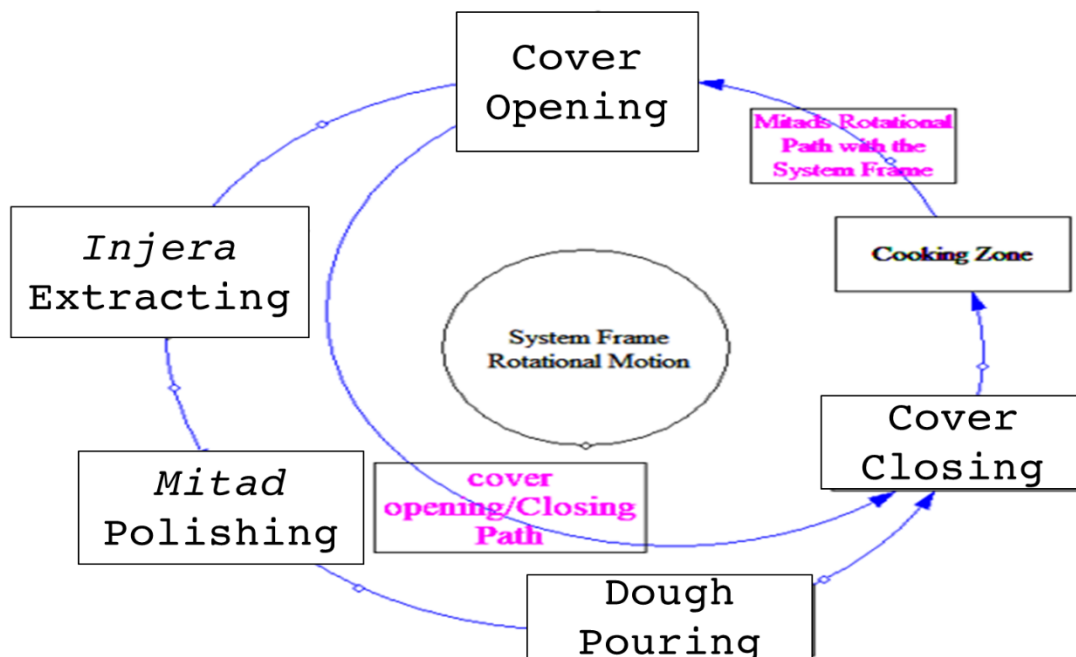


Figure 7: Physical cyclic modeling of *injera* processing in IBM model

During *injera* baking, it needs frequent polishing between two pieces of successive *injera* baking as the first *injera* is taken out. Before extraction, the pan lid needs to be opened and the steam has to be released out within a few seconds. It is extracted by separating the edge lips of it with nail of fingers or very sharp tool; and inserting bamboo mat or flat sheet material through the separated gap between it and *mitad*.

3.3 Setup of Model Specifications of IBM

This study used 12 identical circular electric flat pan with diameter of 42 cm on a circular rotating frame at equal distance. These pans are made of molded clay approximately in total have 60 kg with 4 cm thickness combined with the electric circuits. The model specifications are setup on the Ethiopian Energy Agency (EEA) Standards [14] mostly. The IBM is operated by three electric AC motors, i.e., one for the pan carrier frame rotation, the second for the dough pouring operation and the rest for *injera* extracting operation.

As it is shown in Table 1, *density of *injera* is calculated from the specific volume of *injera* at 180 degree centigrade. Hence, the specific volume of *injera* at 180 °C is $4.3084\text{cm}^3/\text{gram}$. For detail information, the kinematic design is set on Appendix V and Mathcad software programming.

This study has given its system specification as the following as it's listed in Table 1 below:

Table 1: Model specification of IBM

No.	Model Parameter	Symbol	Value
1	Diameter of pan	d_m	42 cm
2	Diameter of pan-Lid	d_c	42 cm
3	Diameter of <i>injera</i>	d_i	40 cm
4	Weight of <i>injera</i>	w_i	350 grams
5	Thickness of <i>injera</i>	t_i	0.3cm
6	Volume of <i>injera</i>	V_i	$3.77 * 10^{-4} m^3$
7	Mass of <i>mitad</i>	M_m	5 kg
8	Frame base diameter	D_b	351.22cm
9	Frame outer diameter	D_o	355.22 cm
10	Frame inner diameter	D_i	271.22 cm
11	Angular speed	N	1/3 rpm
12	No. of pan	N_p	12
13	<i>Mitad</i> type		Single circular clay flat
14	Power Consumption		Electrical energy
15	Motion type and direction		CCW Circular rotary
16	Production rate time	t_p	$0.271t=13/48t$ [s]
17	Flow of current to <i>mitad</i>	I	25 A
18	Startup time (initial delay time)	t_o	15 to 20 min
19	Resistance values	R	22.9 Ω
20	Baking temperature	T_b	180 to 220 $^{\circ}C$
21	Density of <i>Injera</i> *	ρ_m	232.1 kg/ m^3
22	Yield stress of <i>injera</i> [15]	σ_y	0.64 – 0.78 Pa
23	Height of the rotary frame	h	80 cm
24	Effective diameter of the cover	d_{eff}	47 cm
25	Length of extracting finger	l_f	200 mm

3.4 Semi-Automated Rotary Injera Baking System

The main components of a semi-automated *injera* baking machine are *mitad* polishing mechanism, a dough pouring mechanism, and *injera* extracting mechanism. These mechanisms are upgraded from the conventional baking activities of polishing of *mitad*, batter pouring and *injera* extraction by using bamboo mat or very thin sheet plates. All of them are indispensable in *injera* baking system. They work independently within time sequential order.

Before pouring batter on the baking surface of *mitad*, polishing the baking surface of *mitad* is the primary task. Roasted cabbage seed powder, castor ('*gullo*') seed oil, cottonseed oil, and oil contained seeds use for polishing the *mitad* by using polishing pad or cloth. However, the roasted cabbage seed powder is common on usage. The polishing cloth is curled on the hallowed cylindrical spindle that is fixed parallel to the baking surface of the *mitad* within contact. Due to the motion of the *mitad*, the polishing pad also rolled over the baking surface of the *mitad*; follows the motion direction of the *mitad*. The purpose of *mitad* polishing is to avoid the probability of sticking *injera* to the baking surface during extracting and for keeping the quality and cleanness of *injera*.

As the *mitad* is polished, pouring dough on the baking surface of the *mitad* is the second task. Pouring dough over the baking surface of the *mitad* by using a jug like rotating device with nozzle. In semi-automated the dough is poured by using a showerhead like devices with a reciprocating movement to close and open the batter outlet nozzle.

After the batter is added onto the baking surface, the pan-lid is needed to be closed after 5-10 seconds. In conventional method, the time delay after adding batter used for releasing the moisture content from the poured batter and for keeping the light and softness of the *injera* quality.

After 2.5 minutes [14, 5], the *injera* is ready enough to be taken out. The two pairs of fingers that is attached to the scotch yoke mechanism's arm take out *injera* from the thin stainless plate. The scotch yoke mechanism is, operated by AC motor, used to change the rotary motion into intermittent linear motion. The intermittent linear motion helps to take out *injera* from the extracting port and deposits to the *injera* bin position. This motion should fit with the motion of IBM frame with regard to an appropriate time synchronization especially relative to the movement of pan as it is shown in Figure 8 below.

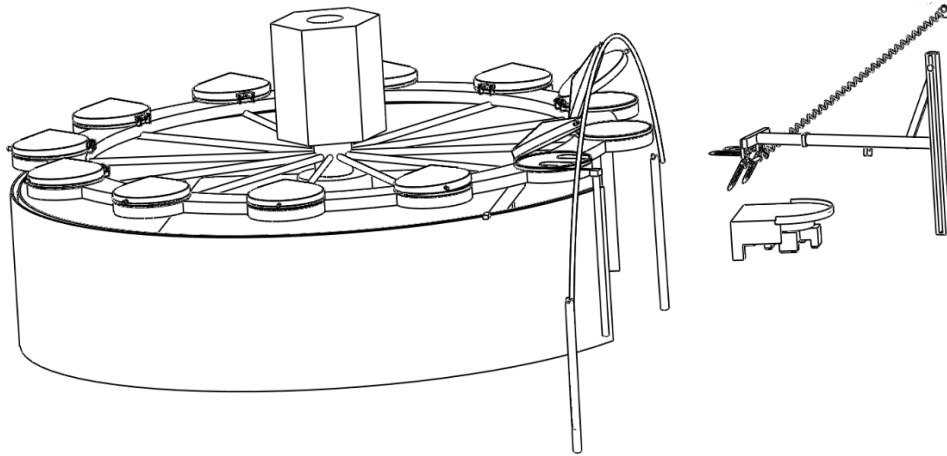


Figure 8: Semi-automated rotary IBM

The pans are arranged on the circular frame at equal distance gap.

3.4.1 Terminology

For the purpose of this study, the following definitions shall apply:

Baking: A process of cooking food such as *injera*, bread, waffle from dough etc.

Cam-guided rod: Pan lid opener and closer curved link.

Clay: A plastic muddy soil when it gets moist and hardy material when it is tempered, that is used for pottery, tile and brick preparation.

DRRD: Dwell- rise-return-dwell cam-guided cover opening curved mechanism.

Time Delay: Duration of time before starting one operation due to a causal-intervention of the operation relative to the other operation/s or system within a relationship. It will also be the interval of time between two sequential operations or tasks.

Flywheel: A rotating disc or circular bar used for rotating to transmit power.

Linkage: A linkage is obtained by fixing one of the links of a kinematic chain to the ground.

Dynamic mechanism: Mechanism under motion with its causal force. It is a motion of any of the movable links results in definite motions of the others.

Gripper fingers: Two pair of fingers to take out *injera* from the circular stainless steel injera extractor plate.

Injera: Ethiopian cultural food, leavened thin flat pancake.

Mitad: a clay pan, a circular griddle made of local clay soil and tempered with fire.

Model: a designation or representation of particular physical characteristics and features of an actual system with respect to some selected dynamic problem.

Scotch yoke mechanism: A mechanism converts linear motion of slider into rotational motion or vice-versa. In this paper, it is used to change rotational motion to linear or intermittent motion by coupled directly to sliding yoke with a slot that engages a pin on the rotating disk with constant angular speed.

Semi-automated IBM: *Injera*-baking machine that is not full automatic operated.

Simulation: it is an imitated operation of the model structure of the physical (may be conceptual) system over a compacted time systematically.

Slider: a component of scotch yoke mechanism that lets the output link free from interruption.

Synthesis: configuring and developing mechanism/s for the required application

Takeout: the word '*taking out*' is used to remove *injera* from the extracting port of the stainless steel plate surface. Even if, the meaning of '*take out*' and '*take off*' are the same, they are used according to time sequence and port position in this thesis.

Takeoff: to remove *injera* onto its temporary storage from *injera* extractor mechanism.

***Injera* extracting mechanism:** *injera* taking out mechanism from the extracting port to the depositing post-port.

3.5 Kinematics of IBM Design Process

The IBM design process starts with meeting the functional requirements of a semi-automated *injera* baking product. Kinematics helps to ensure the functionality of *injera* baking mechanisms, while the role of dynamics is to verify the acceptability of induced forces in the components of the system. Both of them are subjected to various constraints (specifications) imposed on the design.

3.6 Synthesis and Kinematics of Injera Extracting Mechanism

3.6.1 Synthesis of Pan-Lid Linkage Mechanisms

The first work in *injera* extracting is opening the cover. In semi-automated *injera* baking system, the cover also is opened by cam-guide thin trajectory rod. Here, from the minimum to maximum, the lid will be opened to the maximum height of the lid's opening follower path or rod. The maximum height of the lid opener path is 42 cm that equals with the diameter of the pan lid but adding the cover handle it become 45 cm as shown below in Figure 9 and 10. The pan is fixed on the rigid rotating body and the conical lid is hinged at the edge of the pan. In addition, the cover has a handle at the bottom edge of the cover.

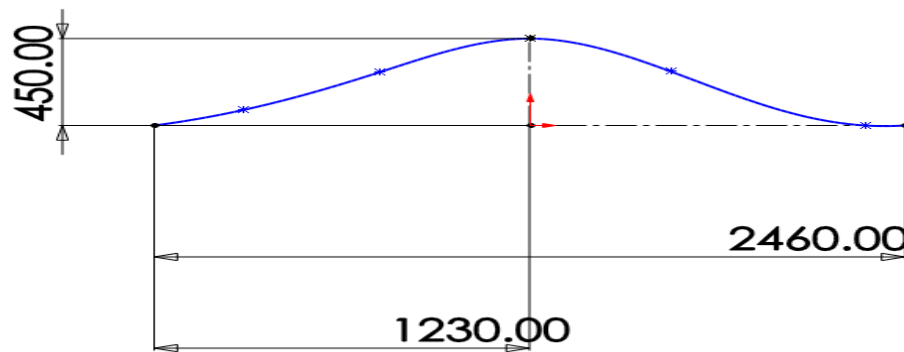


Figure 9: The cam-guide path curve of pan-lid

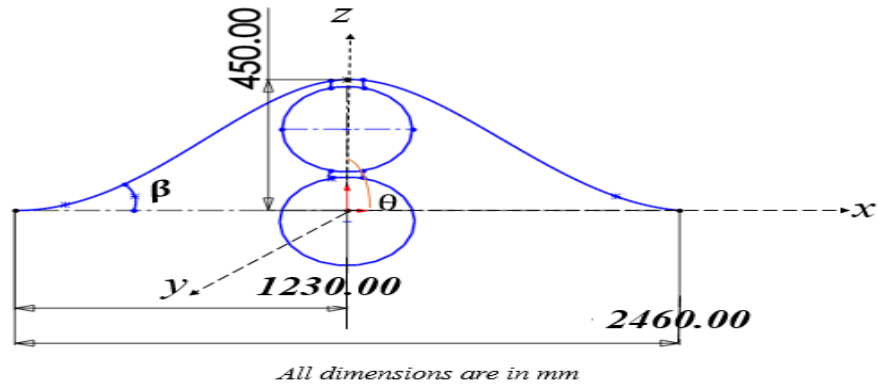


Figure 10: *Opening of cover to x-axis*

The skeleton of the cover opening/closing system will be shown in Figure 11 below as

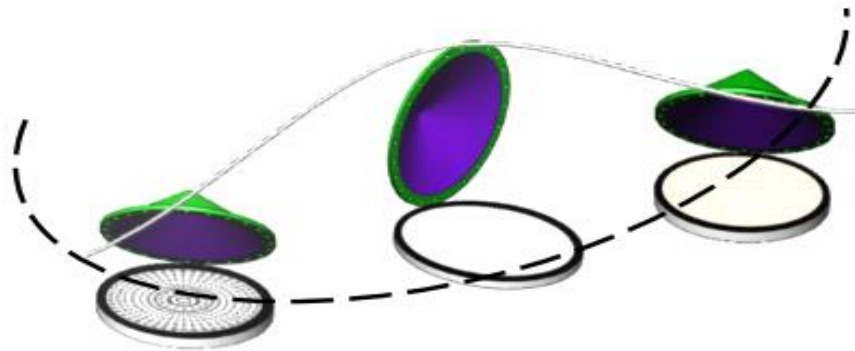


Figure 11: Three ports of IBM with cover opening and closing under (offset) cam-guider mechanism.

The type of the rod path can be considered similar to a dwell-rise-return-dwell (DRRD) [16] curve of cam-guide that guides the opening-and-closing of pan cover motion as shown in figure below. The first dwell curve used to permit the entrance of the rod into the cover's holder, and the end-dwell allows closing the cover on the pan smoothly. The rise curve allows opening of the cover until the cover goes to maximum height that equals the diameter of the cover, and the return curve guides the pan-lid to its place in the same direction of motion of the pan. The dwell-rise-fall type is not proper for this application because the poured batter on the surface of *mitad* needs a few time

for the best quality of gas holes or eyes as it is practiced in the classic way. In order to this case, as it is shown below in Figure 12, the DRRD cam-guide path is an appropriate mechanism.

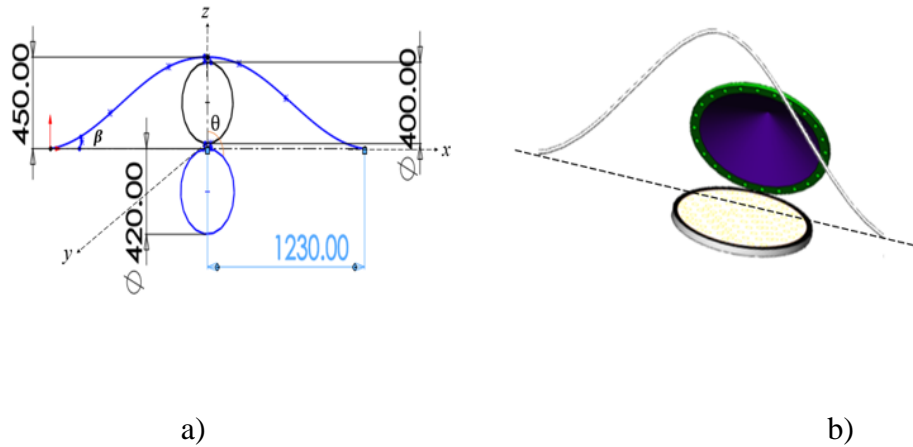


Figure 12: *The translation of cover after dough pouring while the dough is bearing gas holes. (a) skeleton of cover opening through the cam-guide path (b) Cover closing with the poured dough*

The equation of the curve slope will be the same with cam's equation

$$x = f(\theta) \quad (3.1)$$

Where x = cover opening gap or displacement as a function of θ and t

θ = the curve's angle that covered by the pan-cover. However, since the cover follows the curve path at a constant angular velocity as it is shown in Figure 13 below.

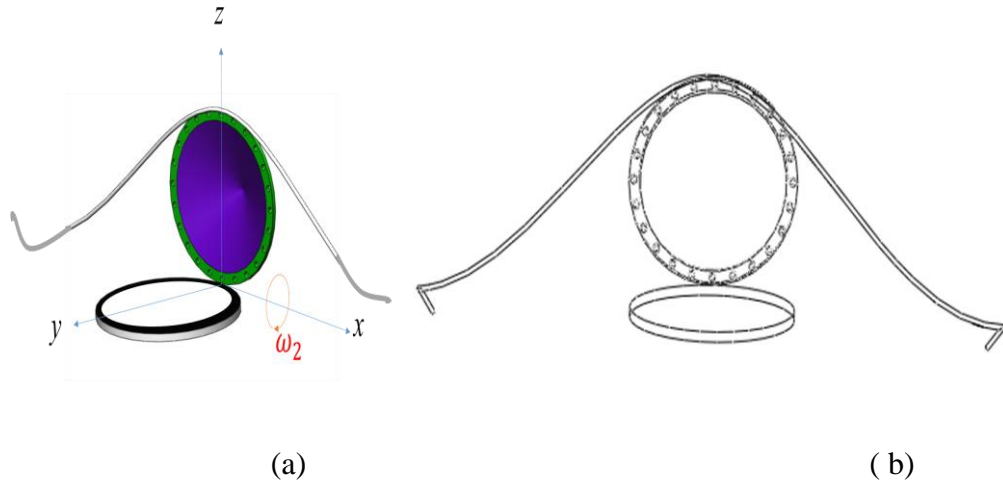


Figure 13: The direction of angular velocity direction to x-axis: (a) Virtual Opening of cover by translating with the means of roller bearing (b) Skeletal representation of the virtual opening of the cover

And the displacement either increases or decreases during rise and returning time respectively as the function of time that can also be written as

$$z = g(t) \quad (3.2)$$

$$\theta = \omega t \quad (3.3)$$

Where t = time to translate the cover through angle θ , sec

ω = Angular velocity of the pan that enables to translate the cover through the curve path, rad/sec

The instantaneous angular rate of change of the displacement and given by

$$z' = \frac{dz}{d\theta} = \text{velocity of cover opening} \quad (3.4)$$

The instantaneous angular rate of change of velocity

$$z'' = \frac{d^2z}{d\theta^2} = \text{Acceleration of cover opening} \quad (3.5)$$

By using the displacement as function of the time, we have the features of the cover opening slope of curve as follows:

Velocity of the cover opening

$$\dot{x} = \frac{dx}{dt} = \left(\frac{d\theta}{dt}\right) \left(\frac{dx}{d\theta}\right) = \omega \left(\frac{dx}{d\theta}\right) = \omega x' \quad (3.6)$$

Acceleration of the cover opening

$$\begin{aligned} \ddot{x} &= \frac{d^2x}{dt^2} = \frac{d}{dt} \left(\omega \frac{dx}{d\theta} \right) = \omega \frac{d}{d\theta} \left(\frac{dx}{d\theta} \right) \left(\frac{d\theta}{dt} \right) \\ &= \omega^2 \left(\frac{d^2x}{d\theta^2} \right) = \omega^2 x'' \end{aligned} \quad (3.7)$$

By using the time function derivative, the dimensionless position θ function gets its unit. Over the complete rise-return motion curve, the following is true due to equal time and angle to rise and fall.

$$\int \ddot{x} dt = 0 \text{ And } \int x'' d\theta = 0 \quad (3.8)$$

3.6.2 Dynamic Determinants of the Operations of the System

The three operations are dependent of time, geometric shape and angle arrangement with each other. The sequence of time, position of *mitads*, and rotational speed of the system play a great role in the baking of *injera* in the rotary semi-automated *injera* baking system among the three tasks. However, the baking time of *injera* depends on the amount of electric power consumption; and this study takes the consumption of energy as a steady condition, replacing the power parameter by baking time, 2.5 minutes and 0.1kWh [5].

The system has a unique time sequential operation at the first round with time index. If the sequence is missed, the work will be interrupted. For instance, if one started by pressing ON, the *injera* extracting motor at the same time with main motor of the IBM of the circular frame, the two fair of fingers of *injera* extractors can destroy the *mitads* at the OP port, as shown below in Fig. 14, IEM is synthesized. At initial time

$t_0 = 0$, the electric power is started by pressing ON and the start or delay time $t_i = 15$ minutes, the *mitad* will be ready to pour dough. At this time ($t = 15\text{min}$) the motor will be started and pouring of dough takes place over the top baking surface of the *mitad* at $t_d = 16$ minute. After each 15 seconds, each next *mitad* arrives to the dough baking port one by one. The first poured on *mitad* arrives to *injera* extracting or output port after 2.5 minutes at 330° angular position of *mitad* movement with a constant angular rotation of $\frac{1}{3} \text{ rpm}$, and the baking time for the first time will be:

$$t_{ij} = t_d + t_{op} \quad (3.9)$$

Where $i = 1, 2, 3 \dots$ the position order of *mitad* on the frame, which is given by the direction of motion and port entrance order. $j = 1, 2, 3 \dots$ the number of revolutions of the frame or batch number, i.e., one batch contains 12 *mitads* per revolution. t_{ij} = *Injera* baking time, t_d = Dough pouring time, and t_{op} = extracting time of *injera*.

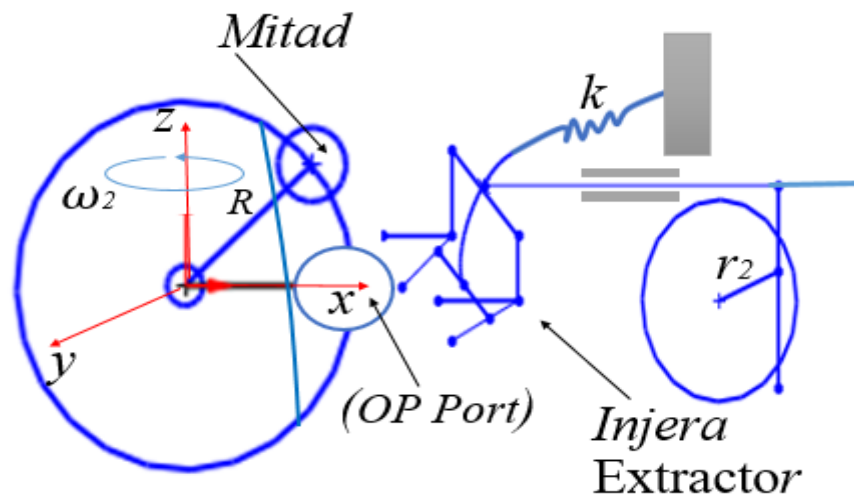


Figure 14: The subcomponent skeletal representation of IBM machine

The motor of *injera* taking out mechanism will start at the first index of t_{ij} equals $t_{11} = 18.5$ minutes. Before the time, t_{11} the position of crank arm (link 2) will be at 0 degree. However, link 2 will be at 360 degree for the next i^{th} position

of pans at their pre-extracting time, $t_{ij}^{(x_0)}$. Where x_0 indicates that the *injera* extractor fingers are at the *injera* taking off bin position. Hence, $t_{11}^{(x_0)}$ means the first *mitad* in the first revolution is arrived to the extracting port (OP) at 360 degree on the pan carrier circular frame and link 2 is at 360 degree on the scotch yoke mechanism. Just at $t = 18.5$ minutes the motor starts and the fingers arrived to the OP port at 18.625 minutes while the link 2 will be at π radians. During this time, the first *mitad* $m_{11}^{x_1}$ will be between the last poured on *mitad* in the first revolution and the OP port around arc length of 20 cm; at this place the first *mitad* will be polished slightly while moving in the speed it was moving. The polishing takes 7.5 sec per each *mitad*. Assume that the first *mitad* is started from $\theta_0 = 0^\circ$, and when it was at the extractor (OP) port, the *injera* will be extracted from the *mitad* at $\theta_{11}^{(x_1)} = 360$ degree. Then the next *mitads* take:

$$\theta_{ij}^{(x_i)} = \theta_{11}^{(x_1)} + \frac{360}{N_p} n \quad (3.10)$$

Where $\theta_{ij}^{(x_i)}$ –is the angle of the next *mitads* when they reach at OP port, $i = 1, 2, 3, N$ – the position rank of *mitad* arrangement. x_0 and x_1 –shows either the *mitad* is arriving or arrived to the OP port respectively, n – indicates number of revolution round and N_p – number of pans on the rotation, $\theta_{11}^{(x_1)}$ –the position vector of the first *mitad* at the OP port.

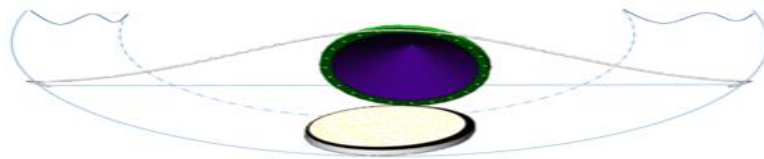


Figure 15: Cover opening and closing mechanism

At the maximum height where the cover is opened to $\theta = 90$ degree, the opening of the cam-guide curve is assumed as $\beta = 90$ degree.

Therefore, the displacement it follows is given by simple harmonic equation

$$z = \frac{h}{2} \left(1 - \cos \left(\frac{\pi\theta}{\beta} \right) \right) \quad (3.11)$$

By using Mathcad software the curve is plotted as shown below in Fig. 16.

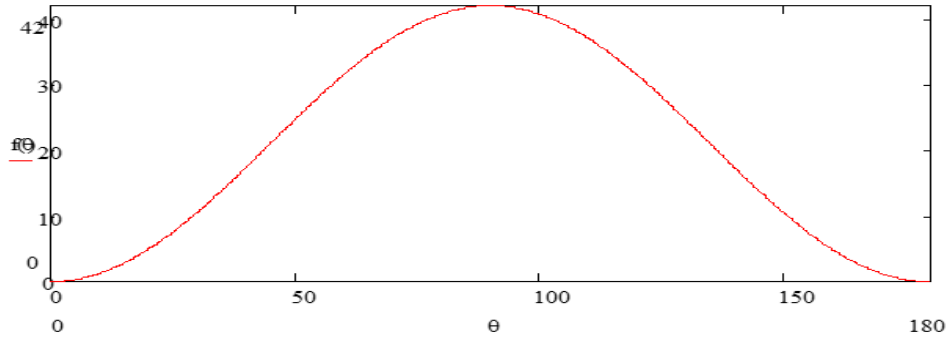


Figure 16 DRRD graph of cover opening and closing position vector curve

The slope curve of the displacement or velocity of the cover opening path by using equation (3.6) will be

$$\begin{aligned} \dot{x} &= \omega x' = \frac{h}{2} \left[0 - \left(\frac{\pi}{\beta} \right) * \dot{\theta} \left(-\sin \frac{\pi\theta}{\beta} \right) \right] \\ &= \frac{h}{2} \left(\frac{\pi}{\beta} \right) * \omega \left(\sin \frac{\pi\theta}{\beta} \right) \end{aligned} \quad (3.12)$$

Acceleration of the cover opening equation (3.7) will be as

$$\begin{aligned} \ddot{x} &= \omega^2 x'' = \frac{h}{2} \left(\frac{\pi}{\beta} \right)^2 * \dot{\theta}^2 \left(\cos \frac{\pi\theta}{\beta} \right) \\ &= \frac{h}{2} \left(\frac{\pi}{\beta} \right)^2 * \omega^2 \left(\cos \frac{\pi\theta}{\beta} \right) \\ &= \frac{h}{2} \left(\frac{\pi\omega}{\beta} \right)^2 \cos \left(\frac{\pi\theta}{\beta} \right) \end{aligned} \quad (3.13)$$

The graphic-sketch of cover opening and closing way is shown below in Fig.17, and the optimized cover opening and closing path is shown below in Fig. 18.

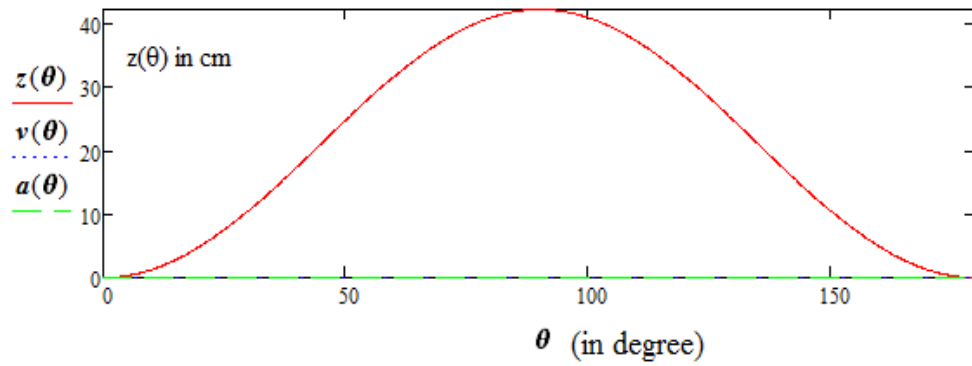


Figure 17: DRRD graph of cover opening and closing curve by Mathcad

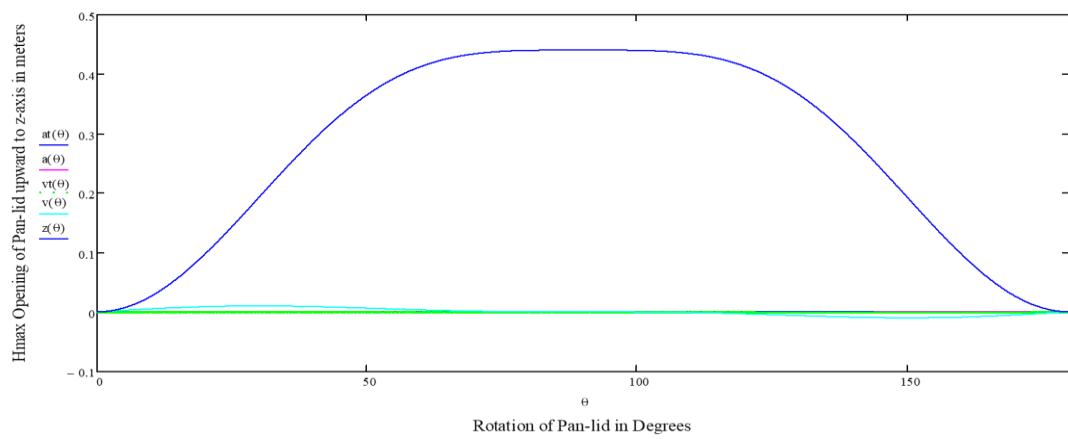


Figure 18: Optimized cam guided cover opener/closer path curve by Mathcad

However, in virtual, the direction of the cover motion is inward to the angular motion of the pan carrying rotary frame as shown below in Fig. 16 and its kinematics is given by

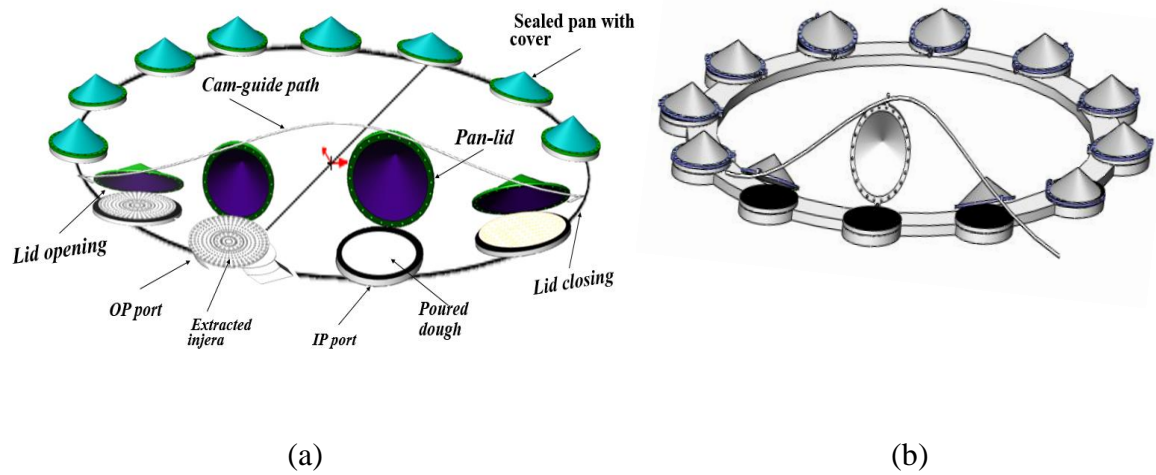


Figure 19: Virtual opening and closing motion path of a semi-automated injera baking system; (a) Subcomponents labeling and ports of IBM (b) Cover opening and closing port

From the above Figure 18, we have the following triangle with the diameter of the pan and the cover is shown as

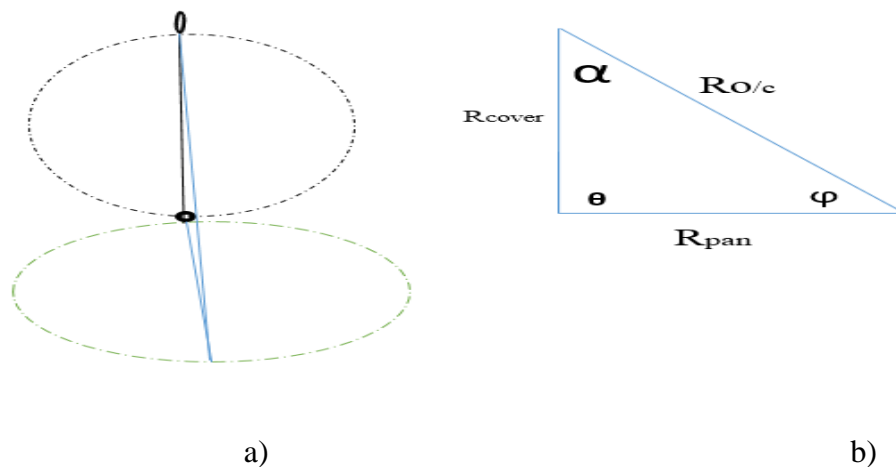


Figure 20: Trigonometric graph of cover opening and/or closing motion a) the maximum opening position of the cover at 90° b) Equivalent trigonometric graph for the maximum height cover opening.

Where $R_{o/c}$ = Radius of cover opening and closing, D_{cover} = diameter of the cover and D_{pan} = diameter of pan.

The displacement of the cover from the pan to backward due to the displacement of equation (3.9) is calculated as:

$$\begin{aligned} R_{o/c} &= \sqrt{D_{pan}^2 + D_{cover}^2} = \sqrt{2}D \cong D \tan \varphi \\ &= D * \tan \varphi \end{aligned} \quad (3.14)$$

Since, $D_{pan} = D_{cover} = D = 420\text{mm}$

$$H_{max} = R_{cover} * \sin \theta$$

$$R_{cover} \leq H_{max} \text{ at } \theta = 90^\circ$$

$\varphi = \alpha$ = the function of time due to the opening and/or closing cover and the $\varphi_{max} = 45^\circ$.

The cover is driven by angular speed of the frame that is given by

$$\omega = \frac{2\pi N}{60} \text{ rad/sec} = 0.035 \text{ rad/sec} \quad (3.15)$$

The backward velocity at $R_{o/c}$ is given by

$$V = \frac{dR_{o/c}}{d\theta} = D \frac{d}{d\theta} \tan \theta = D \frac{d}{d\theta} \left(\frac{\sin \theta}{\cos \theta} \right)$$

Let say $f(\theta) = \sin \theta$, $g(\theta) = \cos \theta$ and $h(\theta) = f(\theta)/g(\theta)$ then the derivatives of them will be

$$v = D \frac{d}{d\theta} h(\theta) \quad (3.16)$$

$$h(\theta) = f(\theta)/g(\theta) \quad (3.17)$$

$$h'(\theta) = \frac{f'(\theta) * g(\theta) - g'(\theta)f(\theta)}{g^2(\theta)}$$

$$\begin{aligned}
&= \frac{\cos\theta * \cos\theta - (-\sin\theta) * \sin\theta}{\cos^2\theta} \\
&= \frac{\cos^2\theta + \sin^2\theta}{\cos^2\theta} \\
&= \frac{1}{\cos^2\theta} \tag{3.18}
\end{aligned}$$

Trigonometric identity for the numerator $\cos^2\theta + \sin^2\theta = 1$

Now substitute equation (3.17) into equation (3.16) gives

$$v = \frac{D\omega}{\cos^2\theta} \tag{3.19}$$

Acceleration of the backward going of cover will be zero from the edge to H_{max} which is given by

$$\begin{aligned}
a = \frac{dv}{d\theta} &= D\omega^2 \frac{d}{d\theta} \left(\frac{1}{\cos\theta} \right) = D\omega^2 \left(\frac{0 - \cos\theta \sin\theta + \cos\theta \sin\theta}{\cos^2\theta} \right) \\
a &= D\omega^2 h''(\theta) = 0 \tag{3.20}
\end{aligned}$$

3.7 Synthesis and Kinematics of *Injera* Extracting Mechanism

Kinematics is the study of motion without consideration of the force that causes the motion. In other words, the objective is to find out the transformation of the motion by identifying the input motion assumptionally [7].

During *injera* extracting, as it is shown below in Fig. 21, the edge circumfenced barrier of the conventional *mitad* does not allow to extract simply. The geometric factor of edge barrier is thought for preventing of dough pour out of the baking surface and blowing of atmospheric air to *injera*. The first challenge is not fact. The dough is poured in the hot baking surface of the pan and the heat suddenly enables the moisture contents to evaporate and the dough starts bearing gas holes (eyes) over the surface of *injera* immediately. So no dough is poured out of the *mitad* if the *mitad* is flat and heated well.

The electric flat mitad, as shown below in Fig. 22, has no edge barrier as it is stated above, factor of high temperature no dough is poured out. Therefore, the absence of edge circumferenced barrier helps to extract *injera* in linear way.



Figure 21: Conventional electric *mitad* with edge barrier

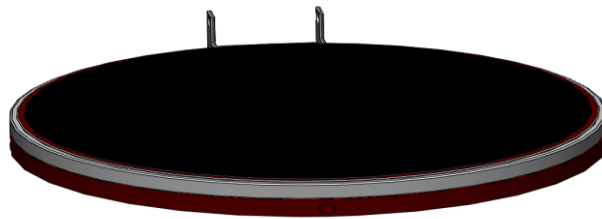


Figure 22: IBM electric flat *mitad* without edge barrier

3.7.1 Synthesis of Injera Extracting Mechanism

The *injera* extracting mechanism is the combination of very thin plate made up of stainless steel with thickness of 0.5 to 1mm and a double parallel arm both with two fingers that the upper fingers are fixed and the lower fingers are free to rotate about y-axis without friction throughout the range of 0 to π radians. The arms are attached to the scotch yoke mechanism in order to get reciprocating motion that helps repetitive task(s) within the same interval of time and distance with a constant velocity. The spring enables the finger to hold *injera* between the lower and upper finger due to the forward motion of the scotch yoke mechanism. When the pin reaches at the opposite end of the disc parallel to the slider arm at 180 degree, the lower finger moves downward and drops *injera* and finds its maximum backward motion by the help of spring's compression and stretch. The stainless steel thin plate whose the same diameter with pan is adjusted within an interval that approaches to zero and fixed at a place of the outer diameter of the pan carrier frame as shown below in Fig. 23.

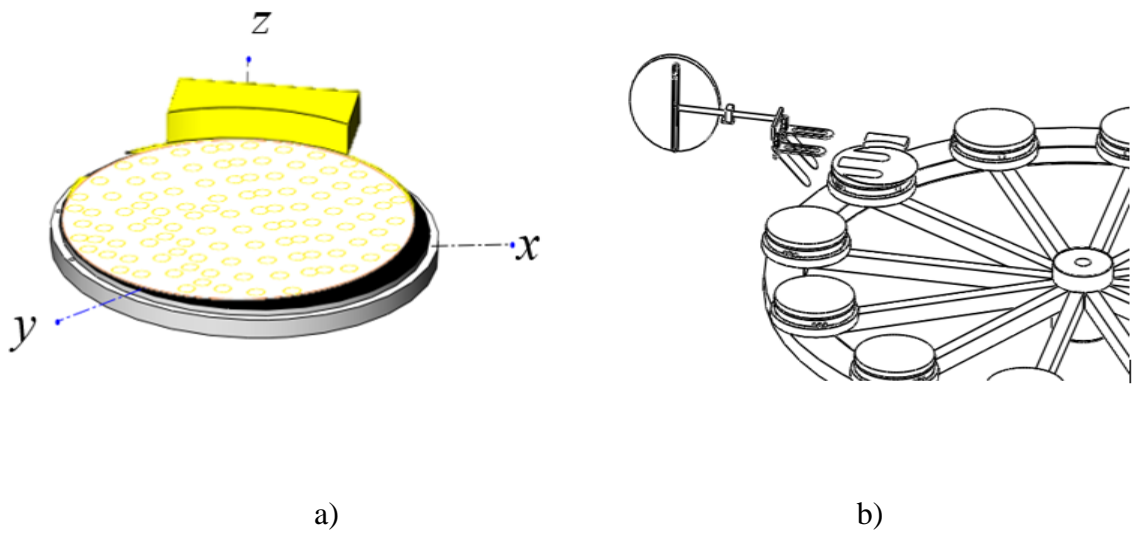


Figure 23: *Injera* extraction, a) *Injera* extracting mechanism b) *Injera* extractor disc by separating it from *mitad*, stainless steel extractor

An *injera* extracting mechanism with a sliding frame, which moves forward and backward through the fixed slider as shown below in Fig. 24.

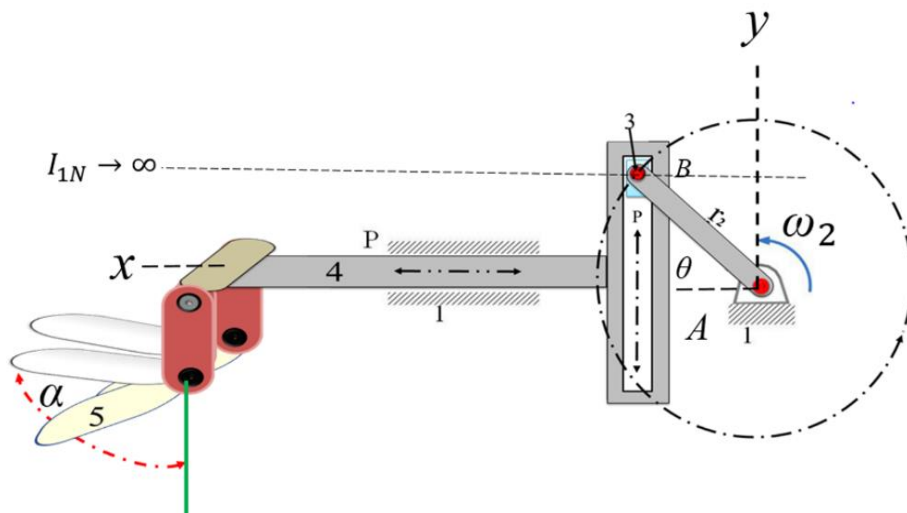


Figure 24: Scotch yoke mechanism with double end-effectors

Here below in Fig. 25, *Injera* extracting mechanism is given with the *injera* slicer up thin plate link.

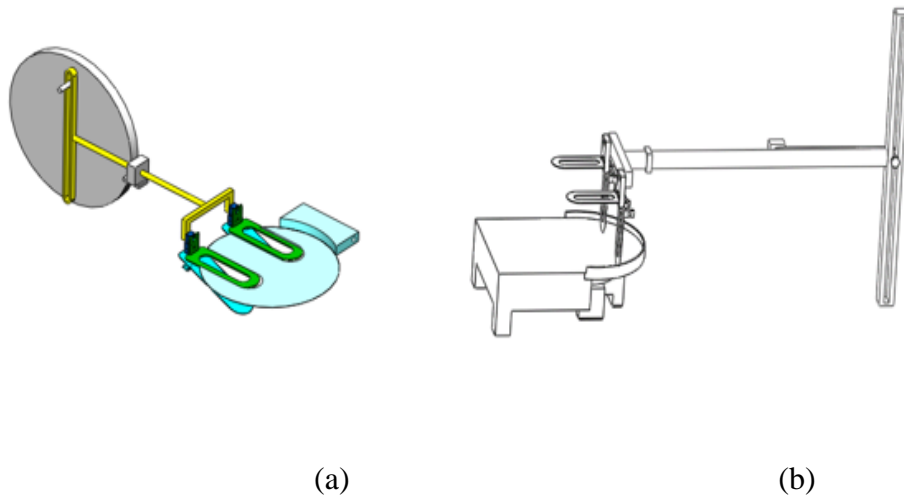


Figure 25: *Injera* extracting mechanism-gripping positions with the circular stainless steel plate: (a) Ready to grip *injera* (b) the fingers dropped *injera* from the thin plate

3.7.2 Skeletal Representation

The skeletal representation of the mechanism is shown below in Fig. 26 as:

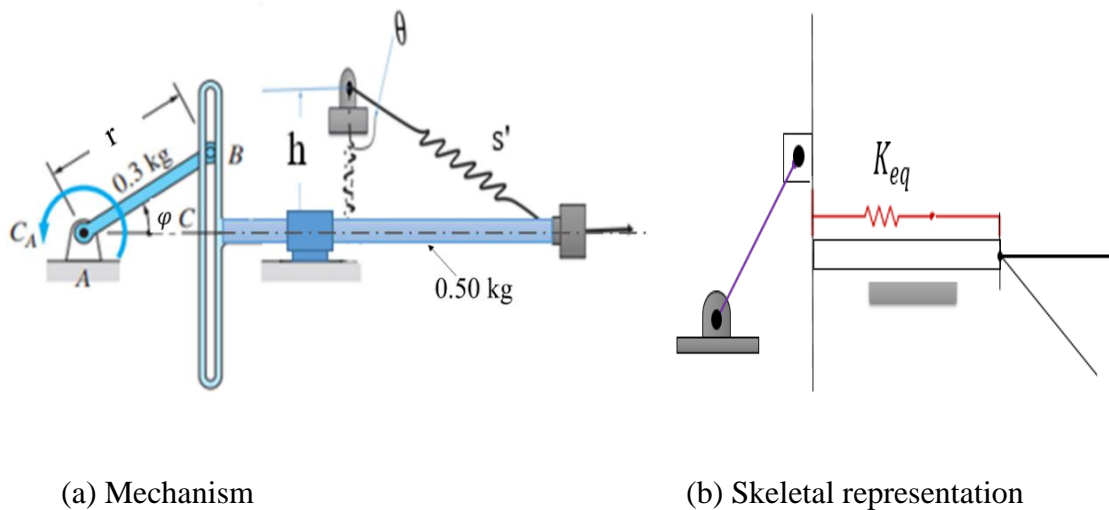


Figure 26: Skeletal representation of scotch yoke mechanism with springs for *injera* extracting mechanism

3.7.3 Mobility of the System

The number of degrees-of-freedom of a linkage is equal to the number of input motions needed to define the motions of the linkage [16]. The number of degrees of freedom (DOF) of

a mechanism to move is known as mobility. By using Kutzbach's criterion of mobility [17], the *injera* extracting mechanism has

$$m = 3(n - 1) - 2j_1 - j_2 \quad (3.21)$$

$$n = 5, j_1 = 5 \text{ and } j_2 = 0$$

$$m = 3(5 - 1) - 2 * 5 - 0 = 2$$

Where n is the number of links, j_1 is the number of low-pair joints, and j_2 is the number of high-pair joints.

3.7.4 Coordinate System

Here, in this study, the main kinematic variables and dimensions of *injera* taking out by position of scotch yoke mechanism with *injera* extractor finger is given as shown below in Fig. 27.

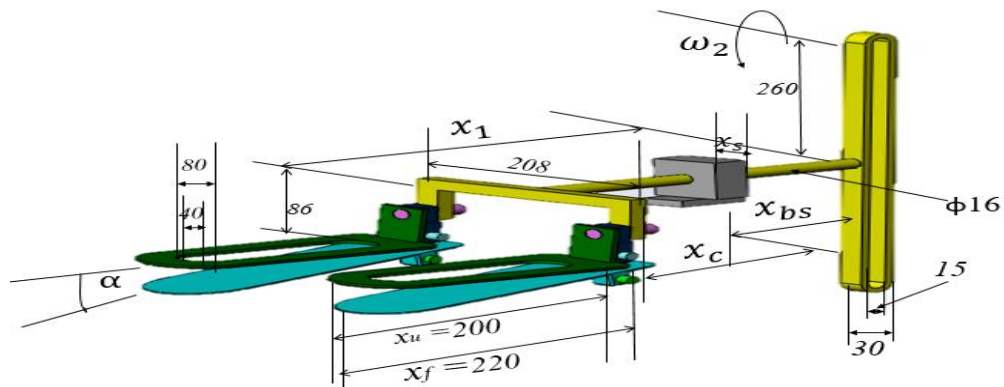


Figure 27: *Injera* extracting mechanism without disk pin as crank

3.7.5 Instantaneous Center of the Injera Extracting Mechanism

A point of a rigid body that has a zero velocity at a given instant is an instantaneous center. It can be thought as a point in the plane about which the link rotate relative to another link whose positions coincide and have the same velocities.

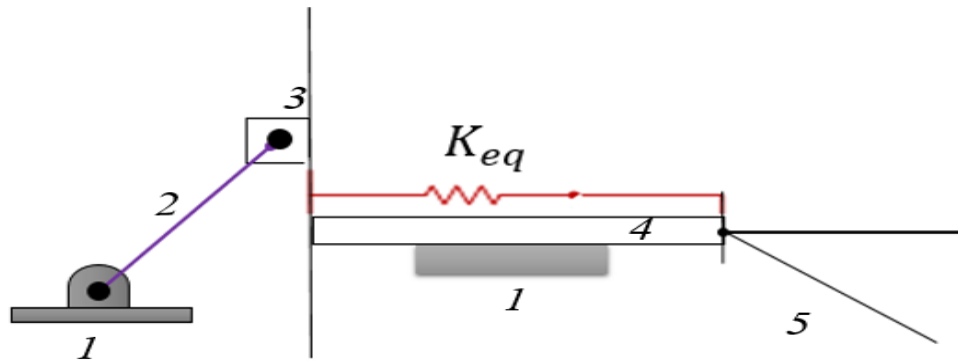


Figure 28: Skeleton of Scotch yoke mechanism

The length of *injera* extractor finger is 200 mm and the rest part of the sliding shaft is given below.

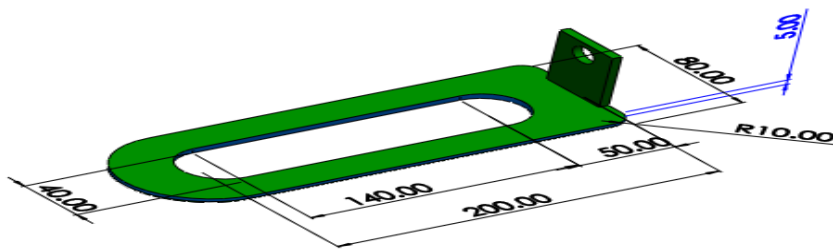


Figure 29: *Injera* extractor finger (upper finger)

There are five numbers of links and the instantaneous $I_{i,j}$ center for the system is given by

$$I_{i,j} = \frac{n(n-1)}{2} = \frac{5(5-1)}{2} = 10$$

Where n = number of links, $i = 1, 2 \dots N$, the predecessor link and $j = 2, 3 \dots N$, the successor link.

Spring is not counted in links but it is considered under kinetics and energy characteristic parameters. By using table we can get, the frequency of each number in folds of itself diagonally, or upside down hypothetical triangle. We obtain the instantaneous center, by reading two digit at a time fixed on the first figure with the down figure or number within a column. Example: $I_{1,2}, I_{1,3}, I_{1,4}, I_{1,5}$ etc. The is has no pair relative with it at the end as shown below in Table 2 with red color.

Table 2: Tabular value of IC for five links

$I_{i,j}$	Number of links				
$i \rightarrow$	i_1	i_2	i_3	i_4	i_5
$j \downarrow$	1	2	3	4	5
j_1	2	3	4	5	
j_2	3	4	5		
j_3	4	5			
j_4	5				

By using Kennedy rule, we can obtain IC as shown below in Fig. 30.

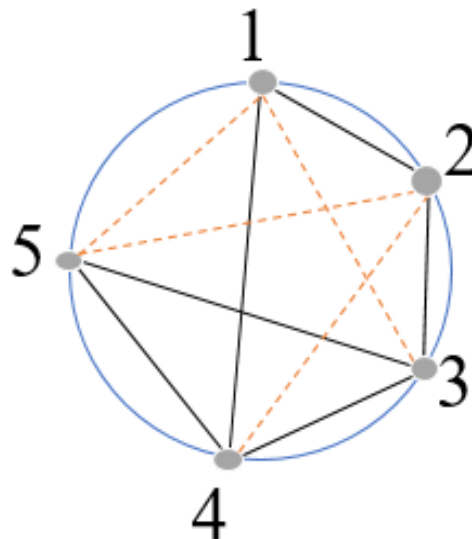


Figure 30: Instantaneous center for *injera* extracting mechanism

As it is labelled above in Fig. 30, the dash lines are the secondary ICs and the solid lines are the primary inspected ICs. They can be located on the skeletal diagram of the mechanism as follows.

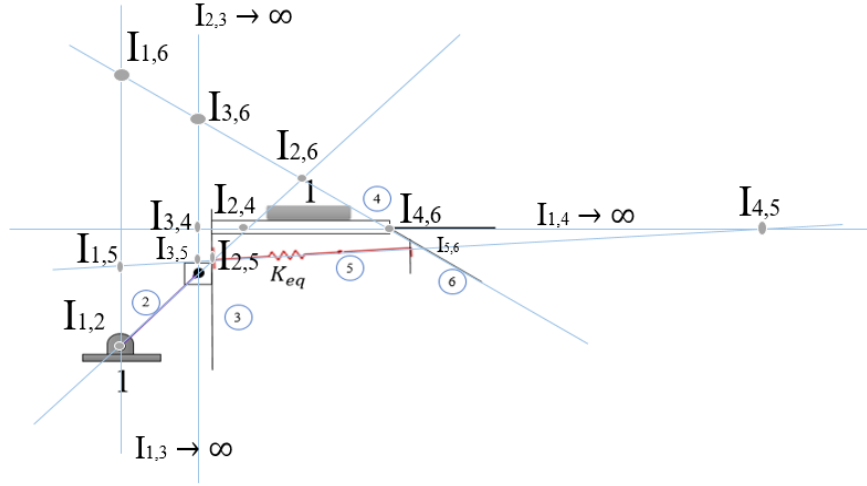


Figure 31: Location of instantaneous center for *injera* extracting mechanism

Link 2 is the crank length r_2 from the revolute A to pin B, and the position to x-axis of point P at any crank angle θ expressed analytically (refer above in Fig. 24 and 26(a)) as:

$$X^P = (x_1 + 200) + r_2 \cos \theta (t) \quad (3.22)$$

The length of x_1 equals r_4 , which is given by

$$r_4(x, \theta) = 2r_2 + x_{bs} + x_s + x_c \quad (3.23)$$

Where x_{bs} : the distance between the fixed slider slot and the scotch yoke disk, x_s : the length that covered by the slider slot fixer, x_c : the distance between the finger frame and the slider slot and assume that $x_{bs} = 20$ mm, $x_s = 60$ mm and $x_c = 50$ mm.

The length of *link 2* is found by considering the diameter of *injera*, the gap (clearance) between the mitad and *injera* dropping and length of fingers that take of *injera* from the stainless steel by entering through the U-shape hole. The diameter of the pan and the crank size, r_2 has a direct relationship with the perspective of geometric size and motion. Hence, $r_2 = x_f + x_g = 460$ mm and equation (3.23) become

$$r_4(X, \theta) = 1.2 \text{ m}$$

By differentiating the position vector, we obtain velocity of the sliding shaft as

$$\dot{x}^p = -r_2 \sin \theta(t) * \frac{d\theta(t)}{dt} = -r\omega \sin \theta(t) \quad (4.24)$$

Acceleration is given by

$$\ddot{x}^p = -r_2 \omega \cos \theta(t) * \frac{d\theta(t)}{dt} = -r\omega^2 \cos \theta(t) \quad (3.25)$$

3.7.6 Characterization of Angles with Link Positions

At *injera* dropping and taking out port the length of link four will be equal, because link 2 be at straight line; i.e., it will be at 180 degree and 360 degree. At other spans it may be given as the theta function of link 2 as it is given in equation (3.26) below:

$$r_4(x, \theta_2) \begin{cases} \leq 1.38\text{m} \text{ if } 0 \leq \theta_2 \leq \pi \\ = 1.38\text{m} \text{ if } \theta_2 = \pi \text{ (at OP port)} \\ \leq r_4(\theta_2) - r_2 \cos \theta_2 \text{ if } \pi \leq \theta_2 \leq 2\pi \\ = 1.38\text{m} \text{ if } \theta_2 = 2\pi \text{ (at injera depositing or dropping port)} \\ \leq r_4(\theta_2) \leq 1.38\text{m} \text{ if } 2\pi \leq \theta_2 \leq 3\pi \\ \text{etc.} \end{cases} \quad (3.26)$$

3.7.7 Kinematic and Dynamic Loop-Closure Equation

By taking the position vector for the offset scotch yoke mechanism without the spring and fingers link, the kinematics of the mechanism will be as shown below in Fig. 32.

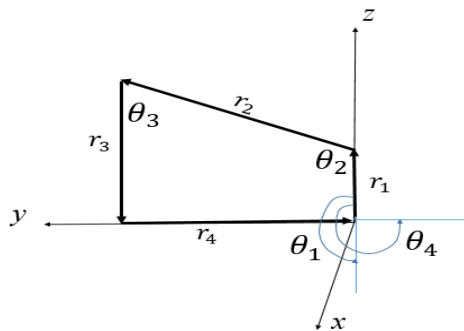


Figure 32: The corresponding vector diagram for an offset scotch yoke mechanism

By applying a loop-closure approach for a sake of universality, the position vector analysis will be given, as the sum of all links equals zero

$$\mathbf{r}_1 \mathbf{Q}_1^T + \mathbf{r}_2 \mathbf{Q}_2^T + \mathbf{R}_3 \mathbf{Q}_3^T + \mathbf{R}_4 \mathbf{Q}_4^T = \mathbf{0} \quad (3.27)$$

Where $Q_i = [\cos \theta_i \sin \theta_i]$ and $i = 1, 2, 3, 4$.

3.7.8 Identification of Input and Output Variables

Here, the length of link 1, r_1 , the length of link 2, r_2 , the velocity of link 1, v_1 , and the velocity of link 2, v_2 , the acceleration of link 1, a_1 , and the acceleration of link 3, a_3 are known input variables the length of link 3, r_3 , link 4, r_4 , velocity of link 3, v_3 , velocity of link 4, v_4 , and acceleration of link 3, a_3 and acceleration of link 4, a_4 are the unknown output variables. From the nature of the motion mechanism, we have an initial condition as $\theta_1 = \pi$, $\theta_3 = 0$ and $\theta_4 = 0.5\pi$ and for the pin and the disc have a relationship as $r_1 = 2r_2$.

3.7.9 Solve the Loop-Closure Equation

3.7.9.1 Position Analysis

To solve the closure equation, the magnitude of the two vectors are unknown and move all unknown vectors to the right-hand side and the equation will be [17]

$$r_3 Q_3^T + r_4 Q_4^T = b P_i^T \quad (3.28)$$

Where b = the sum of all known vectors

$$\mathbf{b} = (b_x \ b_y)^T = \sqrt{b_x^2 + b_y^2} > 0 = - \sum_{i=1, i \neq j}^{N=2} r_i (\cos \theta_i \ \sin \theta_i)^T \quad (3.28.1)$$

$$b_x = - \sum_{i=2}^{N=2} r_i \cos \theta_i \quad (3.28.2)$$

$$b_y = - \sum_{i=1}^{N=2} r_i \sin \theta_i \quad (3.28.3)$$

$$Q_{i,j} = (\cos \theta_{i,j} \ \sin \theta_{i,j}) \quad (3.28.4)$$

$$P_{i,j} = (\cos \alpha_i \ \sin \alpha_i) \quad (3.28.5)$$

Then by using equation (3.28.1)-(3.28.5), equation (3.28) became

$$\mathbf{r}_3(\cos \theta_3 \quad \sin \theta_3)^T + \mathbf{r}_4(\cos \theta_4 \quad \sin \theta_4)^T = b(\cos \alpha \quad \sin \alpha)^T \quad (3.29)$$

The two unknown vectors link three, r_3 and link four, r_4 are calculated by eliminating one of them by pre-multiplying from the left by unit vectors \mathbf{u}_1 and \mathbf{u}_2 that are perpendicular to the vector r_3 and r_4 respectively. Hence, from trigonometric theory

$$\cos \theta_j \sin \theta_i - \sin \theta_i \cos \theta_j = \sin(\theta_j - \theta_i) \quad (3.30)$$

And it is obvious that for any vector \mathbf{A} is perpendicular to \mathbf{B} : $\mathbf{A} \times \mathbf{B} = 0$. Accordingly, then the second vector r_4 will be found by multiplying equation (3.30) by a unit vector $\mathbf{u}_3(\theta_3) = (-\sin \theta_3 \quad \cos \theta_3)^T$ and eliminating r_3 :

$$r_4 = b \frac{\sin(\alpha - \theta_3)}{\sin(\theta_4 - \theta_3)}$$

$$\mathbf{r}_4 = r_2 \cos \theta_2 + \mathbf{x}_1 + \mathbf{x}_f \quad (4.31)$$

Similarly, by using $\mathbf{u}_3(\theta_4) = (-\sin \theta_4 \quad \cos \theta_4)^T$, equation (3.29) become

$$r_3 = b \frac{\sin(\alpha - \theta_4)}{\sin(\theta_3 - \theta_4)} \quad (3.32)$$

By using Mathcad software, we get for r_3 as

$$\mathbf{r}_3(\theta) = \mathbf{r}_1 - \mathbf{r}_2 \sin(\theta_2) \quad (3.33)$$

3.7.9.2 Velocity Analysis

For any vector the magnitude and the direction of the systems which are the functions of time, t , the position vector is given by

$$\vec{\mathbf{r}}(t) = \mathbf{r}(t) \mathbf{Q}^T \quad (3.34)$$

Where \mathbf{Q} is the trigonometric function $[\cos \theta, \sin \theta]$

The time derivative of the position vector represents the velocity vector:

$$\vec{v}(t) = \frac{d\vec{r}(t)}{dt} = \dot{\vec{r}}(t) = \dot{r}(t)\mathbf{Q}^T + r(t)\dot{\mathbf{Q}}^T\dot{\theta}(t) = \mathbf{0}$$

$$\vec{v}(t) = \mathbf{v}_t + \mathbf{v}_r = \mathbf{0} \quad (3.35)$$

$$\mathbf{v}_t = \dot{r}(t)[\cos \theta \sin \theta]^T - \text{Transitional velocity vector}$$

$$\mathbf{v}_r = r(t)\dot{\theta}(t)[- \sin \theta \cos \theta]^T - \text{Rotational velocity vector}$$

\mathbf{v}_r – Is perpendicular to the direction of the original vector and the magnitude of \mathbf{v}_t represents the rate change of the position vector length r .

In this case the magnitude of r_3 and r_4 were the unknown variables and the corresponding velocity $r_3(t)$ and $r_4(t)$ will be:

$$\dot{r}_3(t)[\cos \theta_3 \sin \theta_3]^T + r_3(t)\dot{\theta}_3(t)[- \sin \theta_3 \cos \theta_3]^T + r_4(t)\dot{\theta}_4(t) - \dot{b}_x \sin \theta_4 - \dot{b}_y \cos \theta_4 = 0 \quad (3.36)$$

By using initial condition IC, $\theta_1 = \pi$, $\theta_3 = 0$, $\theta_4 = \frac{\pi}{2}$, and from equation (3.40.2) and (3.40.3), we have $\dot{b}_x = r_1 - r_2 \cos \theta_2(t)$ and $\dot{b}_y = -r_2 \sin \theta_2(t)$. From these IC, we have:

$$\dot{b}_x = r_2 \omega_2(t) \sin \theta_2(t) \quad (3.37.1)$$

$$\dot{b}_y = -r_2 \omega_2(t) \cos \theta_2(t) \quad (3.37.2)$$

Then by using equations (3.37.1) and (3.37.2) and the perpendicular unit vector multiplication for $\dot{r}_3(t)$ and $\dot{r}_4(t)$ respectively, we get equation (3.38) and (3.39).

$$v_3(t) = \dot{r}_3(t) = \dot{b}_x = r_2 \omega_2(t) \sin \theta_2(t) \quad (3.38)$$

In similar way, we obtain

$$v_4(t) = \dot{r}_4(t) = \dot{b}_y = -r_2 \omega_2(t) \cos \theta_2(t) \quad (3.39)$$

3.7.9.3 Acceleration Analysis

Simply, the derivative of, equation (3.38), the velocity vector with respect to time gives acceleration vector, consider $r_2 = \text{constant}$, $\dot{\theta}_2 = \text{constant}$. then

$$a_3(t) = \frac{d}{dt} \dot{r}_3(t) = \ddot{b}_x = r_2 \omega_2^2(t) \cos \theta_2(t) - r_2 \alpha_2(t) \sin \theta_2(t)$$

In the same way, from equation (3.39), we get (3.40)

$$a_4(t) = \frac{d}{dt} \dot{r}_4(t) = \ddot{b}_y = -r_2 \omega_2^2(t) \sin \theta_2(t) - r_2 \alpha_2(t) \cos \theta_2(t) \quad (3.41)$$

The velocity and acceleration vectors of the two sliders' graph is given below in Fig. 33 by Mathcad from Appendix V.

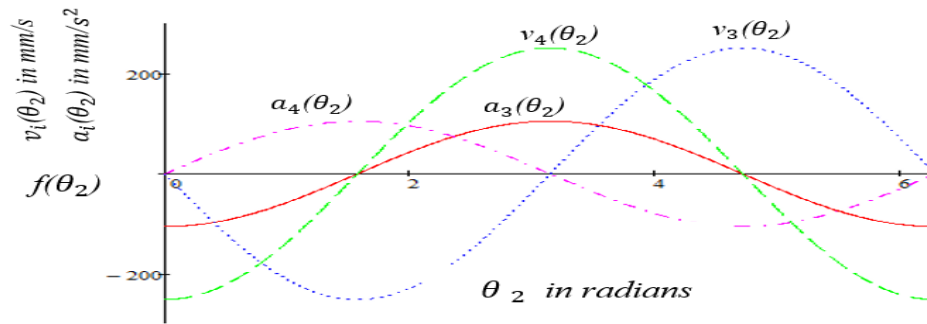


Figure 33: Velocity and acceleration analysis of *injera* extracting mechanism

3.8 Working Principles of *Injera* Extracting Mechanism

The working principle of *injera* extracting mechanism is discussed early under the topic 3.4, entitled as “*Semi-Automated Rotary Injera Baking Machine*” (refer it on page 14 above). As it is shown below in Fig. 34, when the radius of link 2 has been at 360 degrees, the double pair fingers will be opened at 90 degree. This enables to drop *injera* at the temporary *injera* storing position bin. And when the connecting rod will be at 180 degree, the double pair fingers will be closed at *injera* separator blade stationary and capable to grasp *injera* and displace it to the wanted place. During this time, the *injera* delivered *mitad* will be at 345 degree clockwise at polishing position relative to the dough pouring station. Before the extractor fingers arrived to the *injera* taking out place, the stainless thin blade whose thickness of 0.5 mm and diameter of 40 mm separates *injera* from the *mitad*. The *mitad* passes beneath the separator blade and the

separator is fixed at a place. The separator has two holes in the patent of the two double fingers. And the extractor take *injera* from the separator through this two holes by the upward movement of the lower fingers.

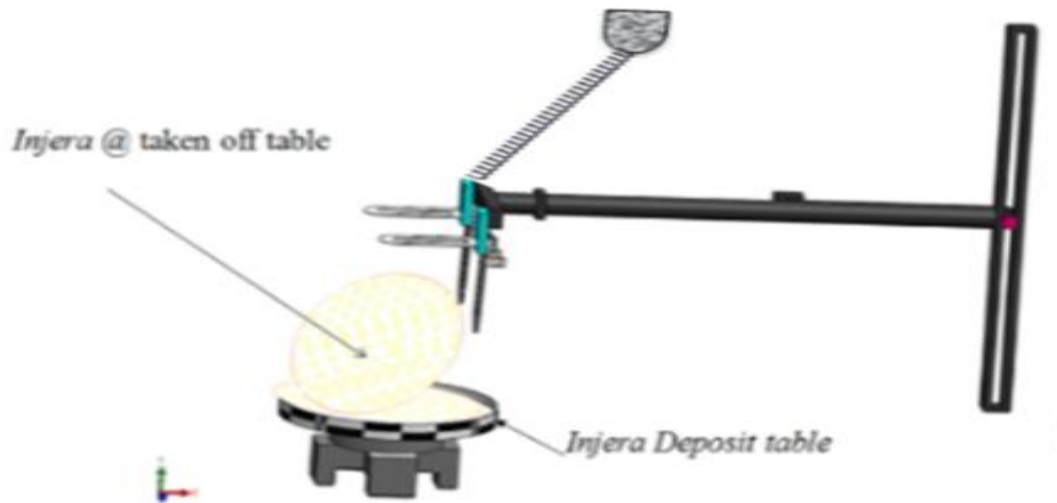


Figure 34: *Injera* extracting mechanism

The scotch yoke driven crank is fixed to the ground and the yoke link joined to the crank by slot joint. The slider link or link 4 is fixed to the scotch yoke link by fixed joint or welding and is joined by translational joint through the slider fixer link. The slider fixer joint makes the *injera* extracting stable and linear movable link.

The simulation is done by dividing the rotating angle size to the required time for each activities in the injera baking and extracting mechanism. The simulation is time dependent events and the rotational angles and translational displacements are kept with their time sequence corresponding to each other.

3.9 Methods to Simulate

The 3D software model is modeled in SOLIDWORK 2018 version and saved in IGS format and imported to ANSYS V.19.2. Dynamic simulation, unlike static analysis and simulation, implies that the model is analyzed or simulated by time representation. A dynamic model is a type of mathematical model that constitutes a numerical or analytical model of the system, is which solved, by the system simulation.

In the level of machine, “*kinetics*” of the completely dynamic system is studied while in the level of mechanisms, the “*kinematics*” of the dynamic system-mechanism is studied.

Accordingly, as this study focused on *injera* extracting mechanism, the results and analysis depend on the kinematics of the system as a level of mechanism. During synthesizes of mechanism, its configuration will be designed by either geometrical or mathematical model. Mostly, the geometric model can be represented by physical model, 3D CAD software, or prototypes, depends on the geometric parameters. While, mathematical dynamic model is the replica of geometrical model by numerical models and analytical models. Analytical model is solved by using deductive logic or mathematic theory. On other hand, computational techniques, procedures and system simulations solve numerical model.

The numerical and graphical analysis of the system is done in Mathcad software. Mathcad software is used to design and mathematical model with keeping every input and output assigned variables with accuracy of the given values until the model is finished. Once you assigned the variable, unless you change and duplicate it, Mathcad software carries the variable all through your document including the SI-unit you given for. In addition, this study used Mathcad software for numerical and graphical plotting.

The simulation is done in rigid body dynamics (RBD) of ANSYS in order to get the kinematic behaviors of the displacement, velocity, and acceleration of *injera* baking machine and its extracting mechanism. The importance of simulation results is for keeping the relative motion of the time dependent sequenced operations of *injera* baking machine. Here, a semi-automated *injera* baking machine (SIBM) is used as a moving reference body and *injera*-extracting mechanism (IEM) is focused. The kinematic responses of *injera* extracting mechanism used time and rotation as an input parameter as a boundary condition the rotation about *z*-axis, $\varphi(t) = 0$ degree at time, $t = 0$ sec and the same initial condition for *injera* baking machine. But in extracting mechanism, the time referring with *injera* baking machine is after the *injera* contained *mitad* is arrived, the extractor reaches to the extractor port immediately. The *mitad* carrier system's frame rotation and *injera* extractor mechanism have to have sequential relationship by time function. Hence, after the first *mitad* leaves the *injera* taking off port, the *injera* taking out fingers have to be reached suddenly the *injera* taking off port and takes out the *injera*. Hence, if the time, $t_{i,j}$ is taken by the *mitad* after one from the next *mitad*, and t_e is the time is taken by *injera* extractor, then

$$f(t) \leq f(t+\Delta t) \leq \tau/2 \rightarrow t_e \leq \frac{t_i+t_j}{4} \leq 7.5 \text{ seconds} \quad (3.42)$$

Where, $f(t)$ is duration of time for extraction at t_e , $f(t+\Delta t)$ is time taken by one fourth of the first and the follower *mitad*, τ is time taken by the leading *mitad*, t_i is time taken by the leading and t_j is time taken by the follower *mitad* on the circular *mitad* carrier frame at motion with a uniform angular velocity.

The above equation (3.42) shows that the angular speed of the *injera* extracting mechanism-driving disc has double fold speed of the pan carrier frames.

The time sequential order of the motion function of the pan carrier circular frame rotates [*in second*] is given as:

$$T_m = f(\theta_1) = \frac{0.5 \cdot \theta_1}{1^\circ} \quad (3.43)$$

The theta function of the motion of *injera* extracting mechanism is given by:

$$T_{ext} = f(\theta_2) = \frac{1}{24^\circ} \theta_2 = \frac{360 (\theta_1 - 360^\circ)}{24 \cdot 30^\circ} = \frac{1}{2} (\theta_1 - 360^\circ), \theta_1 \geq 360^\circ \quad (3.44)$$

The theta function of the motion of *mitad* polishing mechanism is given by:

$$T_{polishing} = f(\theta_3) = \frac{4.7111}{360^\circ} \theta_3 \quad (3.45)$$

It is understood from the above equations that the *injera* extracting mechanism takes a full revolution for each 30 degree of the circular rotating frame of the *mitad* carrier as it's shown below in Fig. 35.

For each $\theta_1 - 15^\circ$, there is a polishing of *mitad* at the fixed polishing port, for $\theta_1 \geq 30^\circ$.

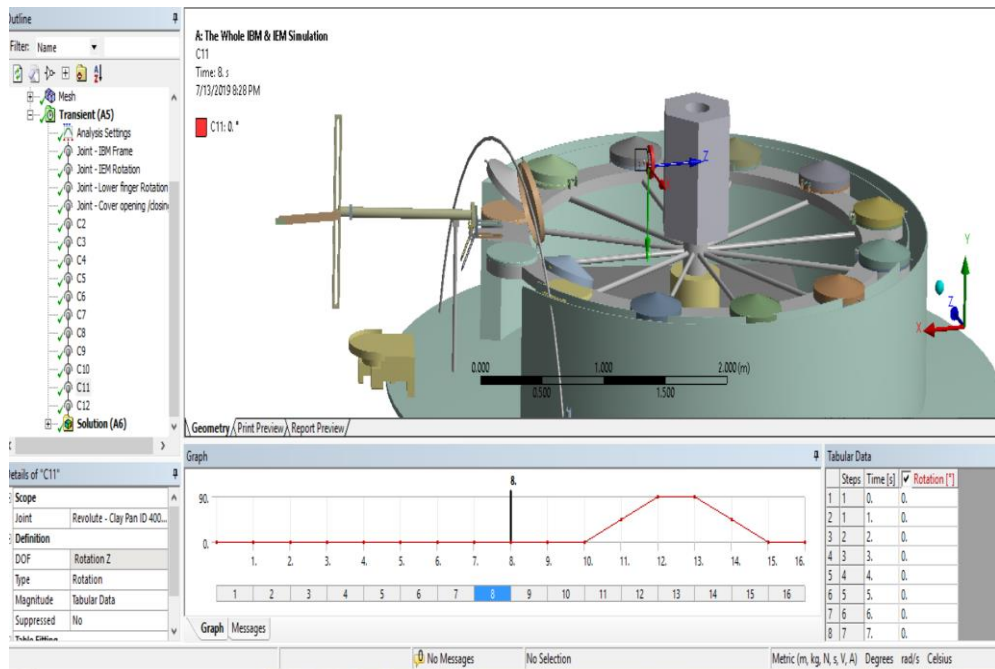


Figure 35: Dynamic Simulation Setting of a Semi-automated IBM in ANSYS
 19.2 Rigid Body Dynamics Model (A4) > Transient (A5) > Kinematic Responses (A6)
 with Input Parameter

Therefore, it takes a half time of a consecutive *mitads*' motion in series within 15 seconds.

As it is dealt under the scope, the scope of this study is the mathematical modeling and simulation of *injera* extracting mechanism, the kinematic graphical responses of *injera* extracting mechanism is represented here. However, the kinematic simulation of a semi-automated *injera* baking machine (IBM) is represented at the last of the document on Appendix IV. This is done by setting the global coordinate system at the motor of *injera* extracting mechanism position and except the extracting mechanism, suppress another systems until the simulation is done.

Identifying the number and types of joints have a vital role in the simulation process. The degree of freedom, DOF is subjected on the types of joints that the links are joined together body to body or body to ground in order to provide the possibility of number of movability. A joint element is typically defined by specifying two neighboring nodes, I and J. These nodes may be arbitrarily positioned in space as it is shown in Fig. 36 below.

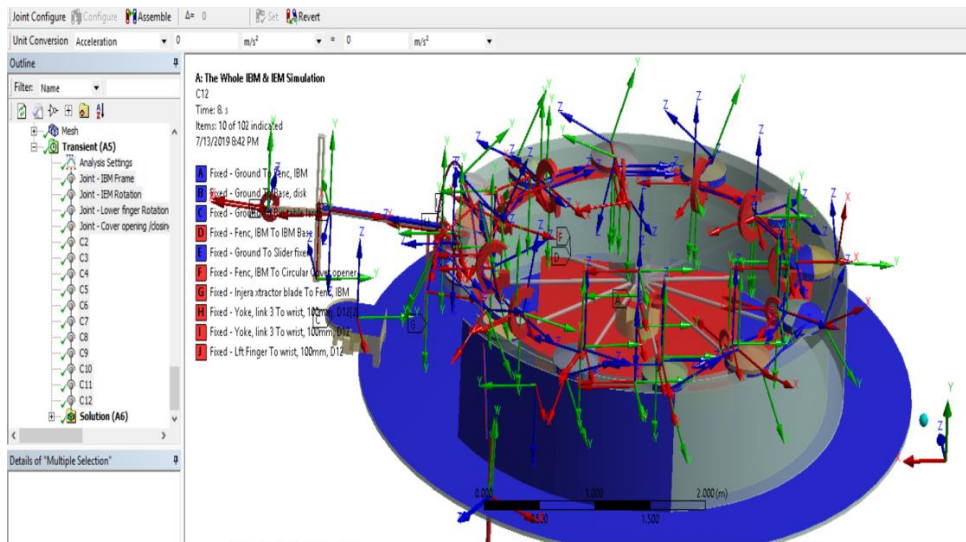
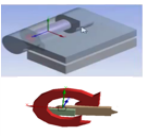
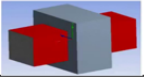
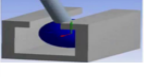
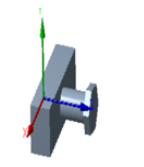


Figure 36: Identifying the number and types of kinematic joints or constraints

In general, according to the IBM and IEM system there are rotational, translational and slot joints are found in the whole system. But in the *injera* extracting mechanism the joints are given in the table below. In the simulation process of *injera* baking and extracting system, the kinematic analysis is achieved by demonstrating the size of rotation or translation and types of joints corresponding to the time sequence of each activities as it is shown in Table 3.

Table 3: Types of joints or constraints in *injera* extracting mechanism

	Types	Symbol	Location	Mobility (DOF)	Angle (deg)
1	Revolute		Link 2 to ground	1	360
			Link 5, lower finger to upper finger	1	0 to 90
2	Prismatic/translational joint		Link 4, in the fixed slider	1	180
3	Slot joint		Link 3, in the scotch yoke	1	90
4	Pin/Fixed Joint		Upper fingers to link 4, link 4 to scotch yoke, base to ground, slider fixer to ground etc.	0	0

Note: The above symbol of joints are taken from ANSYS software package except the last one is taken from the *injera* extracting system.

After the responses are found, one can set the system together by unsuspressing the suppressed systems and adjusting the dynamic initial conditions of the system.

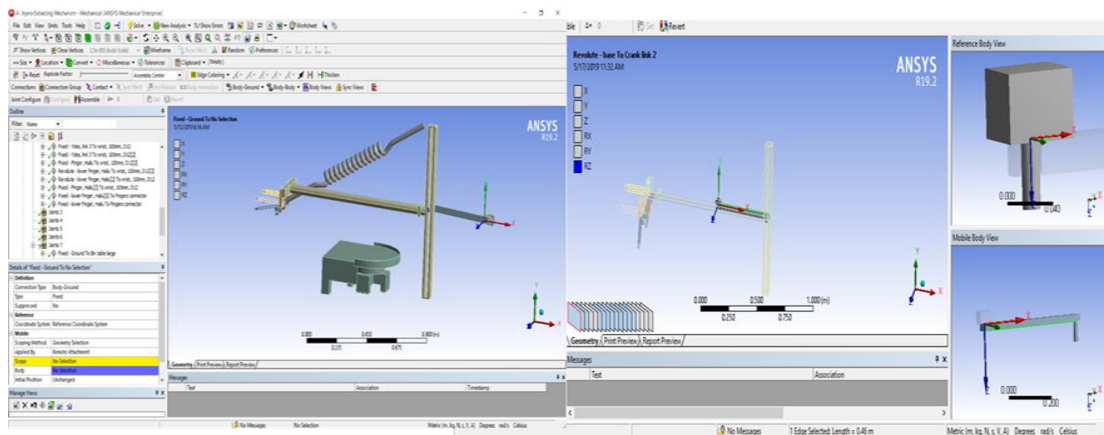


Figure 37: Adjusting the Systems

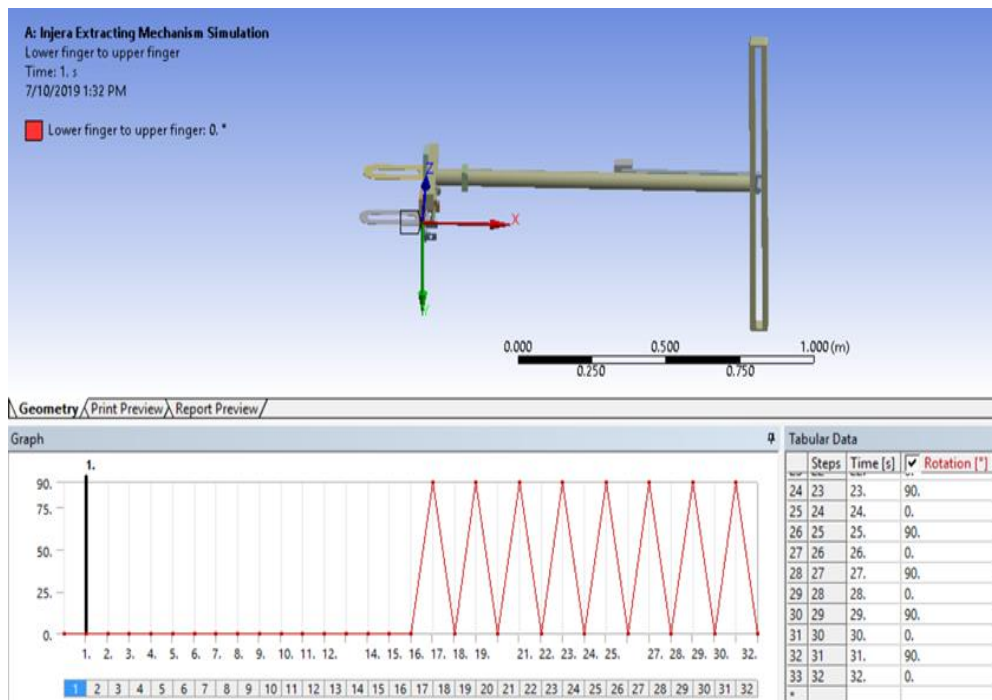


Figure 38: Global coordinates by right selection of the faces of bodies

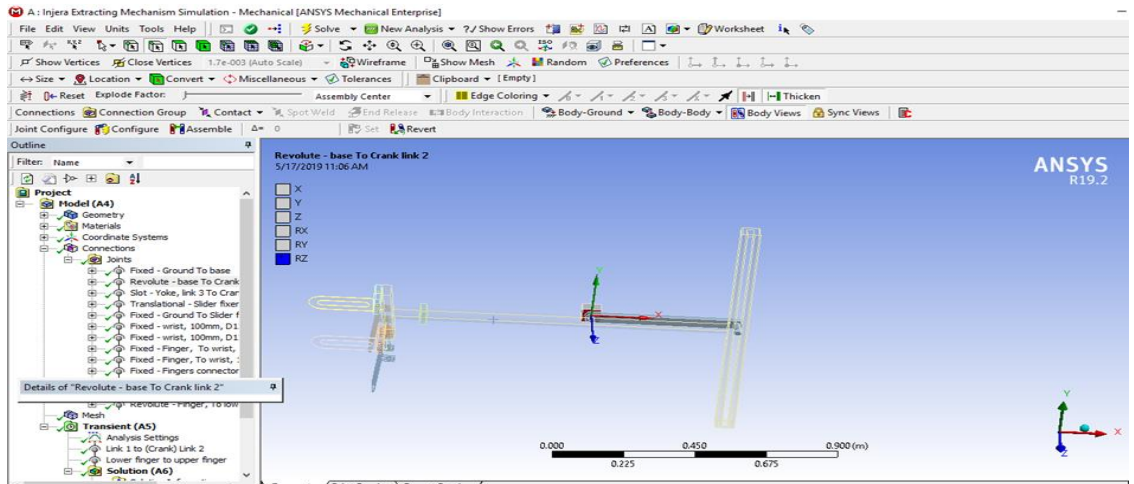


Figure 39: Setting dynamic constraints, their directions and input parameters

Finally, run the analysis of the system in order to obtain the kinematic responses of the system. And by observation of the dynamic behaviors of the system, the responses can be validated as it is shown below in Fig. 40.

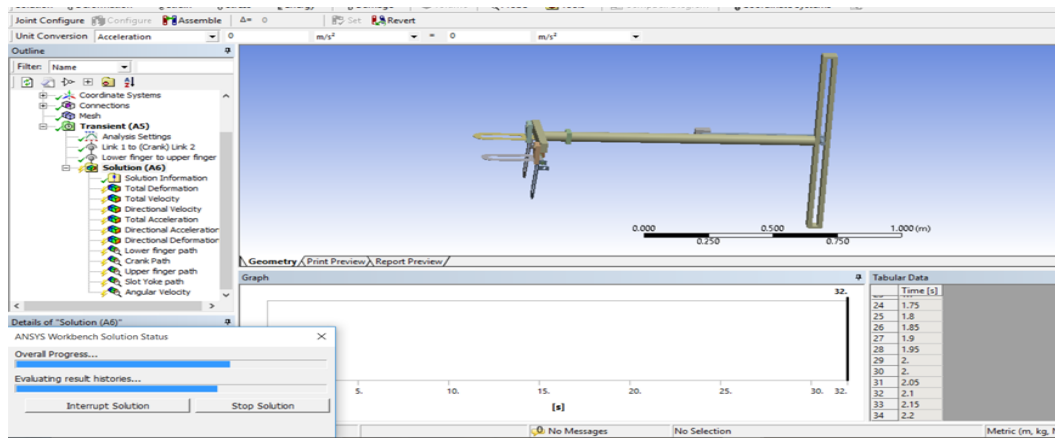


Figure 40: Running the kinematic simulation of the mechanism

The simulation will be explained under the result and discussion part, and the whole IBM is given below in Fig. 41.

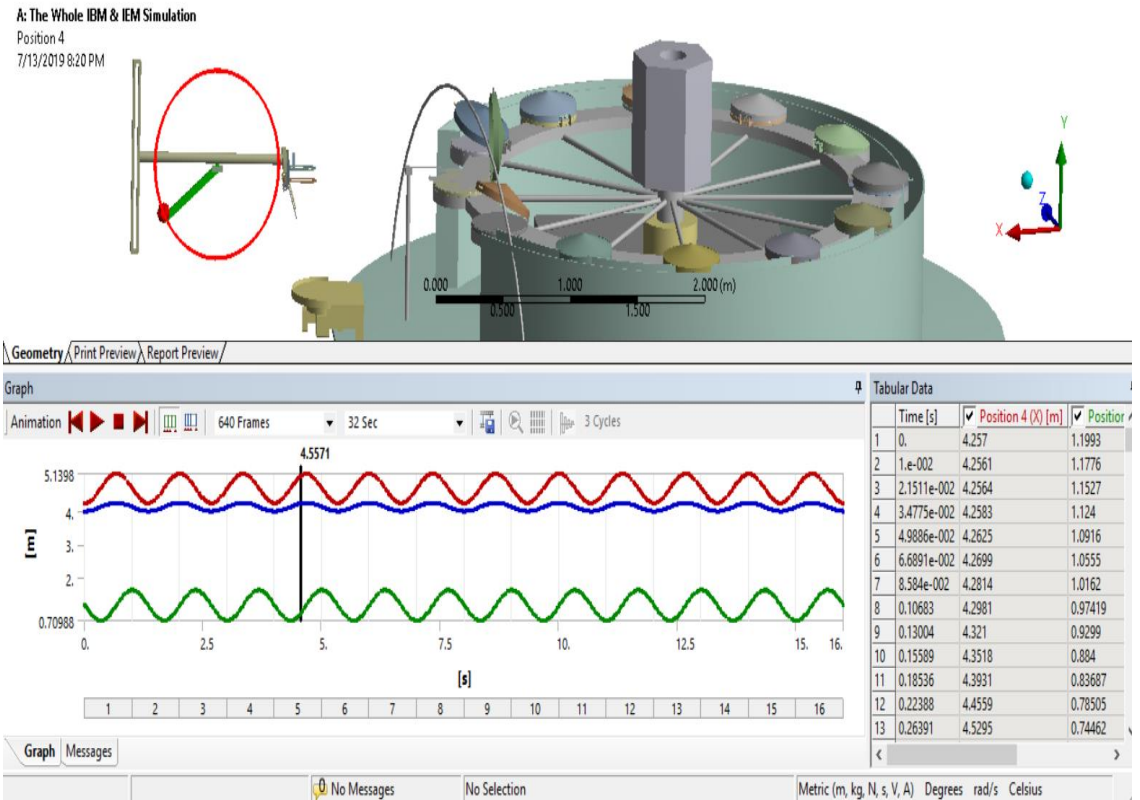


Figure 41: Kinematic simulation or responses of the system

CHAPTER IV

RESULTS AND DISCUSSION

4.1 Kinematic Simulation of *Injera* Extracting

As it was stated under procedures to simulate, to determine the dynamic response, a multi-body dynamic simulation using ANSYS software is performed by using a rigid dynamics FE code ANSYS R19.2 Workbench is selected as a multi-body kinematic calculation platform. For the kinematic simulation of *injera* extracting mechanism, the joint load rotation is selected based on the duration of *injera* baking time and the three basic activities in *injera* baking process; i.e., pan polishing, dough pouring and *injera* extracting. In addition to these activities, the cover opening and closing is considered with joint load rotation within the corresponding sequence of time related to the above activities. Depending on the duration of *injera* baking time, the translational displacement and rotational position are calculated at the appropriate joint loading order to simulate the required motion types.

The baking time of *injera* may be varied according to the performance of *mitad* and amount of electric power. And this needs a selection and control regulation of *mitad*'s performance and *injera* baking machine speed controller. Due to these factors, the speed of *injera* extracting mechanism will be changed corresponding to the changed values of *injera* baking machine and the performance of *mitads*. However, in this study, the simulation is done by considering the baking time, $t = 3 \text{ minutes}$ including the polishing and dough pouring time at $180 \text{ to } 220^\circ\text{C}$. Hence, this time is the full rotation of *injera* baking machine. Actually, the baking time is $t = 2.75 \text{ minutes}$ as the standard deviation time of *injera* baking on the electrical power consumption *mitads* when the cover opens.

4.1.1 Position Simulation of *Injera* Extracting Mechanism

At the beginning, until the first round of the first *mitad*'s *injera* is baked and separated from the *mitad* by the thin stainless *injera* separator blade, the extracting mechanism will be at rest, the rotation angle of the crank or link 2, $\theta_2 = 0$, while at this time, the rotary *injera* baking machine rotates with $\varphi_b = 330$ degree. As the first *mitad* is arrived at $\varphi_b = 330$ degree, the *injera* extracting mechanism will be rotated and arrived to the *injera* extracting port with ω_2 angular velocity. The position analysis of *injera* extracting mechanism is done using by recall equation (3.29) and considering the relative velocity of the mechanism.

$$r_3(\cos \theta_3 \quad \sin \theta_3)^T + r_4(\cos \theta_4 \quad \sin \theta_4)^T + r_5(\cos \theta_5 \quad \sin \theta_5)^T = b(\cos \alpha \quad \sin \alpha)^T$$

The angular velocity of link 2 can be obtained by considering the rpm of *injera* baking machine. According to the reviewed data [13], the standard deviation of *injera* baking time is 2.75 minutes and for the non-baking zone time or time taken by pan polishing $\tau = t + \Delta t = 3$ minutes. According to this data, the rpm of *injera* baking machine and mechanism is obtained as follows in PTC Mathcad Prime 3.0 refer in Appendix V:

Given

$$t := 2.75 \text{ min}$$

$$\Delta t := 15 \text{ sec}$$

The total required time, τ to bake injera including the pan polishing time is calculated as:

$$\tau := t + \Delta t = 180 \text{ s}$$

To build the rotatable injera baking machine, it required the time of injera baking including its pan polishing time which is calculated $\tau := 3 \text{ min}$. This does meant, the rotation needs 3 minutes. Mathematically,

$$N(\text{rpm}) = \frac{1 \text{ rev}}{\text{Period}}$$

$$N := \frac{2 \pi}{3 \text{ min}} = 0.333 \frac{\text{rev}}{\text{min}}$$

$$N = 0.333 \text{ rpm}$$

Depending on the given time, the frequency, f of the rotation of IBM is given by $f := \frac{1}{\tau}$

and it also is possible to find the angular velocity of IBM.

$$\omega := 2 \pi \cdot f = 0.035 \frac{\text{rad}}{\text{s}}$$

$$\omega = 2 \frac{\text{deg}}{\text{sec}}$$

Finally, the rotary injera baking machine has 12 sets of mitads and they need 12 times of injera extracting device per one rotation of injera baking machine. Mathematically, the rpm of IEM, N_{ex} , is calculated as:

$$N_{ex} := \frac{12 \text{ rev}}{\tau} = 4 \text{ rpm}$$

Angular velocity of injera extracting mechanism

$$\omega_{ex} := \frac{12 \text{ rev}}{180 \text{ sec}} = 0.419 \frac{\text{rad}}{\text{s}} \quad \omega_{ex} = 24 \frac{\text{deg}}{\text{s}}$$

Here below in Fig. 42, at the initial position of IEM at link 2 at $\theta_2 = 0^\circ$, IEM is at rest; no motion is recorded. But as the baked *injera* contained *mitad* passes the extracting port, the extracting mechanism is arrived to the extracting port within 7.5 seconds and link 2 will be at $\theta_2 = 180^\circ$ immediately. The real one cycle baking round of IBM machine is performed by IEM as shown below in Fig. 43 in PTC Creo Mathcad Prime 3.0, refer Appendix V.

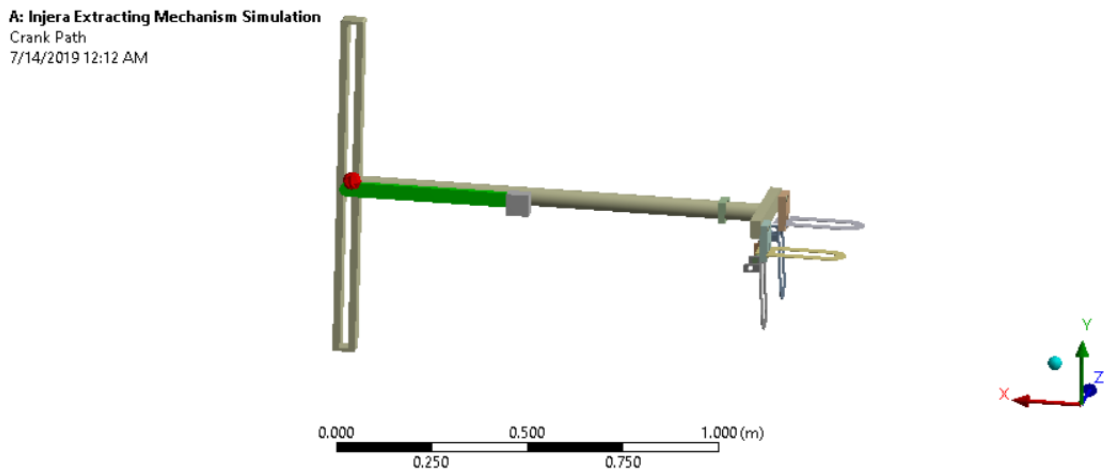


Figure 42: Initial position of IEM

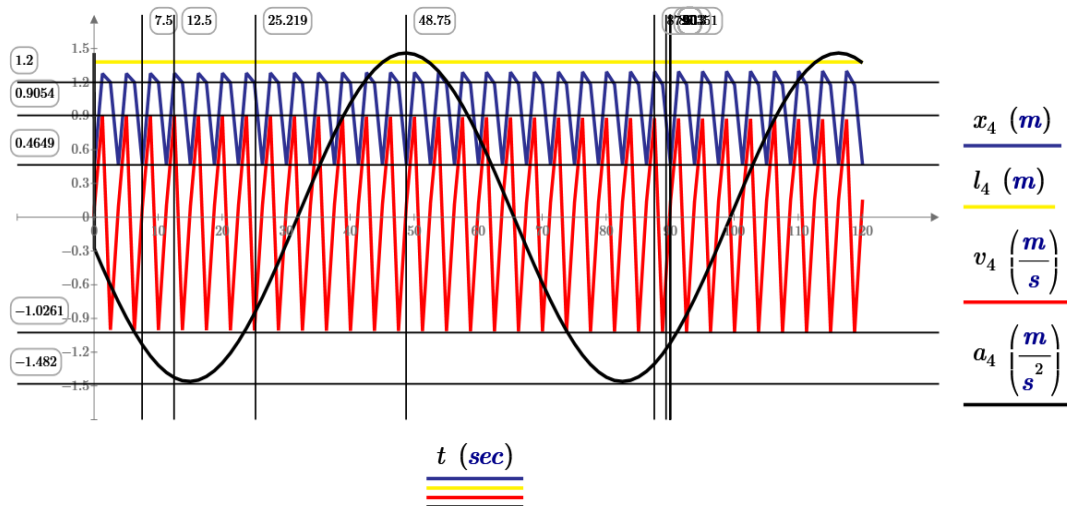


Figure 43: Kinematic analysis of IEM by PTC (Creo V.6.0.0.0) Mathcad Prime 3.0

The above graph in Fig. 43 is the position analysis of *injera* extracting mechanism for $t = 120$ seconds by PTC Mathcad Prime 3.0 and the position analysis is given in Fig. 44 below for $t = 16$ seconds in ANSYS.

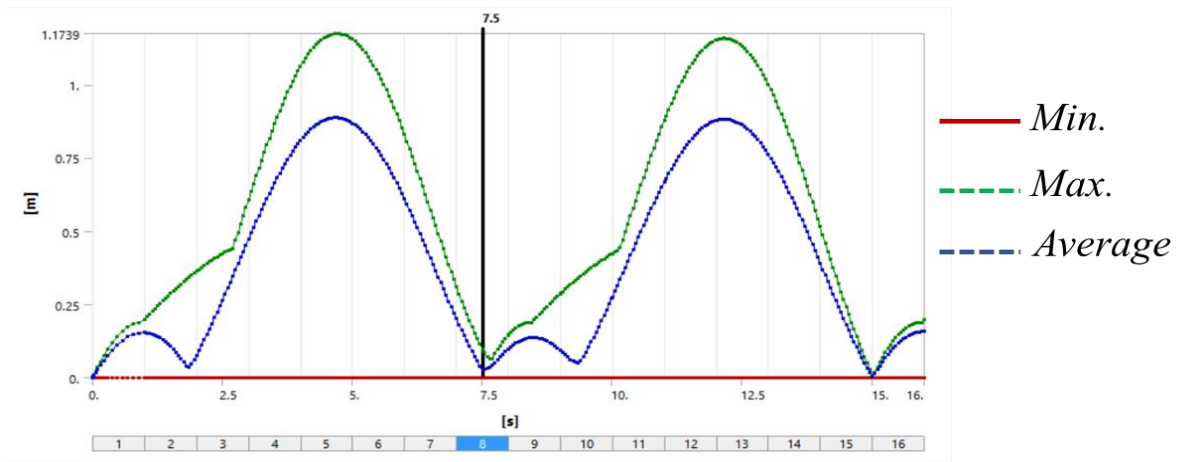


Figure 44: Total displacement vs time simulation of IEM graph by ANSYS MBD
V19.2

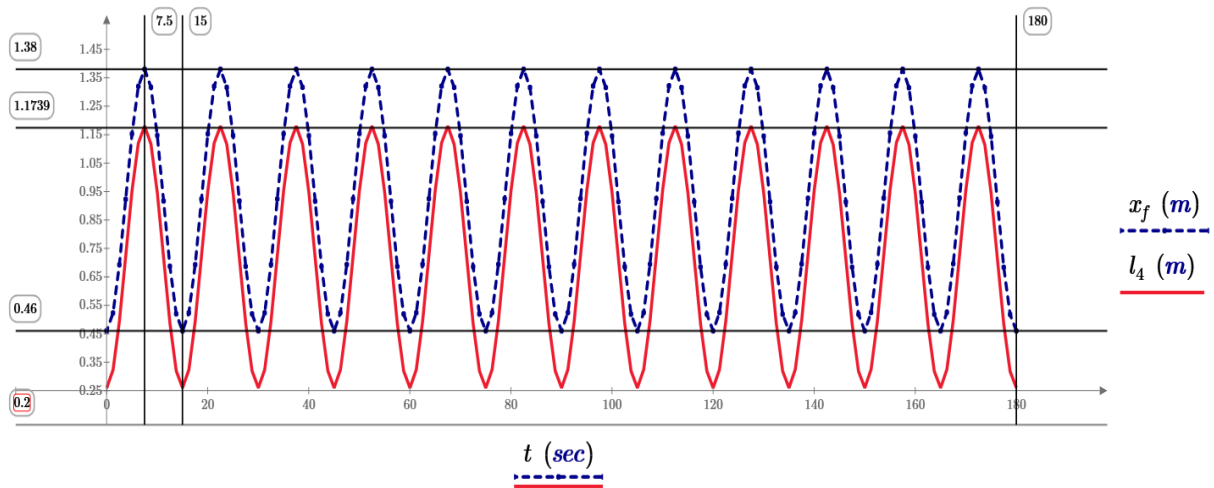


Figure 45: Displacement vs time graph of *injera* extracting mechanism by PTC
Mathcad Prime 3.0

The position analysis of crank or link 2 is shown below in Fig. 46 given as

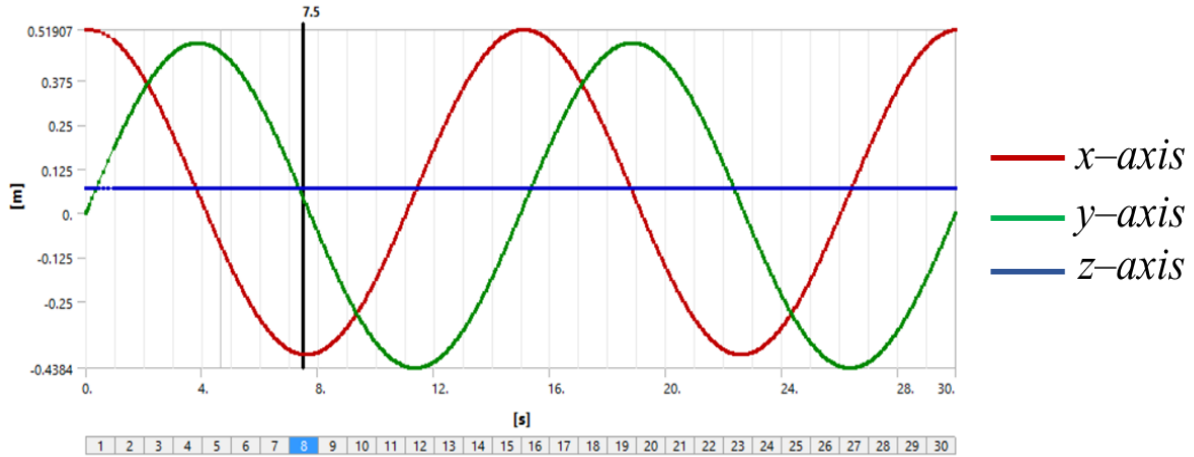


Figure 46: Position analysis of link 2 by ANSYS MBD V19.2

The equation of motion for the above graph is given in Appendix V; by recalling from PTC Mathcad Prime 3.0 equation (49) and (57) for description look Appendix V.

$$X_F = x_1 + r_2 \cdot (1 - \cos(\theta_2))$$

Recall equation (49, 57)

$$y(\theta) = 2 h = 2 r_2 \cdot (1 - \sin(\theta_2))$$

In this study, we need at what angle *injera* will be extracted from the *mitad* and dropped in its storage bin. Hence, as shown above in Fig. 46 by red color, the maximum values was obtained at $\theta_2 = 180^\circ$ and the minimum values was obtained at $\theta_2 = 360^\circ$. The corresponding time is $t = 7.5$ seconds and $t = 12.25$ seconds. However, in the graph above in Fig. 46, it is observed at 7.5 sec the value is minimum. Let us demonstrate it by using the magnitude of position along x-axis as shown below in Fig. 47, then we obtain the following graph which makes the above claim true. The value is the same in PTC Mathcad Prime 3.0 as shown above in Fig. 45 by blue color. Here below in Fig. 48, the graph illustrates that IEM grips *injera* at $t = 7.5\beta$ seconds and $\theta_2 = \mu\pi$ degrees. Where, $\beta = 2 \cdot N$, $N =$ natural number which indicates the number of strokes to grip *injera* and $\mu = \frac{N}{2}$ Rev, $N =$ natural number which

indicates the number of revolution; and Rev = number of revolution.

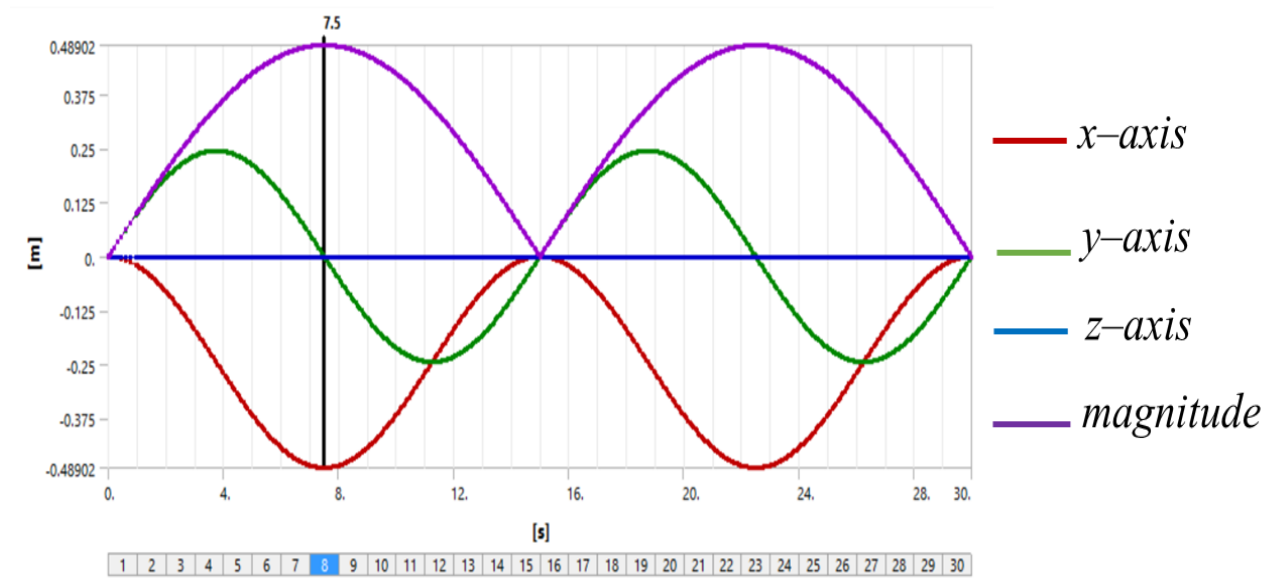


Figure 47: Magnitude position analysis of link 2 by ANSYS 19.2

The above graphs shows the following closed loop path of link 2 as shown in Fig. 48 below by red color.

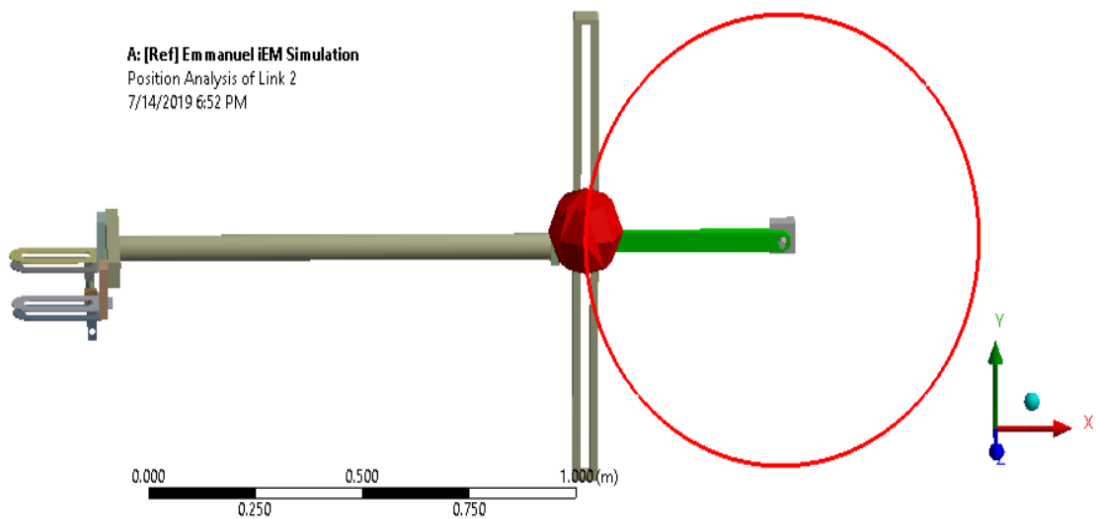


Figure 48: 3D position analysis path of link 2 of IEM by ANSYS 19.2

Position analysis of link 3, or the scotch yoke link (refer Fig. 10 and 11 in Appendix V to visualize how it works) is given below in Fig. 49.

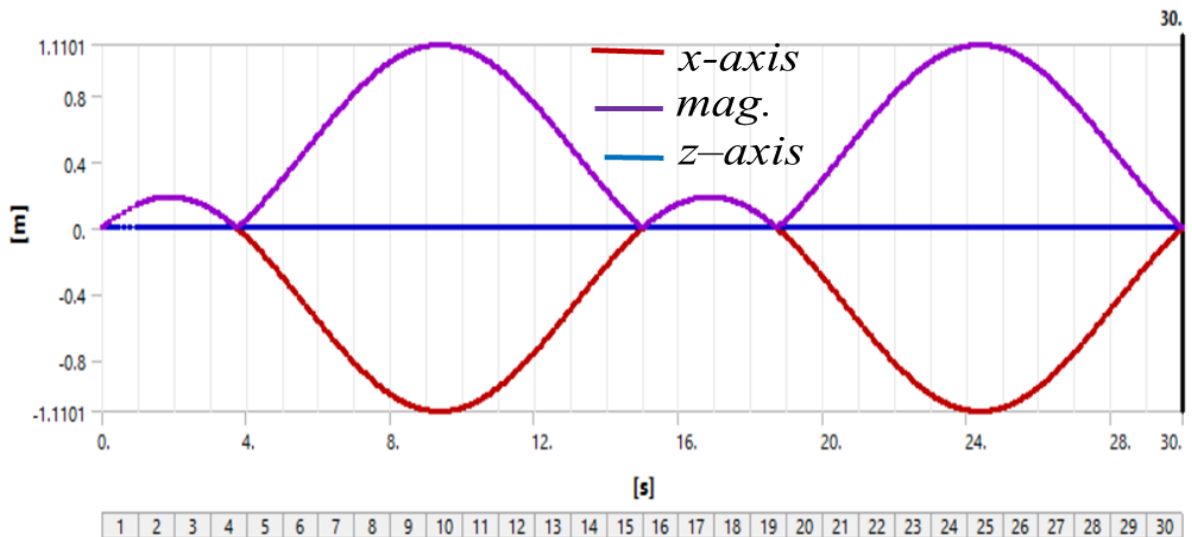


Figure 49: Link 3 or translational link position analysis by ANSYS

This graph shows, in Fig. 50, the slider link, $l_4(\theta)$ is arrived to approximately 1.11 m at the *injera* extracting port for $t \geq 7.5$ sec and turns back to 1.18 m which means the tip of the slider link will be at the storage bin during the *injera* is dropped, as shown in Fig. 51. Refer equation (55) on Appendix V and Fig. 49 shown below is taken from PTC Mathcad Prime 3.0 kinematic analysis.

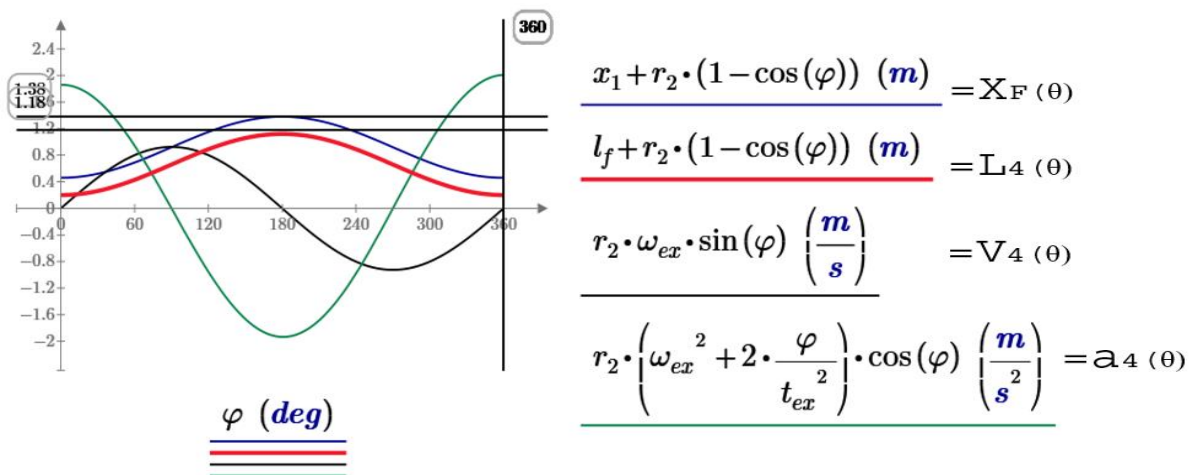


Figure 50: Magnitude of kinematic analysis of slider link or link 4 by PTC Mathcad Prime 3.0

The lower finger has a great role to grasp and drop *injera* as the with the help of spring as shown in Fig. 11 in Appendix V. The double lower fingers has the same position analysis as it is shown below in Fig. 51.

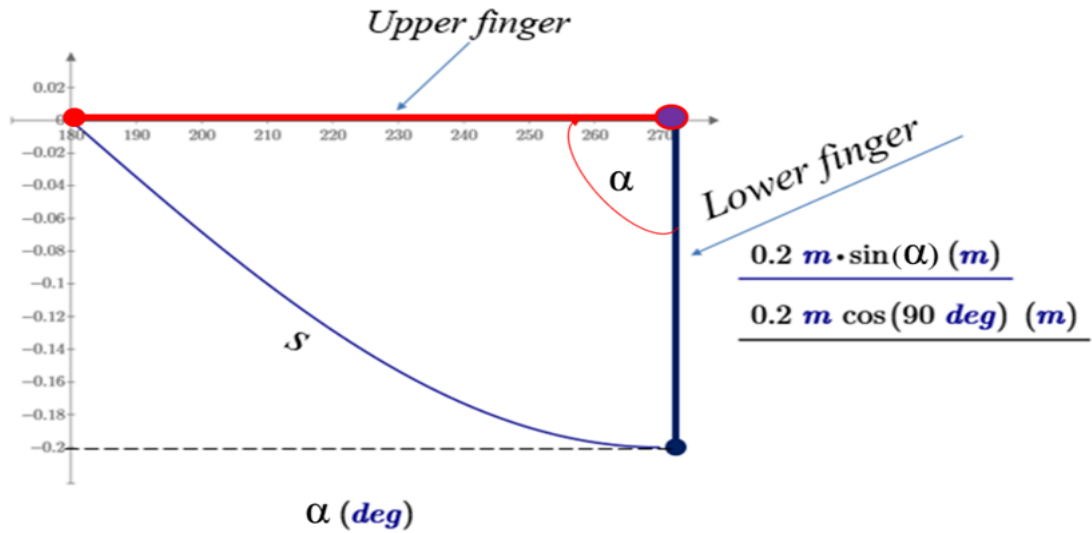


Figure 51: Position analysis of the lower finger by PTC Mathcad Prime 3.0

At 7.5 sec the graph shows that the lower finger is approached to the upper finger with 3 to 3.5 mm gap which enables *injera* not to be smudged out and at 15 sec it drops *injera* over the table as it is shown below in Fig. 52 and above in Fig. 51.

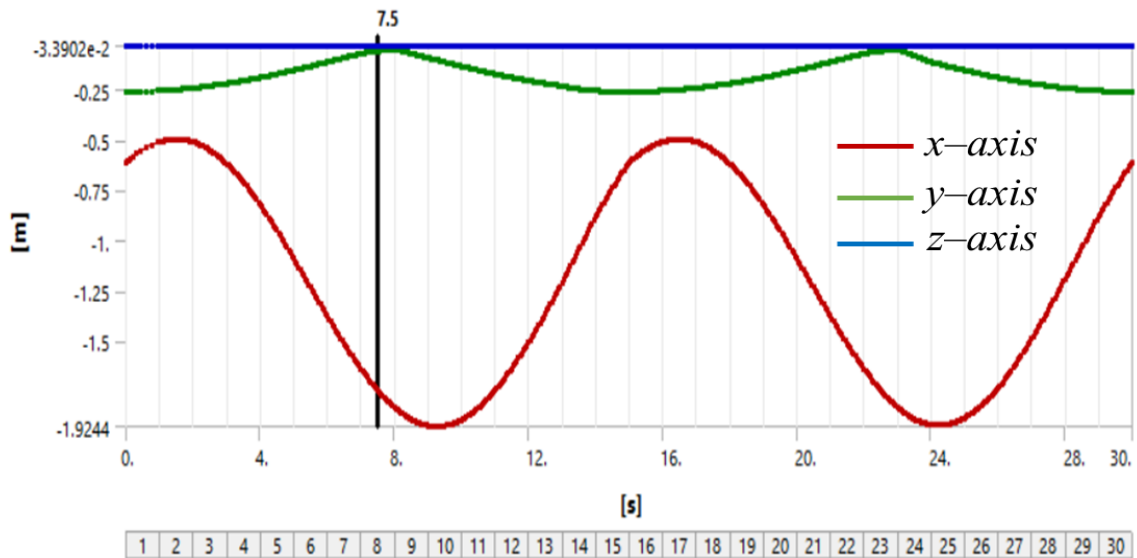


Figure 52: Position analysis of lower finger by ANSYS 19.2.

As shown below in Fig. 53, the upper fingers are fixed in both y – and z -axis but moves to x -axis and has the following directional position analysis in order to assist the lower fingers to grasp *injera* at the extracting port.

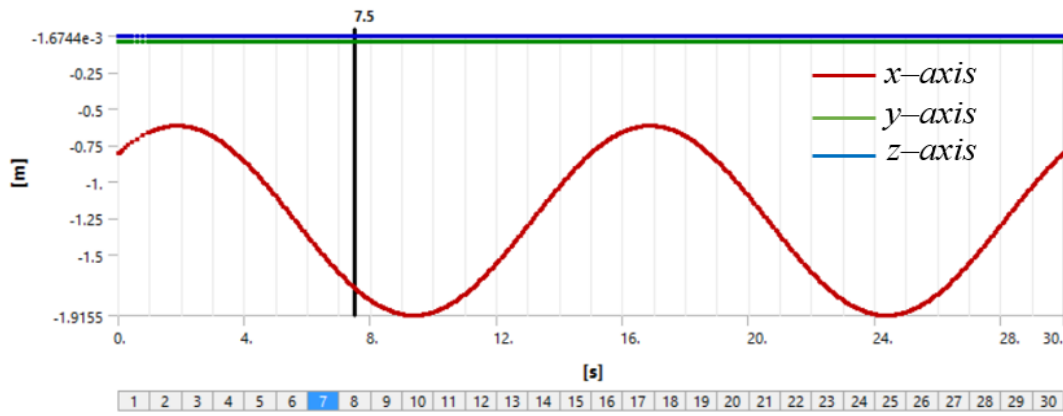


Figure 53: Upper fingers directional position analysis

According to Fig. 52 and 53, the green color position path shows the directional displacement in y –axis and the lower finger grasps *injera* from the *injera* separator blade at 7.5 seconds and it drops *injera* at $t = 15$ seconds corresponding to motion of link 2. The red color shows the motion analysis on the x-axis and here below as in Fig. 54, it shows the path of position along x-y coordinates with illustration of gripping and dropping *injera* at both ends respectively.

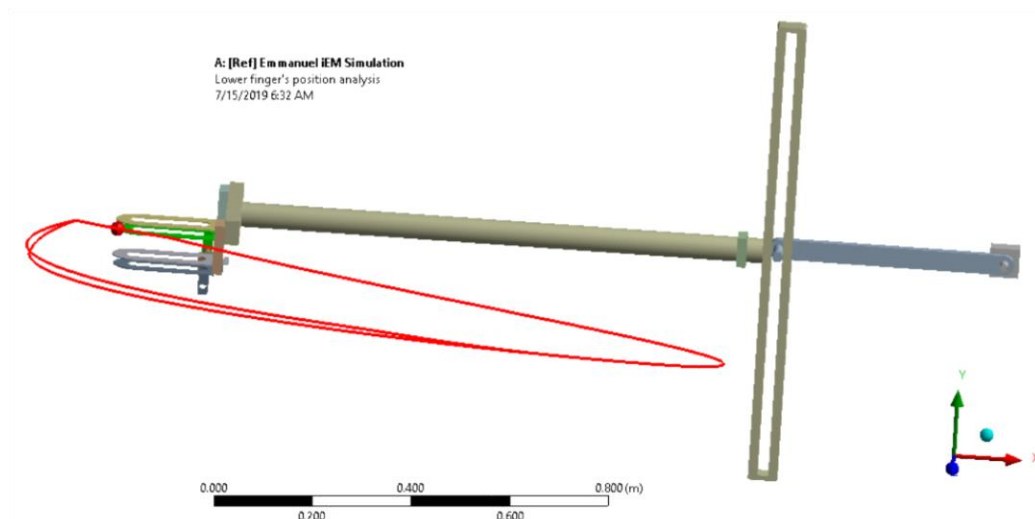


Figure 54: One loop lower finger *injera* grasping and dropping analysis

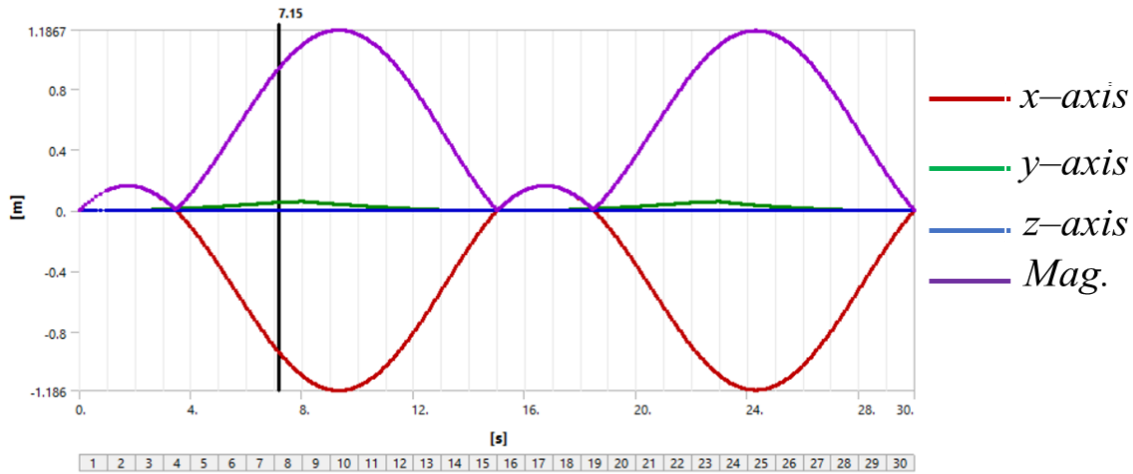


Figure 55: Directional position analysis of lower fingers

Totally, *injera* extracting mechanism works $s = 1.38$ m displacement including the finger length and the link 4 covers the displacement from the analysis as shown in both Fig. 55 and 56.

$$x = \sqrt{x_{min}^2 + x_{max}^2} = \sqrt{(0.2)^2 + (-1.186)^2} = 1.204 \text{ m}$$

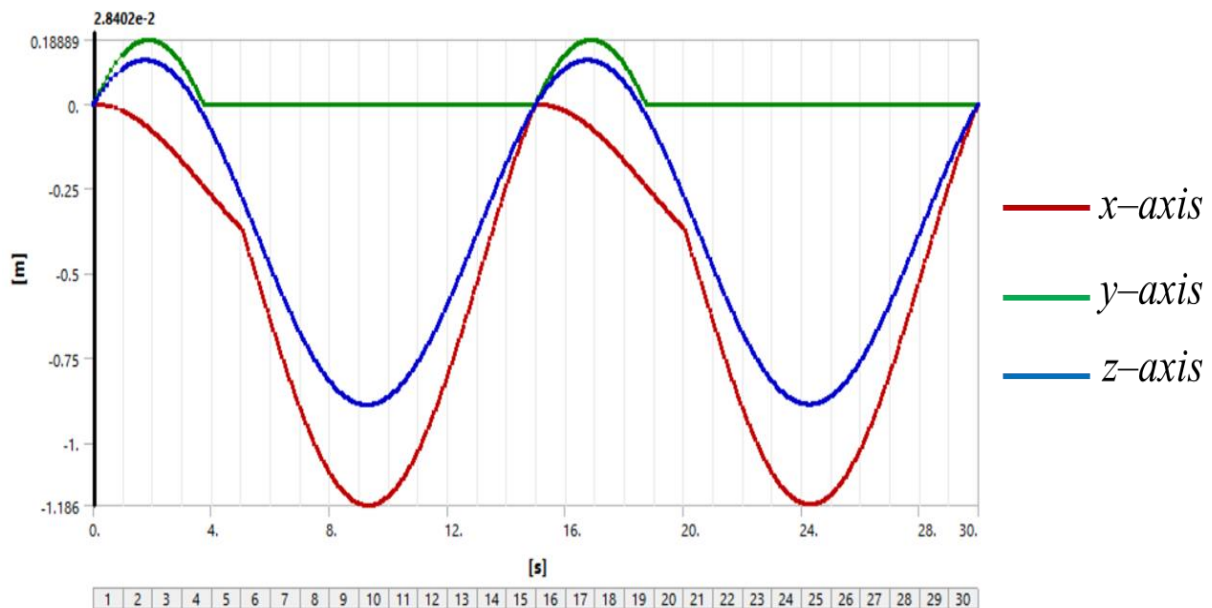


Figure 56: Position analysis of *injera* extracting mechanism

4.1.2 Velocity Simulation of Injera Extracting Mechanism

As it stated in chapter three under the velocity analysis in equation (3.35), the velocity analysis is done, by the time derivatives of the given position vector of *injera* extracting mechanism. Recall equation (3.35):

$$\vec{v}(t) = \frac{d\vec{r}(t)}{dt} = \dot{\vec{r}}(t) = v_{e_r} + v_{e_\theta} = \mathbf{0} \quad [\text{Recall equation (4.35)}]$$

$$\vec{v}(t) = \dot{r}(t)[\cos \theta \sin \theta]^T + r(t)\dot{\theta}(t)[- \sin \theta \cos \theta]^T$$

Where, v_{e_r} = Transitional velocity vector and v_{e_θ} = Rotational velocity vector


Through the yoke the slot joint has the y-axis velocity and is shown below in Fig. 56 by green color.

$$v_3(t) = \dot{r}_3(t) = r_2 \omega_2(t) \sin \theta_2(t) \quad [\text{Recall equation (4.38)}]$$

In similar way, we obtain velocity along the x-axis as shown in Fig. 56 below

$$v_4(t) = \dot{r}_4(t) = -r_2 \omega_2(t) \cos \theta_2(t) \quad [\text{Recall equation (4.39)}]$$

As it is shown in Fig. 59, the angular velocity has positive direction but the motion has negative direction against to x-axis and due to this the above recalled equation (3.39) has negative sign. Actually, the equation is done in Mathcad as given in Appendix V as:

<p>Velocity along x-axis</p> $v_4(t) = \frac{d}{dt} (r_2 \cdot (1 - \cos(\theta_2)))$ $v_4(t) = r_2 \cdot \omega_2 \cdot \sin(\theta_2)$		<p>Velocity along y-axis through the slot joint</p> $v_3(t) = \frac{d}{dt} (r_2 \cdot (1 - \sin(\theta_2)))$ $v_3(t) = -r_2 \cdot \omega_2 \cdot \sin(\theta_2)$
<p>(Hint: $r_2 = \text{constant}$) +</p>		

According to the recalled equation, the directional velocity of *link 3 and 4* is given as shown in Fig. 57 below.

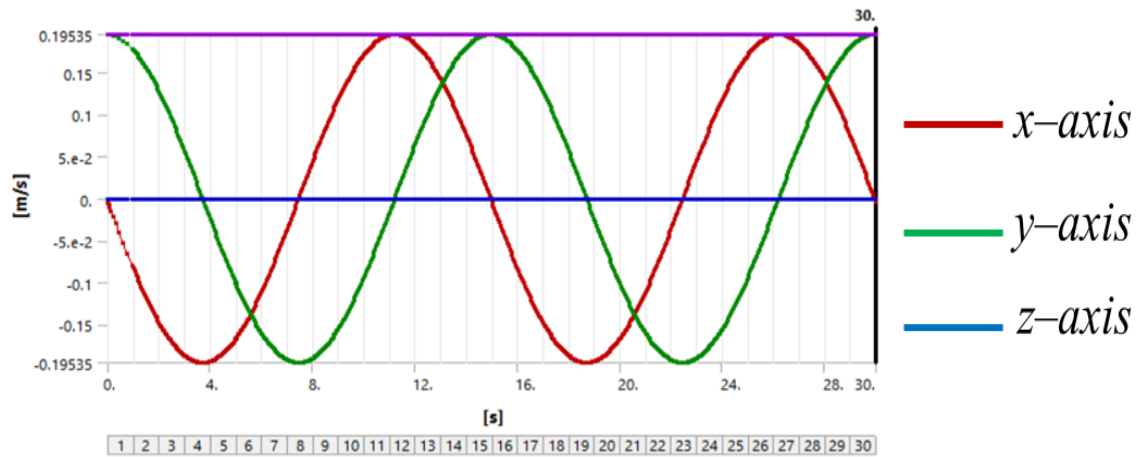


Figure 57: Total velocity analysis of link 3 and link 4 for 30 seconds

As shown in Fig. 58 below, the velocity and acceleration analysis graph is obtained by PTC Mathcad Prime 3.0; as it is indicated to the right of the graph at legend, the blue path shows the velocity analysis and the red one shows acceleration analysis to the x-axis. Hence, both the graph approximately have the same sinusoidal values of velocity.

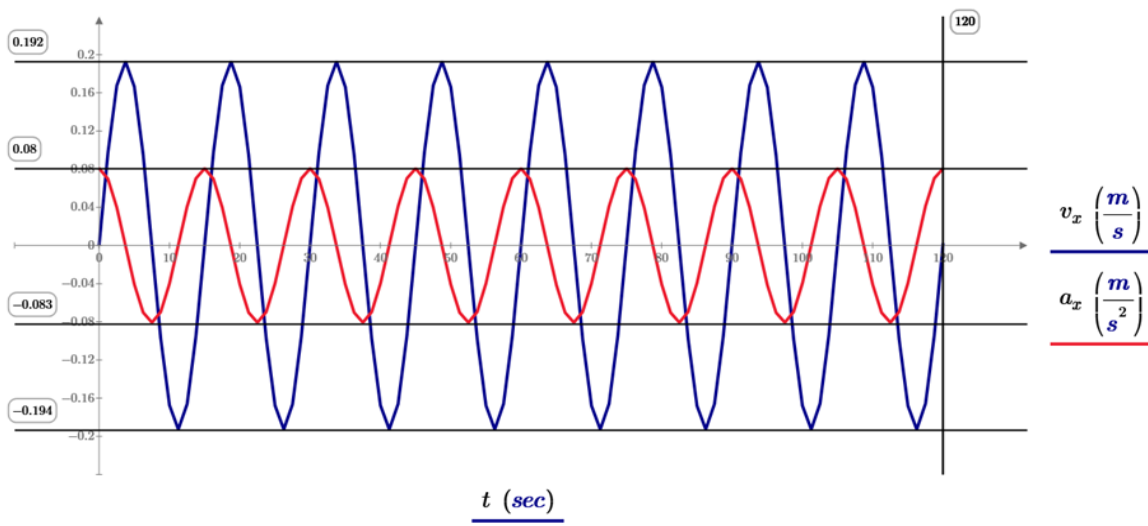


Figure 58: Total velocity analysis of IEM for 120 seconds by PTC Mathcad Prime 3.0

According to the above graphs, the velocity of link 3 through the slot joint or yoke and link 4 are given in Appendix V, in Mathcad.

$$v_{4max} := 0.19535 \frac{m}{s}$$

$$v_{4min} := -0.19535 \frac{m}{s}$$

$$v_{3max} := 0.19535 \frac{m}{s}$$

$$v_{3min} := -0.19535 \frac{m}{s}$$

$$v_{max} := \sqrt{v_{3max}^2 + v_{4max}^2} = 0.276 \frac{m}{s}$$

$$v_{min} := \sqrt{v_{3min}^2 + v_{4min}^2} = 0.276 \frac{m}{s}$$

From the above expression, it is analyzed that when the finger arrived at the tip of *injera* extraction port or grasped *injera* at $t=7.5$ sec. where the mitad is set and dropped *injera* where the lower finger is opened 90 degree at $t = 15$ sec., the velocity of $v_4(x)$ became zero while the velocity along y-axis got its minimum value at $t = 7.5$ seconds and its maximum value at $t = 15$ seconds. At $\theta_2 = \frac{\pi}{2}$ and $\frac{3}{2}\pi$ radians to the corresponding time $t = \frac{\pi}{2\omega_2}$ and $\frac{3\pi}{2\omega_2}$ seconds the $v_4(x)$ got its minimum and maximum values. But the system works with the magnitude of the velocity $v = 0.276 \frac{m}{s}$.

The velocity analysis of the lower finger is calculated above and given by graphs below in Fig. 59 as:

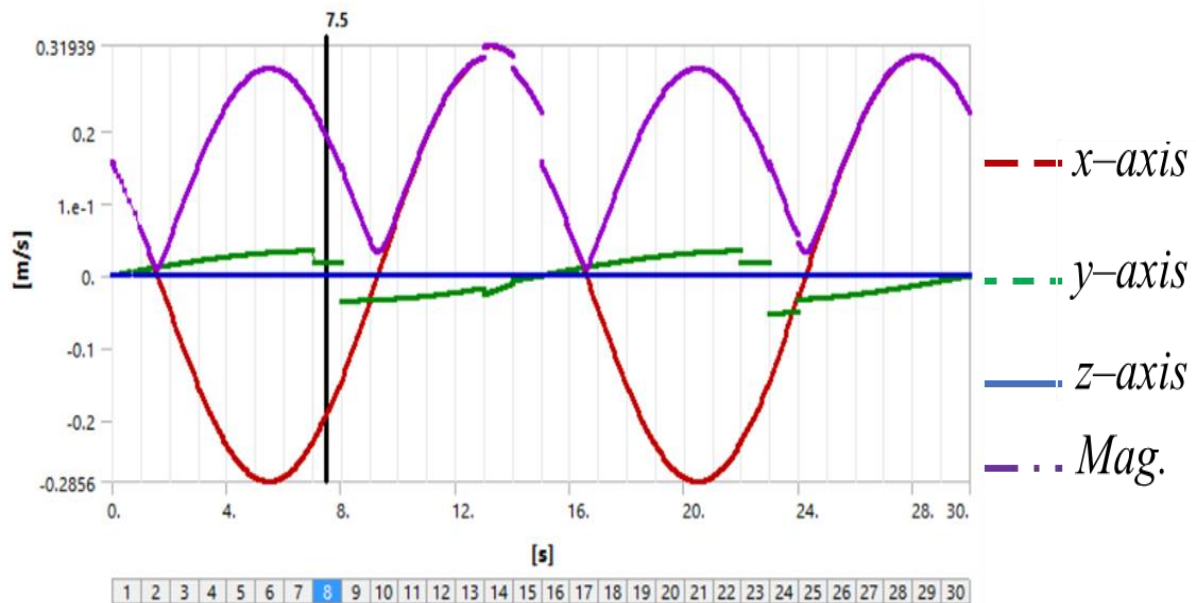


Figure 59: Velocity analysis of lower finger

At $t = 7.5$ sec the lower finger has a directional velocity with angular velocity $\omega_5 = 0.3142 \frac{rad}{sec}$ along x-axis and y-axis.

According to as it is mentioned previously, the angular velocity of *injera* extracting driven input link or link 2 was obtained from ANSYS analysis as shown below in Fig. 60:

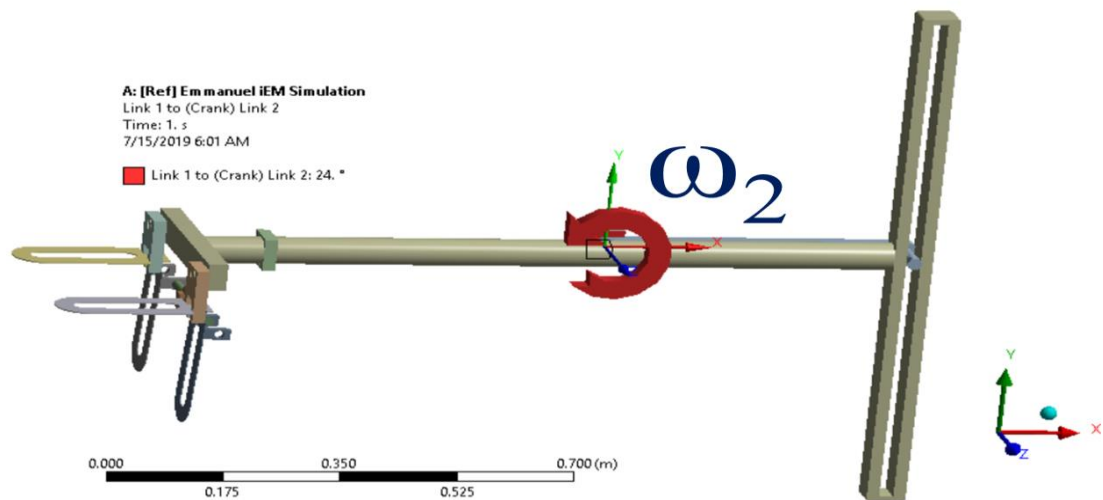


Figure 60: Assigning the revolute joint constraint of link 2 to the ground

As it is solved in PTC Creo Mathcad Prime 3.0 in Appendix V, the directional velocities are given below as follows.

By using relative velocity analysis, the velocity of the lower fingers is calculated as:

$$v_x = (\omega_5 - \omega_4) \times l_5 + \omega_5 \times l_4 + \omega_2 \times r_2 + v_A$$

$$v_y = \frac{dy}{dt} = \frac{d(r_5 \cdot \cos(\alpha))}{dt} = -r_5 \cdot \omega_5 \cdot \sin(\alpha)$$

The size and direction of the lower finger is known but the angular velocity of it is not known. From ANSYS analysis we can obtain the vertical velocity as

$$v_y := 3.4648 \cdot 10^{-2} \frac{m}{s} = 0.035 \frac{m}{s}$$

$$v_x := 0.31857 \frac{m}{s}$$

The magnitude of the lower finger at injera grasping port was obtained

$$v := \sqrt{v_x^2 + v_y^2} = 0.32 \frac{m}{s}$$

Due to the spring stretched the direction of the angular velocity of the link 5 will be negative upward to grasp and positive downward to drop *injera*. From the model of geometer, $r_5 := 200 \text{ mm}$ and opening and closing angle α varies $0 \leq \alpha \leq 90$

As it is shown in Fig. 61, the angular velocity of input link is zero both through the scotch yoke slot joint and along x-axis about the z- axis.

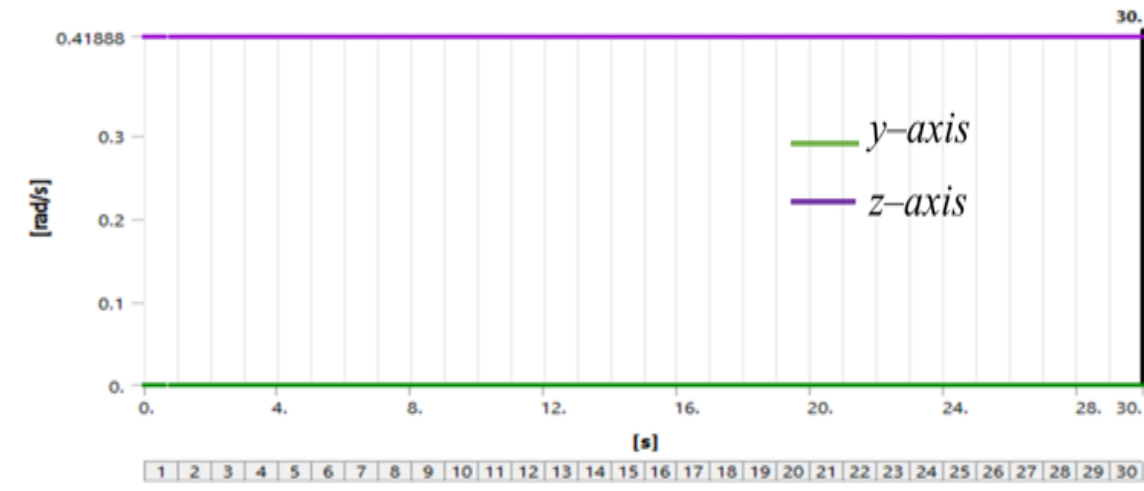


Figure 61: Angular velocity analysis of link 2 by ANSYS

As it is calculated in PTC Mathcad Prime 3.0, in Appendix V, the value of angular velocity of link 2 was obtained $\omega_2 = \frac{0.42rad}{sec}$ from graph above in Fig.60. This point is very important value in the design of *injera* extracting mechanism for integrated with *injera* baking machine whose rotary components. Either wise, if the angular velocity of *injera* baking and extracting mechanisms are not proportional as the motion is requested, they cannot be in appropriate task without clashing each other.

4.1.3 Acceleration Analysis of IEM

By using the time derivatives of the equations that are used for the position and velocity vectors, the acceleration of the extracting mechanism is given below in Fig. 62 as

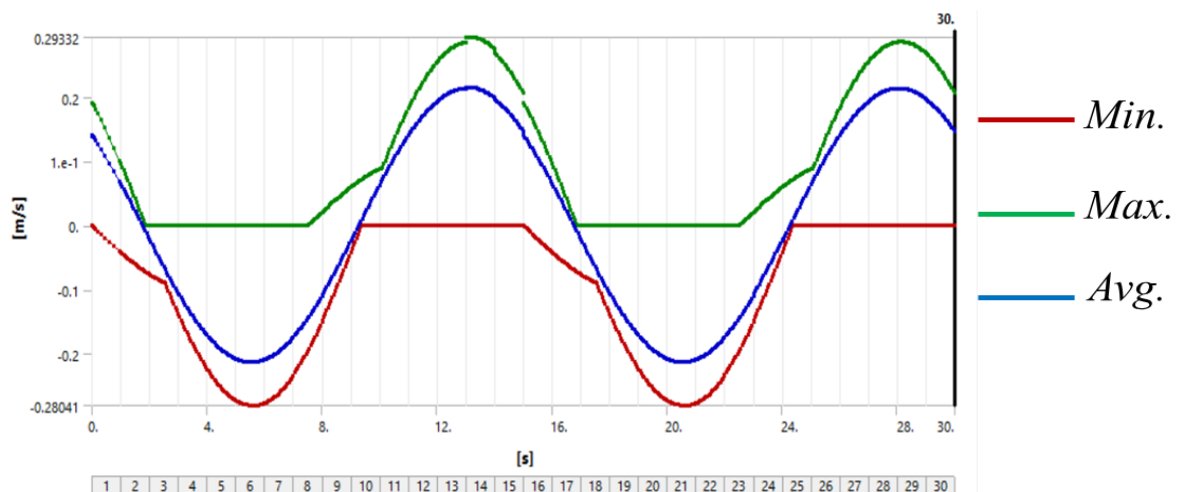


Figure 62: Directional acceleration analysis of *injera* extracting mechanism

And it is approximately similar in PTC Creo Mathcad Prime 3.0, in Appendix V, as shown below in Fig. 63.

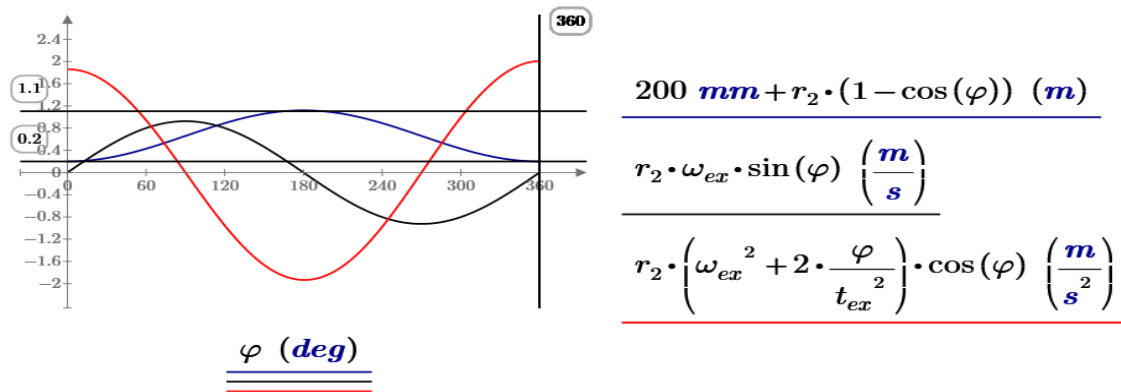


Figure 63: Directional acceleration analysis of *injera* extracting mechanism by PTC Mathcad Prime 3.0.

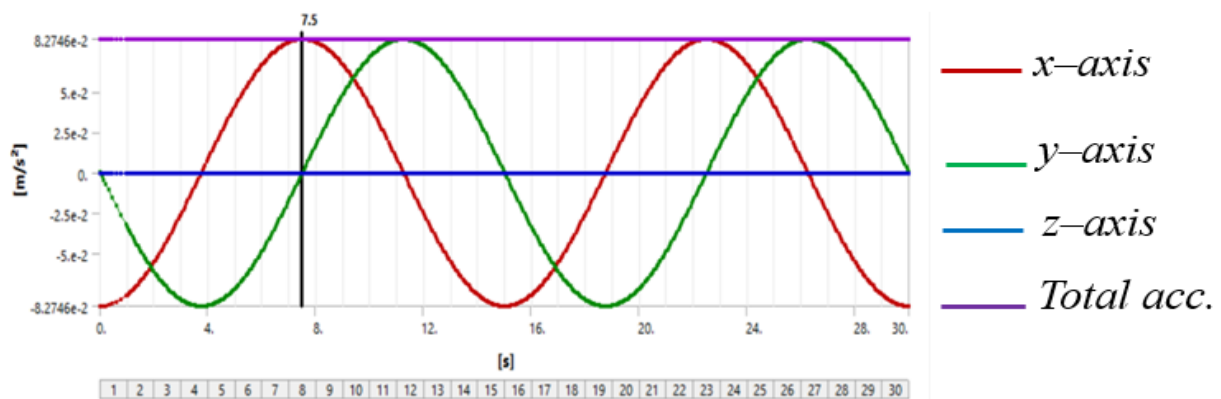


Figure 64: Acceleration analysis of link 2 by ANSYS 19.2

As shown above in Fig. 64, link 2 has a maximum directional acceleration at $t = 7.5$ second at $\theta_2 = \pi$ rad and minimum at $t = 0$ and $t = 15$ seconds. On other hand, link 3 has its maximum vertical acceleration at $t = 11.25$ seconds for extracting one piece of *injera*.

Acceleration analysis result of link 4 is given below in Fig. 65 as

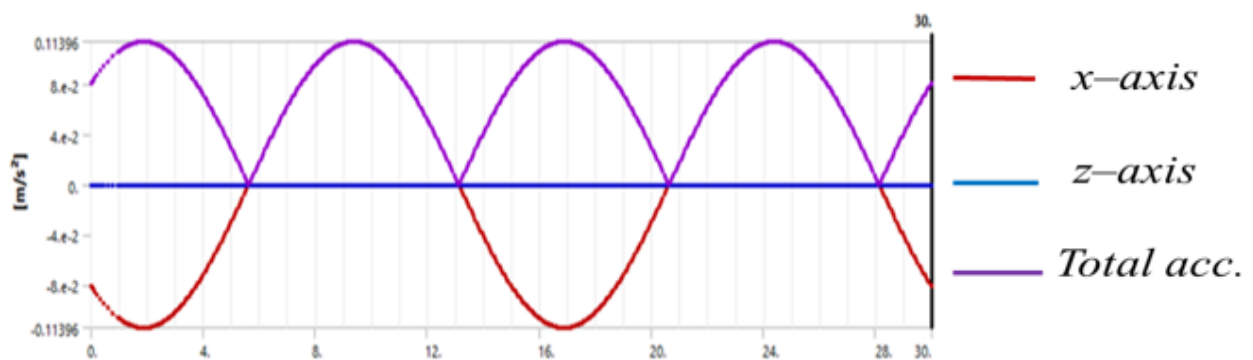


Figure 65: Acceleration analysis of link 4

According to the simulation result as shown above in Fig. 65, the acceleration of lower fingers will be zero at the extracting port and the upper fingers stays constant along the x-axis. The upper finger has a uniform directional acceleration, speed and angular velocity, to make the system stable due to the link 4 slider is fixed.

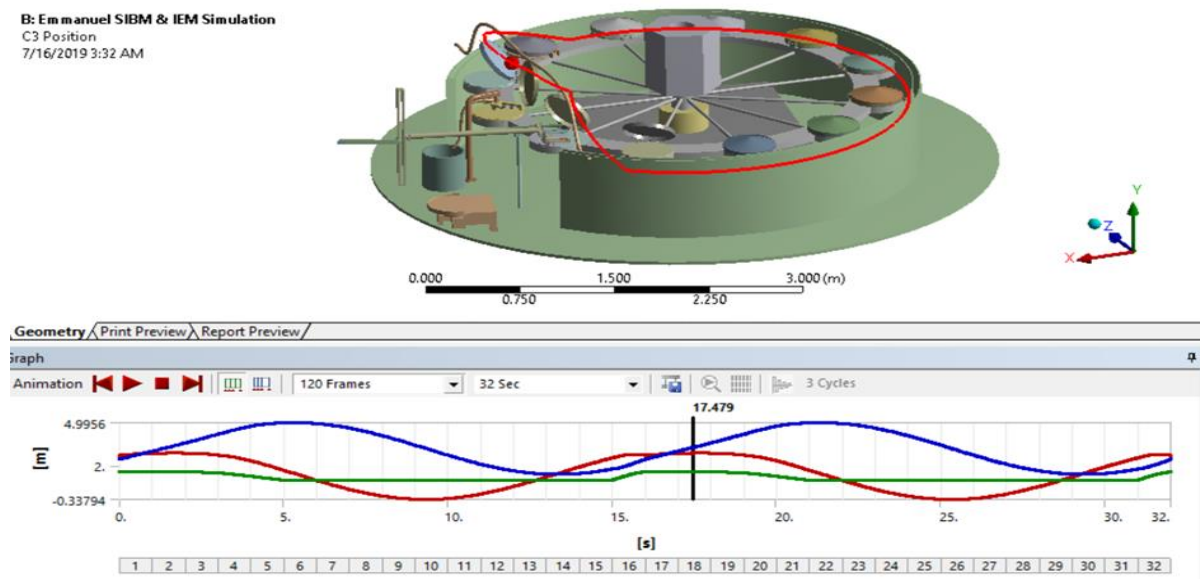


Figure 66: Kinematics analysis of baking machine integrated with *injera* extracting mechanism

As it was observed above, from Fig. 66, the cover is opened and running to be closed at 5 seconds from the instant time while *injera* extracting mechanism stays on its place and arrived to the extracting port at $t = 17.5$ seconds after it finished the round step for time step 1:5 scale simulation.

The kinematic analysis of IBM integrated with IEM was proportional according to the time sequence of activities and the kinematic behavior of *injera* extracting mechanism is valid. According to this kinematic modeling and simulation results we can design and optimize the *injera* baking machine (IBM).

Machines without motion are structures and they are not machines and are studied in static. Machines are composed of mechanisms and the operation of the machine is based on the mobility of the mechanism/s which made it. And the mechanism/s is/are valid by its/their number of DOF it/they has/have. Accordingly, the IBM is valid with its main mechanisms as IEM, dough pouring, pan polishing, cover opening and closing, the whole IBM rotating mechanism and etc. motion validation.

CHAPTER V

CONCLUSION AND FUTURE WORK

5.1 Conclusion

This research addressed the modeling and simulation of *injera* extracting mechanism of a semi-automated *injera* baking machine (IBM) for massive production purpose. It deals with a dynamic modeling and its responses of the *injera* extracting mechanism including the basic related dynamic parameters of *injera* baking machine during baking and extracting *injera*.

The purpose of this research was to model and simulate *injera* extracting mechanism in order to develop the design and manufacture of *injera* baking machine. Modeling and simulation of *injera* extracting mechanism referring to *injera* baking machine helps us to automate the system by keeping the dynamic behaviors or parameters regarding to the time sequential events. According to the dynamic modeling and simulation of *injera* extracting mechanism, in the rotary *injera* baking machine, it can be concluded that keeping the time sequence and the speed of *injera* extracting and the motion of *mitad* as well as the cover opening and closing are very important events. The results indicate that during *injera* extracting, the double lower finger should hold up and drop down *injera* at 180 and 360 degree respectively.

The *mitad* rotates uniformly under a circular motion at a constant speed with the vector from the center of the circular frame to the *mitad* has a constant magnitude and changing direction so is not constant in time with time derivative.

It used both graphic and mathematical modeling of the principal components of a semi-automated *injera* baking machine that are related to *injera* extracting. It focused on modeling and simulation of extraction of *injera* with regarding to the kinematics of *injera* baking machine. The kinematics of *injera* baking machine is studied and it influences directly the dynamic parameters of the extraction mechanism. The mathematical modeling of *injera* extraction mechanism was used time as the input parameter from the bases of classic method of *injera* baking on electrical pan. This parameter is the guidance variable for *injera* baking machine and extraction system. Depending on the input parameter, dynamic events, behaviors, and geometries of kinematic events of the *injera* extracting mechanism was studied.

The extraction system used scotch yoke mechanism as a means of both motion transmission and for extracting purposes. In this study, the scotch yoke mechanism converts the rotational motion into a linear motion. It is obvious that to rotate any machine or mechanism motor power is needed. However, under modeling and simulation of this study, the *injera* baking time was an input for all parameters taking as an angle division and the position vector, angular velocity and rotational speed, rpm of the system was calculated from the baking time. Hence, by using these parameters and software analysis the optimized motor power and torque will be found for the valid design.

The output result parameters of this simulation was position, velocity and acceleration of *injera* extracting mechanism inclusively the cover opening and closing mechanism. As it was discussed, under results and discussion, the kinematic analysis of *injera* extracting mechanism is valid with the kinematic analysis of *injera* baking machine. Changing in the baking time by using a better performance qualified *mitad* changes the angular velocity and the production rate will be increased accordingly to the increment of motion that depends on the performance of *mitad*. The performance of *mitad* plays a great role in *injera* baking machine.

Finally, depending on this kinematic modeling and simulation results we can design and optimize the *injera* baking machine for the massive production.

5.2 Recommendation

I recommended the future studies on the targeted area during the design and modeling of *injera* baking machine and extracting in order to make it automated, it is better to consider the baking time, dough pouring mechanism timing and appropriate mechanism, selection of *mitad* and their performance, geometrical optimization of *injera* baking machine, etc.

It is obvious that *injera* extracting and dough pouring are the difficult task to automat *injera* baking process. It is not easy as mothers pour batter onto the surface of the upper *mitad* and bake conventionally the well baked *injera* from the *mitad* easily. Here, the curved edge of the upper surface of the *mitad* and the softness texture of *injera* against to *injera* extraction and the encircling zoom in spiral motion of dough pouring makes the activity difficult to automate *injera* baking machine.

5.3 Future Work

Nowadays, cooking appliances and baking devices are well improved in the developed countries and advanced from labors to robotic (or semi- and fully- automated machines). Baking food devices need many amount of heat and according to the baking food types, it consumes time and labor power. Typically, *injera* baking is one among the baking foods in Ethiopia (both in the country and abroad) and rarely in Eritrea, Somalia, and Sudan.

Although, it is a staple food over the country, except numerous studies studied on the performance of *injera*'s pans, there is no plenty developments done on *injera* baking machine. Therefore, the future works has to be done on improving the performance of *mitad*, design and manufacturing of fully automated *injera* baking machine, design and analysis of power *control* and optimization of *mitads* and using their applications on an automated *injera* baking machine, digitizing or programing the whole system by using PLC programs, thermal and structural FEA of *injera* baking machine, design development and synthesis of dough pouring mechanism and its CFD analysis, etc. are the areas in most needed in our country case.

REFERENCES

- [1] Hassen, A.A. Performance investigation of Solar Powered Injera Baking Oven for Indoor Cooking: Proceedings of ISES Solar World Congress, Kassel, Germany, 2011.
- [2] Mulugeta, W. Rotary Baking System and Method. Aug. 4,2011; US2011/0189364 A1
- [3] 14. Gulilat, A. Stove Testing Results: A Report on Controlled Cooking Test Results Performed on ‘Mirt with Integrated Chimney’ and Institutional Mirt’ Stoves. May 23, 2011.
- [4] Tesfaye, A.H., et al. Design and Development of Solar Thermal Injera Baking: Steam Based Direct Baking. ISES Solar World Congress. 2013; 57(2014): 2946-2955.
- [5] Hailu, H.M., et.al. Energy Consumption Performance Analysis of Electrical *Mitad* at Mekelle City.2017; *V9 (1):43-65*.
- [6] Shigley’s Mechanical Engineering Design, 9th ed. McGraw-Hill publication.
- [7] Tesfaye, A.H., et al. Solar Powered Heat Storage for Injera Baking in Ethiopia. 2013 ISES Solar World Congress. 2013; 57(2014): 1603 -1612.
- [8] Oleg, V. Fundamentals of Kinematics and Dynamics of Machines and Mechanisms.2009; ISBN 0-8493-0257-9.
- [9] Tsegaye, M.M. Design and Manufacture of a Laboratory Model for Solar Powered Injera Baking Oven.
- [10] Yayeh, M. Integration of Scheffler Concentrator and Thermal Storage Device for Indoor Injera Baking. April 2013.
- [11] Admassu, W. Zelalem Injera Machine. Making Injera the New-Fashioned Way. June 20, 2006.
- [12] Abraha, A. Genetic Variation in Barely Enables a High Quality *Injera*, the Ethiopian Staple Bread, Comparable to Teff. July 1, 2013.
- [13] *Moges, G. Electric Injera Mitad Energy Efficiency Standards and Labeling, Challenges and Prospects. Ethiopian Energy Agency. VIENNA ENERGY FORUM 2017.*
- [14] Darling, W.A. Influence of Processing Parameters on Eye Size and Elasticity of Teff Based Injera. December 2014.
- [15] Harold, A. Rothbart. Cam Design Handbook. McGraw-Hill Handbooks. 2004. P. 40-50.
- [16] Alexander S. Fundamentals of Design: Topic 4 Linkages. January 1, 2008

- [17] Oberg, E. Machinery Handbook 27th Edition: A Reference Book for the Mechanical Engineer, Designer, Manufacturing Engineer, Draftsman, Toolmaker, and Machinist. 2004. P87.
- [18] Dicker J.J.Theory of Machines and Mechanisms, 3rd Ed. New York Oxford, Oxford University Press, 2003.

Appendix I

Glossary: Amharic-English Lexicon

These words are mostly common in Ethiopia but rare in abroad; are Amharic words. Here, they are listed as help for good understanding for they are written interchangeably somewhere.

Amharic

English

Akenbalo

Pan-cap or lid, cover

Absit

Restarter of dough molecules

Injera

Flat leavened soft bread, Ethiopian pancake

Teff

Gluten-less cereal, love grass, annual bunch grass

Massesha

Pan cleaner, caressing brush, polishing pad

Mitad

Clay griddle, Pan

Appendix II

Major Geometric Design Model of Semi-automated IBM

1. Dimensioning

The medium diameter of the circular frame that carries 12 *mitads* at equal distance gap between the two successors (not in cascade series) *mitads* illustrates the geometry of the *mitads* and assuming the gaps as the circles on the circular frame.

Then according to Erick Oberg and Franklin D. Jones, et.al. [17], the diameter of the centerline of the *mitads* and the gaps will be:

$$\begin{aligned} D_b &= \frac{d_m}{\sin\left(\frac{180^\circ}{N_m}\right)} + \frac{d_g}{\sin\left(\frac{180^\circ}{N_g}\right)} & (1) \\ &= \frac{0.42 \text{ m}}{\sin\left(\frac{180^\circ}{12}\right)} + \frac{0.40 \text{ m}}{\sin\left(\frac{180^\circ}{12}\right)} \\ &= \underline{\underline{3.513 \text{ m}}} \end{aligned}$$

Where the number of gaps equals the number of mitads, $N_g = N_m = 12$,

As it is shown in Fig. 67, D_b is the base diameter of the centerline of the *mitads* and the gaps, D_o is the outer diameter of the frame that passes through the centerline of the mitads and gaps. D_i is the internal diameter of the frame and d_m is the diameter of the *mitad*, d_g is the diameter of the gap (i.e., the arc length of the gap between two *mitads* is considered as the diameter of the gap), N_m is the number of *mitads* and N_g is number of gaps on the frame. Then the outer diameter is given by

$$D_o = D_b + dm \quad (2)$$

$$D_o = 3.513 \text{ m} + 0.42 \text{ m} = \underline{\underline{3.933 \text{ m}}}$$

The inner diameter of the circular frame will be:

$$D_i = D_b - dm \quad (3)$$

$$D_o = 3.513 \text{ m} - 0.42 \text{ m} = \underline{\underline{3.11 \text{ m}}}$$

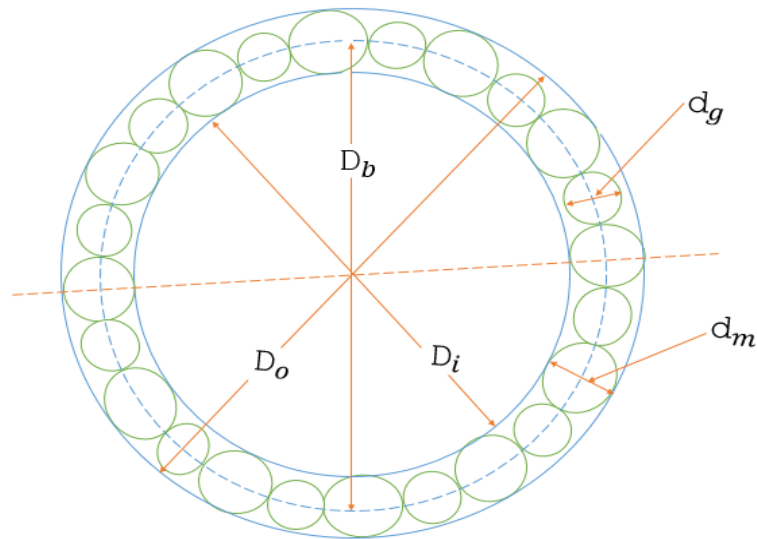


Figure 67: Diameter formulation for the IBM system

However, the above formula cannot be specifically applicable for an application where two different diametric size circles are enclosed or encompassed in/on the largest circle. Further, it is solved simply by adding the two diameters with the number of items and equating them by the circumference formula:

$$C = N_m d_m + N_g d_g = N_m (d_m + d_g) = \pi D_b \quad (4)$$

$$\begin{aligned} D_b &= \frac{N_m (d_m + d_g)}{\pi} \\ &= \frac{12(0.42 \text{ m} + 0.40 \text{ m})}{\pi} \\ &= \underline{\underline{3.132 \text{ m}}} \end{aligned}$$

Then in the same way as in equation (ii) and (iii), the outer and the inner diameters will be solved:

$$D_o = D_b + dm$$

$$D_o = 3.132 \text{ m} + 0.42 \text{ m} = \underline{\underline{3.552 \text{ m}}}$$

The inner diameter of the circular frame will be:

$$D_i = D_b - dm$$

$$D_o = 3.132 \text{ m} - 0.42 \text{ m} = \underline{\underline{2.712 \text{ m}}}$$

Figure 68 below shows the diameters calculated based on equation (4) and follows equation (3) and (2) are either right or wrong in arrangement. The arrangement and diametric size evaluation is satisfied by equation (4) and equation (1) does not satisfies the arrangement of the input parameters. Therefore, equation (4) is the chosen formula for different circles size enclosed around a largest circle.

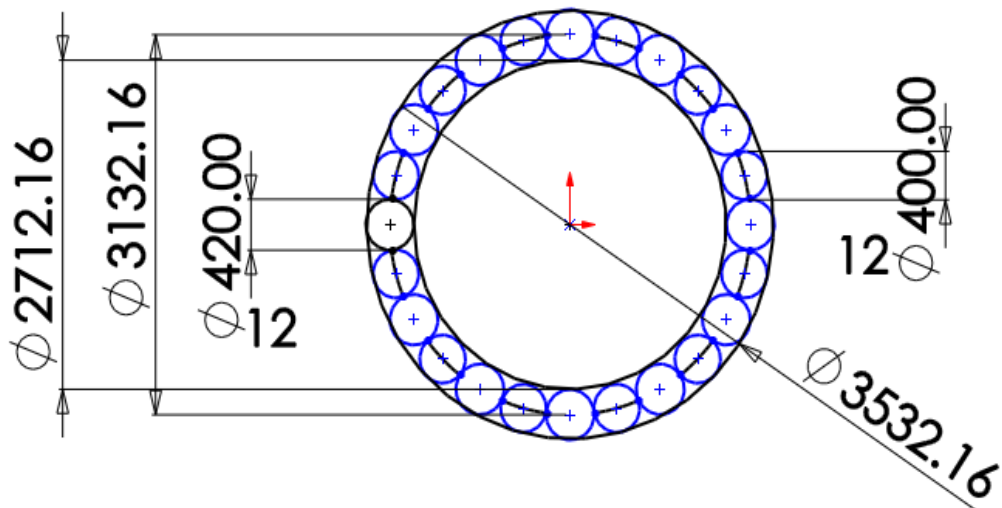


Figure 68: Centerline diameter calculation and demonstration with different size of small circles on the largest circle.

The dimension of cover is given as below in Fig. 69 and its height is calculated by the considering the height of the classic covers and using Pythagorean theory of the triangle. The height of cover of the classic mitad is 0.2 of the diameter of the cover. Based on this information, the height, h of the cover in this model is calculated as:

$$h = k * D_c \quad (5)$$

Where $k = 0.2$ is the constant factor that relates the height with the diameter of the cover, $D_c = 0.42 \text{ m}$. Then the height is:

$$h = 0.2 * 0.42 \text{ m} = 0.084 \text{ m} = \underline{\underline{8.4}} \text{ cm}$$

The geometry of the cover does satisfy the two side equilateral triangle properties and the lateral length of the cover, l_1 is given by Pythagorean theory by splitting the triangle into two equal sides each has common h size. Then:

$$l_1 = \sqrt{h^2 + \left(\frac{D_c}{2}\right)^2} = \underline{\underline{23.55}} \text{ cm} \quad (6)$$

The effective diameter that plays role in the cover opening/closing mechanism is the $D_{\text{effective}}$ that equals the sum of cover diameter, clearance, c_1 and cover opener handle c_2 at one edge of the cover.

$$D_{\text{effective}} = D_c + c_1 + c_2 \quad (7)$$

$$D_{\text{effective}} = 42 \text{ cm} + 2 \text{ cm} + 3 \text{ cm} = \underline{\underline{47}} \text{ cm}$$

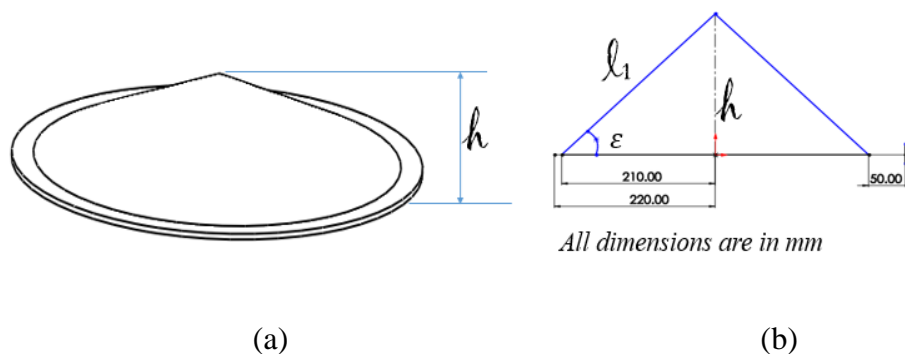


Figure 69: Dimension of pan lid; (a) pan lid (b) Equivalent dimensions of pan lid in trigonometric representation

2. Inertia Moment of the Main Components of Injera Baking Machine

The main geometric properties of a semi-automated *injera* baking machine is given as follows:

A= Area

G= Location of (mass) centroid

$I_x = \int x^2 dA$ = second moment of area about x axis

$I_{xy} = \int xy \, dA$ = mixed moment of area about x and y axis

$J_G = \int r^2 \, dA = \int (x^2 + y^2) \, dA = I_x + I_y$ = second polar moment of area about axis through G.

$k_x^2 = \frac{I_x}{A}$ = Squared radius of gyration about x axis

The components to be calculated under this topic are shaft, circular rotary frames, pans as shown in Fig. 70, circular connector rods, the disks, etc.

The mass of the connector rods are calculated as

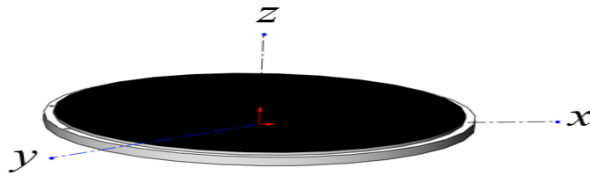


Figure 70: Geometric properties of *mitad* model

The properties formula is taken from the round disks formula [6], by neglecting the spiral electric wires as particles consider the pan as round disc:

$$A = \pi \frac{d_m^2}{4} = 0.14 \, \text{m}^2, \text{ volume, } V = A * t = 0.003 \, \text{m}^3$$

Density of mitad $\rho = 2887.2 \, \text{kg/m}^3$, then the mass of mitad is given as

$$m = \frac{V}{g} \rho = \frac{\pi d^2 t \rho}{4g} = \frac{\pi (0.42 \, \text{m})^2 (0.02 \, \text{m}) (2887.2 \, \text{kg})}{4 * 9.81 \frac{\text{m}}{\text{s}^2}} = 8.16 \, \text{Kg}$$

$$I_x = I_y = m \frac{d^2}{16} = 8.99 * 10^{-2} \, \text{kgm}^2$$

$$I_z = m \frac{d^2}{8} = 0.1799 \, \text{kgm}^2$$

$$I_{xy} = I_x + I_y = I_z = 0.1799 \, \text{kgm}^2$$

3. Baking Time and Production Rate

Per one revolution the number of production will be = $1 \times 12 = 12$ injeras

One output port produces 12 *injeras* per a revolution. Then the production rate is given by

Production Rate = Number of *Mitads* \times Number of Op Ports \times Number of Revolutions

$$PR = N_m * N_p * N_R \quad (8)$$

$$N_R = \frac{P_R}{N_m N_p} \quad (9)$$

Where R_m = radius of the pan or mitad

N_R = Number of revolution

P_R = Number of production rate

The baking time is depended on the type of pan. For the rotary baking type, if 1 *injera* takes t_i times then one batch *injeras* are baked per 1 rev within

$$T_B = t_i + \frac{t_{rev}}{N_p} * (N_p - 1) \quad (10)$$

However, t_i depends on the amount of temperature the *mitad* consumed for the first *injera* baking from input to output to be baked enough. Hence, the baking rev. rotation takes 150 seconds. In this case, the number of pans are 12, the pan carrier frame rotates one turn per 3 minutes and the first *injera* takes 2.5 minutes then a batch of *injera* is baked within:

$$T_B = 2.5 + \frac{180sec}{12} * (N_p - 1) \quad (11)$$

$$= 2.5 * 60 + 15 * 11 = 315 \text{seconds} = 5.25 \text{ min.}$$

Where, T_B = One batch baking time

t_i = time taken by the first pan to bake *injera*

t_{rev} = One revolution per time

t_{rev/N_p} = One revolution time per number of pans

N_p = Number of pans on the frame

In one hour the production rate will be

$$\frac{60 \text{ min}}{TB} * N_p = \underline{277} \text{ injeras/hour} \quad (12)$$

Appendix III

Mathematical Model of the Circular Rotary Frame of *Injera* Baking Machine with *Mitad* and Polishing Pad

3.1) Mathematical Model of the Circular Rotary Frame with Fixed Mitads

Consider the *mitads*' carrier circular frame rotates about the z-axis horizontally and the mitads are fixed at the edge of it; and the parametric equation of the first one mitad in the first sequential order pointed as AB on the circle is given as shown in Fig. 71 below:

$$x = R \cos \alpha \quad \text{and} \quad y = R \sin \alpha \quad (13)$$

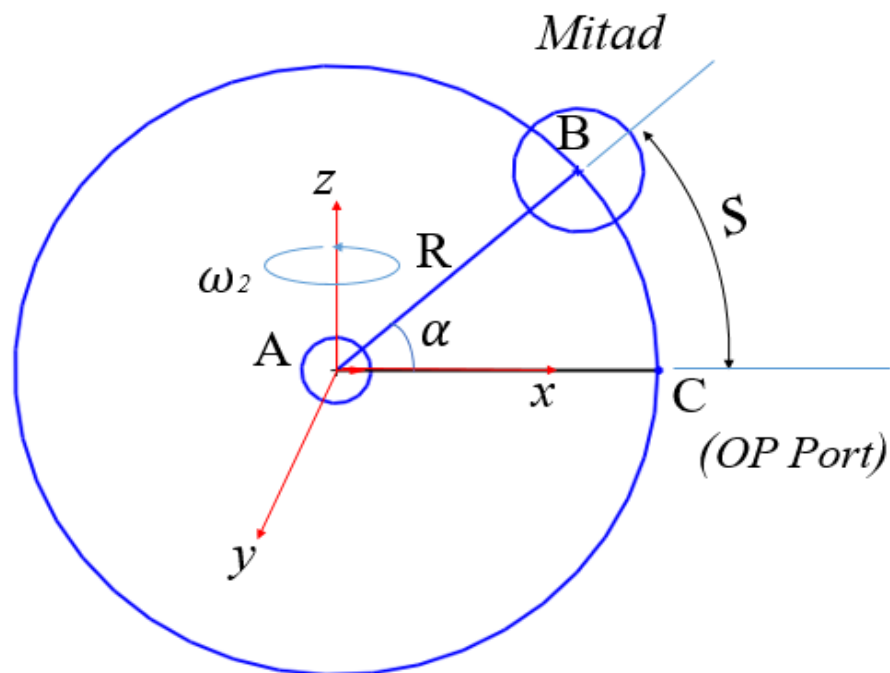


Figure 71: Location of a *mitad* on the circular frame for an *injera* extracting fixed at its place and an observer moving with the circular frame

Where α = the angle of the *mitad* moves from its origin (OP port), x = the position of the moving *mitad* in horizontal direction, y = the covered position in the y direction during from C to B.

By using Pythagoras theorem, the displacement of mitad from the center of the circle (Radius pointed from A to C) is nothing but the radius it covers by the arc \widehat{CB} is given by:

$$R = \sqrt{x^2 + y^2} \quad (14)$$

The angular velocity of the mitad is already known from the nature that the time taken to bake one injera per a revolution $\omega = 0.0349$ rad/sec. However, our intention is to know the time relation for the kinematic modeling with relative to *injera* extracting mechanism, so the angular displacement is given by:

$$\alpha = \omega t \quad (15)$$

Back substitution, and our R is already known then by substituting equation (15) into (13), we obtain:

$$x = 1.565 \cos \omega t \text{ and } y = 1.565 \sin \omega t \quad (16)$$

By using the first and second order differential equation with respect to time, we obtain velocity and acceleration of the *mitad* respectively as:

$$\dot{x} = -R\omega \sin \omega t \text{ and } \dot{y} = R\omega \cos \omega t \quad (17)$$

$$\ddot{x} = -R\omega^2 \cos \omega t \text{ and } \ddot{y} = -R\omega^2 \sin \omega t \quad (18)$$

Then the velocity v (in cm/s) vector is given as

$$v(t) = -5.48 \sin(0.035t) \hat{i} + 5.48 \cos(0.035t) \hat{j}$$

Then the magnitude of the resultant velocity and acceleration of the mitad is given by:

$$\begin{aligned} v &= \sqrt{\dot{x}^2 + \dot{y}^2} = \sqrt{(-R\omega \sin \omega t)^2 + (R\omega \cos \omega t)^2} \\ &= R\omega \sqrt{(\sin^2 \omega t + \cos^2 \omega t)} = R\omega \sqrt{1} = R\omega \end{aligned} \quad (19)$$

And

$$a = \sqrt{\ddot{x}^2 + \ddot{y}^2} = \omega^2 R \sqrt{(\cos^2 \omega t + \sin^2 \omega t)}$$

$$= \omega^2 R \quad (20)$$

Since, equation (19) and (20) shows that the *mitad* has a constant velocity and acceleration for the same radius around the circular frame and the rest N number of *mitads* for the same radius on this circular frame have equal velocity and acceleration.

The tangential velocity of the *mitad* to the circular path through the centerline of *mitads* equals the magnitude of the resultant velocity that is solved above in equation (19) and equation (20) will become:

$$a = \left(\frac{v}{R}\right)^2 R = \frac{v^2}{R} = \underline{0.2 \text{ cm/s}^2} \quad (21)$$

$$\text{Since, } \omega = \frac{v}{R}$$

Equation (21) shows the Newton law is succeeded in showing geometrically that a *mitad* performing a circular motion that accelerates a magnitude of $\frac{v^2}{R}$ directed toward the center of the circular frame that carries the *mitads*. Then each *mitad* has the numerical value of the tangential velocity **5.48 cm/sec** on diameter that passes through the centerline of the *mitads*.

At the OP port, $\alpha = 0, 2\pi, 4\pi, 6\pi, \dots$ etc.

The first *mitad* is found at 30 degree from the Op port as is shown in Fig. 71 above, which has the arc length s and is calculated as:

$$s = \frac{\pi r \alpha}{180} \quad (22)$$

$$s = \frac{\pi * 175.5 \text{ cm} * 30}{180} = \mathbf{91.8915 \text{ cm}}$$

$$s = \underline{\underline{0.919 \text{ m}}}$$

All the twelve *mitads* around the circular pan carrier frame are set at the same distance s are one after another as shown below in Fig. 72 and 73.

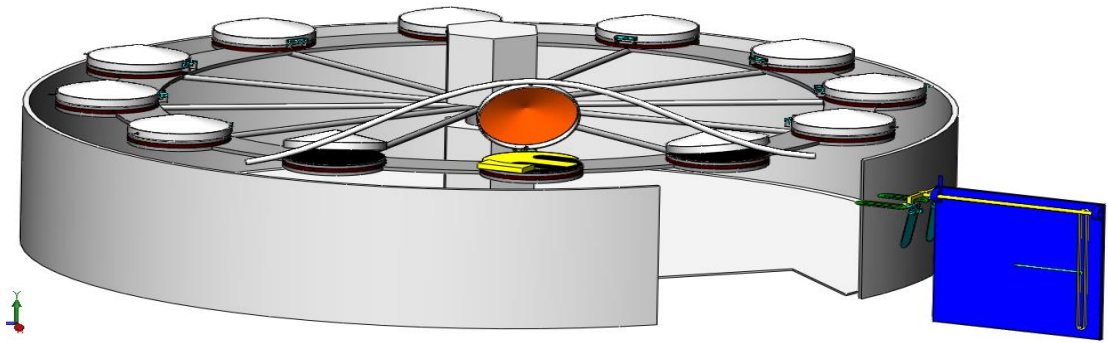


Figure 72: IBM 3D Draft

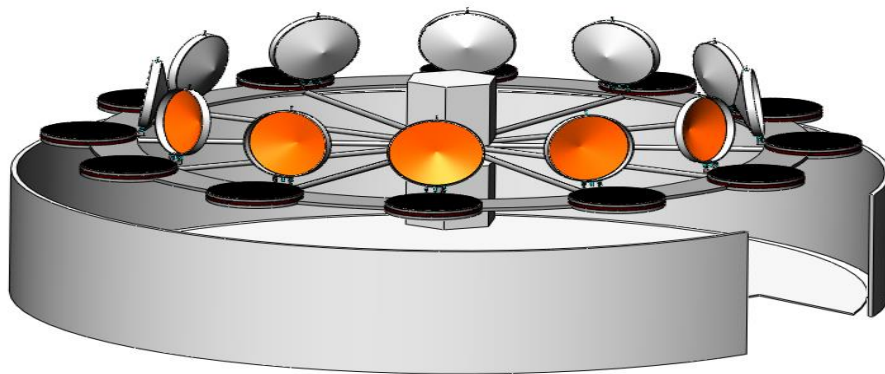


Figure 73: IBM Subcomponents before operation (here the cover are opened to show all covers are able to be opened during rotation at the cover opening port)

3.2 Mitad-Cleaning Roller Mechanism

The top surface of the pan is cleaned by the translational movement of the mitad relative to the roller cylinder on the fixed axis as it's shown in Fig. 74.

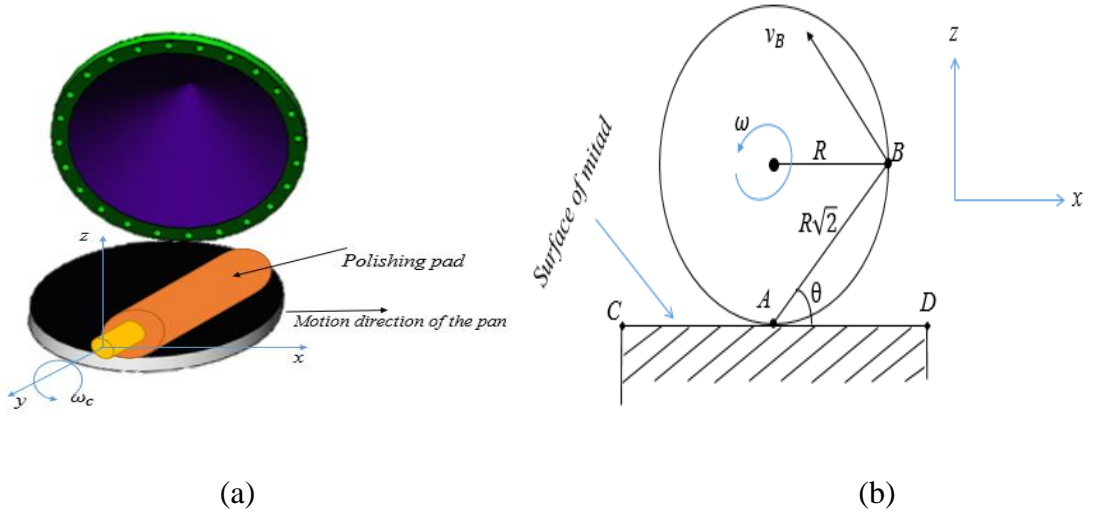


Figure 74: Rolling cylinder to the x-direction due to friction from the *mitad*: (a) Polishing of *mitad* between the dough pouring IP port and the OP port (b) Equivalent skeletal representation of the polishing pad on the *mitad* surface.

Point A shows the contact surface between the *mitad* and the cylinder, the *mitad* has an infinite instantaneous center with respect to the rolling cylinder. Due to friction, the rotational motion of the *mitad* rotates the cylinder in the direction of its movement. Hence, angular velocity of the *mitad* is $\omega_m = 0.035 \text{ rad/sec}$. The rolling cylinder, whose length L_{CD} equals to the diameter of the *mitad*, is driven by the upper surface of *mitad*, is adjusted horizontally on a shaft and has the same velocity with the *mitad*. Therefore, the rolling cylinder has

$$\omega_c = \frac{\omega_m R_f}{R_c} \quad (23)$$

$$\omega_c = \frac{0.035 \frac{\text{rad}}{\text{s}} * 160.282 \text{ cm}}{4 \text{ cm}} = 1.311 \frac{\text{rad}}{\text{s}}$$

$$N_c = 12.522 \text{ rpm i.e., } \omega_c = 1.311 \text{ rad/sec.}$$

Where ω_c – angular velocity of the rolling cylinder about y-axis, ω_m – angular velocity of the *mitad*, R_c – radius of rolling cylinder and R_f – radius of *mitad*-carrying rotational frame. R_c is 40mm and the cleaning cylinder finished the surface of the *mitad* by 1.592 rev, $\theta = \omega t = 3.184\pi$ after 0.125 min. Then at $\theta = 45^\circ$:

$$\vec{v}_B = \vec{\omega}_c \hat{j} \times \vec{r}_{AB} \quad (24)$$

$$\vec{v}_B = \vec{\omega}_c \hat{j} \times (-R\sqrt{2} * \cos\omega_c t \hat{i} + R\sqrt{2} * \sin\omega_c t \hat{k}) \quad (25)$$

Equation (24) can be written as

$$\vec{v}_B = \begin{vmatrix} \hat{i} & \hat{j} & \hat{k} \\ 0 & \vec{\omega}_c & 0 \\ -R\sqrt{2} * \cos \omega_c t & 0 & R\sqrt{2} * \sin \omega_c t \end{vmatrix}$$

$$\vec{v}_B = R\omega_c \sqrt{2} * \sin \omega_c t \hat{i} + R\omega_c \sqrt{2} * \cos \omega_c t \hat{k} \quad (26)$$

$$v_B = 1.034 \times 10^{-3} \hat{i} + 0.075 \hat{k} \left[\frac{m}{s} \right] = \sqrt{V_{Bx}^2 + V_{Bz}^2}$$

$$= 0.075 m/s$$

The acceleration of the rolling cylinder will be as

$$a_B = R\sqrt{2} * \omega_c^2 \cos \omega_c t \hat{i} - R\sqrt{2} * \omega_c^2 \sin \omega_c t \hat{k} \quad (27)$$

Then the time in second is given by:

$$t = 4.711 * \frac{\theta}{360^\circ} \quad (28)$$

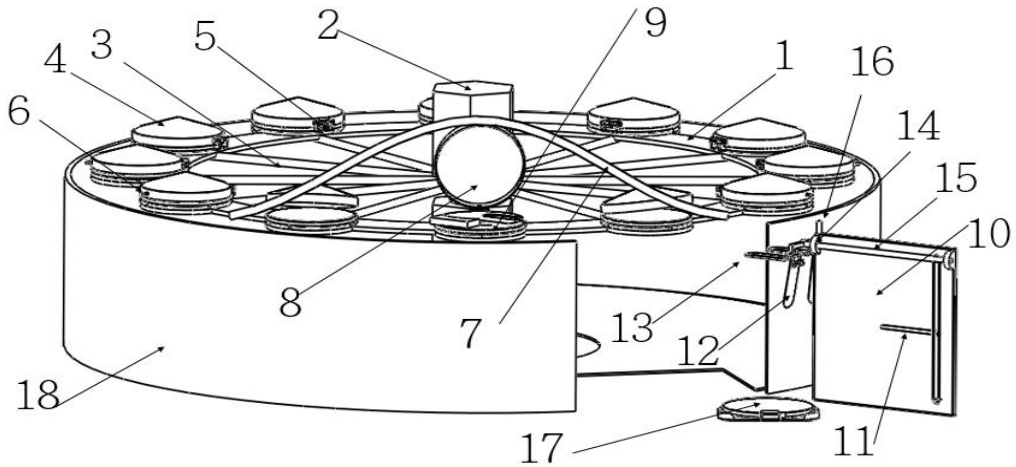


Figure 75: Semi-automated *injera* baking machine

The labelled parts above in figure are given in Table 4 as

Table 4: Subcomponents of semi-automated *injera* baking machine

No.	Parts Name	Material	Quantity
1	Rotary circular frame	Cast iron	1
2	Vertical hub with shaft	Mild steel	1
3	Cylindrical rod	Cast iron	12
4	<i>Mitad</i>	<i>Clay</i>	12
5	Cover hinge frame	Cast iron	12
6	Cover handle	Teflon coated Stainless Steel	12
7	Cover-guider rod	Stainless steel	1
8	Cover	Sheet metal	12
9	<i>Injera</i> separator	Stainless steel	1
10	Scotch yoke mechanism (Here, used as <i>injera</i> extracting mechanism)		1
11	Crank (Link 2)	Cast iron	1
12	Lower finger	Stainless steel	2
13	Upper finger	Stainless steel	2
14	Slotted joint supporter	Cast iron	2
15	Extractor arm (Sliding shaft)	Cast iron	1
16	Spring fixer frame	Mild iron	1
17	<i>Injera</i> deposit place	Woody straw mat (Plastic)	1
18	IBM House	Sheet metal	1

Table 5: Calculation of kinematics of *injera* baking machine

t(sec)	ω (rad/s)	ϕ (deg)	Xf(m)	v(m/s)	a(m/s ²)
0	0.0349	0	0	0.05598	0.001953688
5	0.0349	9.99811	0.0279	0.05598	0.001953688
10	0.0349	19.9962	0.05135	0.05598	0.001953688
15	0.0349	29.9943	0.08964	0.05598	0.001953688
20	0.0349	39.9925	0.14161	0.05598	0.001953688
25	0.0349	49.9906	0.20568	0.05598	0.001953688
30	0.0349	59.9887	0.27991	0.05598	0.001953688
35	0.0349	69.9868	0.36204	0.05598	0.001953688
40	0.0349	79.9849	0.44957	0.05598	0.001953688
45	0.0349	89.983	0.53985	0.05598	0.001953688
50	0.0349	99.9811	0.63013	0.05598	0.001953688
55	0.0349	109.979	0.71767	0.05598	0.001953688
60	0.0349	119.977	0.79982	0.05598	0.001953688
65	0.0349	129.975	0.87408	0.05598	0.001953688
70	0.0349	139.974	0.93819	0.05598	0.001953688
75	0.0349	149.972	0.9902	0.05598	0.001953688
80	0.0349	159.97	1.02855	0.05598	0.001953688
85	0.0349	169.968	1.05205	0.05598	0.001953688
90	0.0349	179.966	1.06	0.05598	0.001953688
95	0.0349	189.964	1.05216	0.05598	0.001953688
100	0.0349	199.962	1.02876	0.05598	0.001953688
105	0.0349	209.96	0.99051	0.05598	0.001953688
110	0.0349	219.958	0.93859	0.05598	0.001953688
115	0.0349	229.957	0.87455	0.05598	0.001953688
120	0.0349	239.955	0.80036	0.05598	0.001953688
125	0.0349	249.953	0.71825	0.05598	0.001953688
130	0.0349	259.951	0.63074	0.05598	0.001953688
135	0.0349	269.949	0.54046	0.05598	0.001953688
140	0.0349	279.947	0.45018	0.05598	0.001953688
145	0.0349	289.945	0.36262	0.05598	0.001953688
150	0.0349	299.943	0.28044	0.05598	0.001953688
155	0.0349	309.942	0.20616	0.05598	0.001953688
160	0.0349	319.94	0.14201	0.05598	0.001953688
165	0.0349	329.938	0.08995	0.05598	0.001953688
170	0.0349	339.936	0.05156	0.05598	0.001953688
175	0.0349	349.934	0.028	0.05598	0.001953688
180	0.035	359.9	0.02	0.056	0.001954
185	0.0349	369.93	0.02779	0.05598	0.001953688
190	0.0349	379.928	0.05114	0.05598	0.001953688
195	0.0349	389.926	0.08933	0.05598	0.001953688
200	0.0349	399.925	0.14122	0.05598	0.001953688
205	0.0349	409.923	0.20521	0.05598	0.001953688
210	0.0349	419.921	0.27938	0.05598	0.001953688
215	0.0349	429.919	0.36146	0.05598	0.001953688
220	0.0349	439.917	0.44896	0.05598	0.001953688
225	0.0349	449.915	0.53923	0.05598	0.001953688
230	0.0349	459.913	0.62952	0.05598	0.001953688
235	0.0349	469.911	0.71709	0.05598	0.001953688
240	0.0349	479.909	0.79929	0.05598	0.001953688
245	0.0349	489.908	0.87361	0.05598	0.001953688
250	0.0349	499.906	0.93779	0.05598	0.001953688
255	0.0349	509.904	0.9899	0.05598	0.001953688
260	0.0349	519.902	1.02833	0.05598	0.001953688
265	0.0349	529.9	1.05194	0.05598	0.001953688
270	0.0349	539.898	1.06	0.05598	0.001953688
275	0.0349	549.896	1.05226	0.05598	0.001953688

Table 6: Kinematic behavior calculation of IEM

t(sec)	ω (rad/s)	θ (deg)	Xf(m)	v(m/s)	a(m/s ²)	L4
0	0.41893	0	0.26	0	0.080732	0.46
0.015	0.41893	0.360047	0.260009	0.001211	0.080731	0.4600091
1.265	0.41893	30.36394	0.323097	0.0974128	0.069658	0.5230973
2.515	0.41893	60.36783	0.492562	0.1675063	0.039917	0.6925622
3.765	0.41893	90.37172	0.722984	0.1927053	-0.00052	0.9229843
5.015	0.41893	120.3756	0.952607	0.1662559	-0.04082	1.1526066
6.265	0.41893	150.3795	1.119886	0.0952472	-0.07018	1.3198863
7.515	0.41893	180.3834	1.17999	-0.001289	-0.08073	1.3799897
8.765	0.41893	210.3873	1.116808	-0.097481	-0.06964	1.316808
10.02	0.41893	240.3912	0.947275	-0.167545	-0.03989	1.1472749
11.27	0.41893	270.3951	0.716828	-0.192705	0.000557	0.9168283
12.52	0.41893	300.3989	0.487232	-0.166216	0.040852	0.6872318
13.77	0.41893	330.4028	0.320021	-0.095179	0.070198	0.5200211
15.02	0.41893	360.4067	0.260012	0.001368	0.08073	0.4600116
16.27	0.41893	390.4106	0.323287	0.0975482	0.069625	0.5232868
17.52	0.41893	420.4145	0.492888	0.1675839	0.039859	0.692888
18.77	0.41893	450.4184	0.723359	0.1927042	-0.00059	0.9233591
20.02	0.41893	480.4223	0.95293	0.1661765	-0.04088	1.1529298
21.27	0.41893	510.4262	1.120071	0.0951107	-0.07021	1.3200714
22.52	0.41893	540.4301	1.179987	-0.001446	-0.08073	1.379987
23.77	0.41893	570.434	1.116618	-0.097616	-0.06961	1.3166183
25.02	0.41893	600.4378	0.946949	-0.167623	-0.03983	1.146949
26.27	0.41893	630.4417	0.716454	-0.192704	0.000622	0.9164536
27.52	0.41893	660.4456	0.486909	-0.166137	0.040909	0.6869086
28.77	0.41893	690.4495	0.319836	-0.095042	0.070231	0.5198361
30.02	0.41893	720.4534	0.260014	0.001525	0.08073	0.4600144
31.27	0.41893	750.4573	0.323477	0.0976836	0.069592	0.5234767
32.52	0.41893	780.4612	0.493214	0.1676613	0.039802	0.693214
33.77	0.41893	810.4651	0.723734	0.192703	-0.00066	0.9237338
35.02	0.41893	840.469	0.953253	0.1660969	-0.04094	1.1532529
36.27	0.41893	870.4729	1.120256	0.0949741	-0.07025	1.3202563
37.52	0.41893	900.4767	1.179984	-0.001603	-0.08073	1.3799841
38.77	0.41893	930.4806	1.116428	-0.097751	-0.06958	1.3164283
40.02	0.41893	960.4845	0.946623	-0.1677	-0.03977	1.146623
41.27	0.41893	990.4884	0.716079	-0.192702	0.000688	0.9160788
42.52	0.41893	1020.492	0.486586	-0.166057	0.040965	0.6865856
43.77	0.41893	1050.496	0.319651	-0.094906	0.070263	0.5196514
45.02	0.41893	1080.5	0.260018	0.001682	0.080729	0.4600175

Table 7: Kinematics boundary condition calculation of IEM and IBM

S.NO.	1 round time (32 steps) (sec)	Time (16 steps) (sec)	IBM Deg	IEM Deg	Finger Deg	Spur Gear Deg	x Rack mm	Pouring Deg
0	0	0	0	0	0	0	0	0
1	10.78125	11.25	22.5	0	0	17280	18.75	16200
2	21.5625	22.5	45	0	0	34560	37.5	32400
3	32.34375	33.75	67.5	0	0	51840	56.25	48600
4	43.125	45	90	0	0	69120	75	64800
5	53.90625	56.25	112.5	0	0	86400	93.75	81000
6	64.6875	67.5	135	0	0	103680	112.5	97200
7	75.46875	78.75	157.5	0	0	120960	131.25	113400
8	86.25	90	180	0	0	138240	150	129600
9	97.03125	101.25	202.5	0	0	155520	168.75	145800
10	107.8125	112.5	225	0	0	172800	187.5	162000
11	118.59375	123.75	247.5	0	0	190080	206.25	178200
12	129.375	135	270	0	0	207360	225	194400
13	140.15625	146.25	292.5	0	0	224640	243.75	210600
14	150.9375	157.5	315	0	0	241920	262.5	226800
15	161.71875	168.75	337.5	270	0	259200	281.25	243000
16	172.5	180	360	540	0	276480	300	259200
17	183.28125	191.25	382.5	810	90	293760	281.25	275400
18	194.0625	202.5	405	1080	0	311040	262.5	291600
19	204.84375	213.75	427.5	1350	90	328320	243.75	307800
20	215.625	225	450	1620	0	345600	225	324000
21	226.40625	236.25	472.5	1890	90	362880	206.25	340200
22	237.1875	247.5	495	2160	0	380160	187.5	356400
23	247.96875	258.75	517.5	2430	90	397440	168.75	372600
24	258.75	270	540	2700	0	414720	150	388800
25	269.53125	281.25	562.5	2970	90	432000	131.25	405000
26	280.3125	292.5	585	3240	0	449280	112.5	421200
27	291.09375	303.75	607.5	3510	90	466560	93.75	437400
28	301.875	315	630	3780	0	483840	75	453600
29	312.65625	326.25	652.5	4050	90	501120	56.25	469800
30	323.4375	337.5	675	4320	0	518400	37.5	486000
31	334.21875	348.75	697.5	4590	90	535680	18.75	502200
32	345	360	720	4860	0	552960	0	518400

Table 8: Cover opening and closing boundary condition magnitude of position inputs

Time(sec)	C1	C2	C3	C4	C5	C6	C7	C8	C9	C10	C11	C12
0	0	0	0	0	0	0	0	0	0	0	0	0
1	80	0	0	-45	0	0	0	0	0	0	0	0
2	80	95	0	-90	-90	0	0	0	0	0	0	0
3	80	95	45	-90	-90	-90	0	0	0	0	0	0
4	80	95	95	-90	-90	-90	0	0	0	0	0	0
5	80	95	95	-90	-90	-90	45	0	0	0	0	0
6	80	95	95	0	-90	-90	90	45	0	0	0	0
7	80	95	95	0	0	-90	90	90	45	0	0	0
8	80	95	95	0	0	0	90	90	90	45	0	0
9	80	95	95	0	0	0	0	90	90	90	45	0
10	80	95	95	0	0	0	0	45	90	90	90	45
11	80	95	95	0	0	0	0	0	45	90	90	90
12	80	95	95	0	0	0	0	0	0	45	90	90
13	70	95	95	0	0	0	0	0	0	0	45	90
14	0	80	45	0	0	0	0	0	0	0	0	45
15	0	0	0	0	0	0	0	0	0	0	0	0
16	0	0	0	0	0	0	0	0	0	0	0	0
17	0	0	0	0	0	0	0	0	0	0	0	0
18	80	0	0	-45	0	0	0	0	0	0	0	0
19	80	95	45	-90	-90	0	0	0	0	0	0	0
20	80	95	95	-90	-90	-90	0	0	0	0	0	0
21	80	95	95	-90	-90	-90	0	0	0	0	0	0
22	80	95	95	-90	-90	-90	45	0	0	0	0	0
23	80	95	95	0	-90	-90	90	45	0	0	0	0
24	80	95	95	0	0	-90	90	90	45	0	0	0
25	80	95	95	0	0	0	90	90	90	45	0	0
26	80	95	95	0	0	0	0	90	90	90	45	0
27	80	95	95	0	0	0	0	45	90	90	90	45
28	80	95	95	0	0	0	0	0	45	90	90	90
29	80	95	95	0	0	0	0	0	0	45	90	90
30	70	95	45	0	0	0	0	0	0	0	45	90
31	0	80	0	0	0	0	0	0	0	0	0	45
32	0	0	0	0	0	0	0	0	0	0	0	0

Appendix IV

Kinematic Simulation Result Graphs of *Injera* Baking Machine

Table 9: Total displacement IBM rotation for the real time event to simulator time scale 1:12

Time (sec)	x(m)	y(m)	z(m)	total(m)
0	0	0	0	0
0.01	-9.9E-09	-2.2204E-16	4.33E-07	4.3356E-07
0.03	-3.5E-08	0	1.3E-06	1.3007E-06
0.07	-1.1E-07	0	3.03E-06	3.0348E-06
0.12	-2.3E-07	0	5.2E-06	5.2023E-06
0.17	-4E-07	0	7.36E-06	7.3692E-06
0.22	-6.11E-07	-2.22E-16	9.52E-06	9.54E-06
0.27	-8.64E-07	0.00E+00	1.17E-05	1.17E-05
0.32	-1.16E-06	0.00E+00	1.38E-05	1.39E-05
0.37	-1.5E-06	0.00E+00	1.6E-05	1.60E-05
0.42	-1.9E-06	0.00E+00	1.81E-05	1.82E-05
0.47	-2.3E-06	-2.22E-16	2.02E-05	2.03E-05
0.52	-2.8E-06	-2.22E-16	2.23E-05	2.25E-05
0.57	-3.3E-06	0.00E+00	2.44E-05	2.47E-05
0.62	-3.8E-06	-2.22E-16	2.65E-05	2.68E-05
0.67	-4.4E-06	0.00E+00	2.86E-05	2.90E-05
0.72	-5E-06	0.00E+00	3.07E-05	3.11E-05
0.77	-5.7E-06	-2.22E-16	3.28E-05	3.33E-05
0.82	-6.4E-06	0.00E+00	3.48E-05	3.54E-05
0.87	-7.2E-06	0.00E+00	3.68E-05	3.75E-05
0.92	-7.9E-06	0.00E+00	3.89E-05	3.97E-05
0.97	-8.8E-06	0.00E+00	4.09E-05	4.18E-05
1	-9.3E-06	0.00E+00	4.21E-05	4.31E-05
1	-9.3E-06	0.00E+00	4.21E-05	4.31E-05
1.05	-1E-05	0.00E+00	4.4E-05	4.52E-05
1.1	-1.1E-05	0.00E+00	0.000046	4.73E-05
1.15	-1.2E-05	0.00E+00	4.79E-05	4.94E-05
1.2	-1.3E-05	0.00E+00	4.99E-05	5.15E-05
1.25	-1.4E-05	0.00E+00	5.18E-05	5.37E-05
1.3	-1.5E-05	0.00E+00	5.36E-05	5.58E-05
1.35	-1.6E-05	0.00E+00	5.55E-05	5.78E-05
1.4	-1.7E-05	0	5.73E-05	5.9937E-05
1.45	-1.9E-05	0	5.91E-05	6.2021E-05
1.5	-2E-05	-2.2204E-16	6.09E-05	6.4098E-05
1.55	-2.1E-05	0	6.27E-05	0.00006617
1.6	-2.2E-05	0	6.44E-05	6.8235E-05
1.65	-2.4E-05	0	6.62E-05	7.0293E-05
1.7	-2.5E-05	-2.2204E-16	6.78E-05	7.2345E-05
1.75	-2.7E-05	0	6.95E-05	7.4389E-05
1.8	-2.8E-05	0	7.11E-05	7.6427E-05
1.85	-2.9E-05	0	7.27E-05	7.8457E-05
1.9	-3.1E-05	0	7.43E-05	8.0479E-05
1.95	-3.2E-05	0	7.59E-05	8.2494E-05
2	-3.4E-05	-2.2204E-16	7.74E-05	8.4501E-05
2	-3.4E-05	-2.2204E-16	7.74E-05	8.4501E-05
2.05	-3.6E-05	0	7.89E-05	0.0000865
2.1	-3.7E-05	-2.2204E-16	8.03E-05	0.00008849
2.15	-3.9E-05	0	8.17E-05	9.0472E-05
2.2	-4E-05	0	8.31E-05	9.2445E-05
2.25	-4.2E-05	0	8.45E-05	9.4409E-05
2.3	-4.4E-05	-2.2204E-16	8.58E-05	9.6364E-05
2.35	-4.6E-05	0	8.71E-05	0.00009831
2.4	-4.7E-05	0	8.84E-05	0.00010025
2.45	-4.9E-05	0	8.96E-05	0.00010217
2.5	-5.1E-05	0	9.08E-05	0.00010409
2.55	-5.3E-05	-2.2204E-16	9.19E-05	0.000106
2.6	-5.5E-05	0	9.3E-05	0.00010789
2.65	-5.7E-05	0	9.41E-05	0.00010978
2.7	-5.8E-05	0	9.51E-05	0.00011166
2.75	-6E-05	0	9.61E-05	0.00011352

As it is shown in Figure 76 below, the maximum and minimum results of the graph is attached to the right side of the graph for the real time event to simulator time scale given as 1:12 for all the IBM with IEM simulation in this study except the *injera* extractor mechanism is simulated alone.

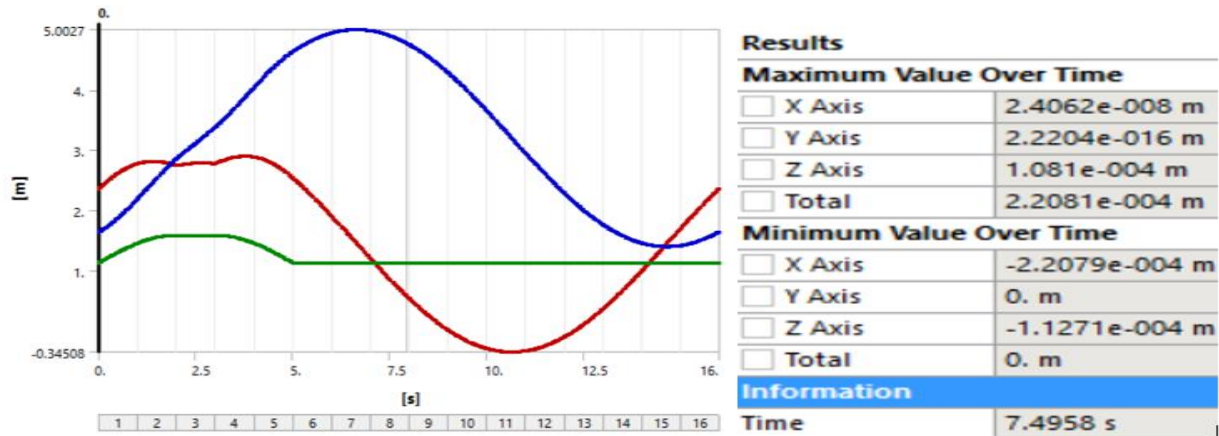


Figure 76: Displacement Analysis of One cycle rotation of the IBM circular frame with cover opening and closing

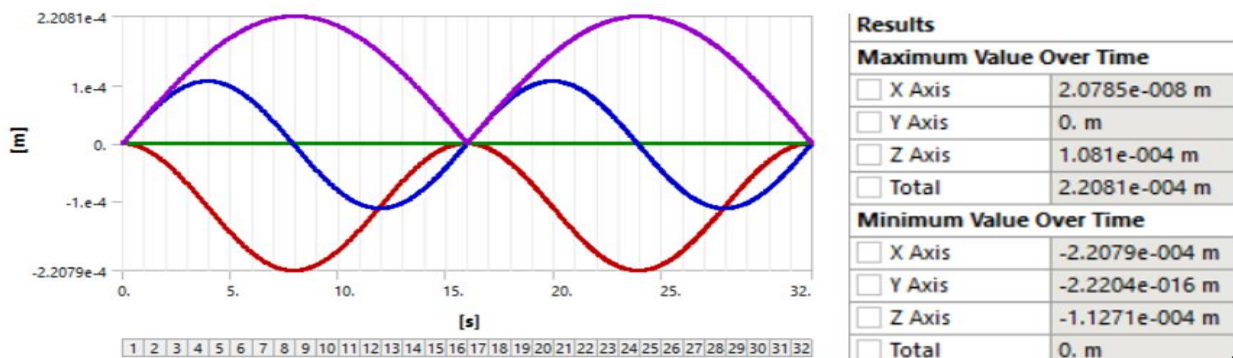


Figure 77: Total displacement analysis of two cycle rotation of IBM with mitad carrier frame

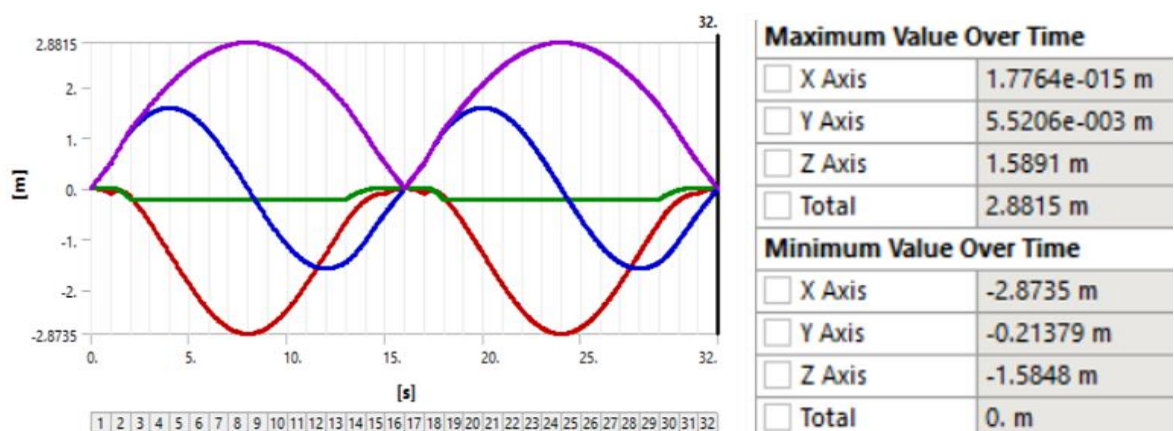


Figure 78: Total displacement analysis of two cycle rotation of IBM frame with Cover opening and Closing (Time scale 1:12)

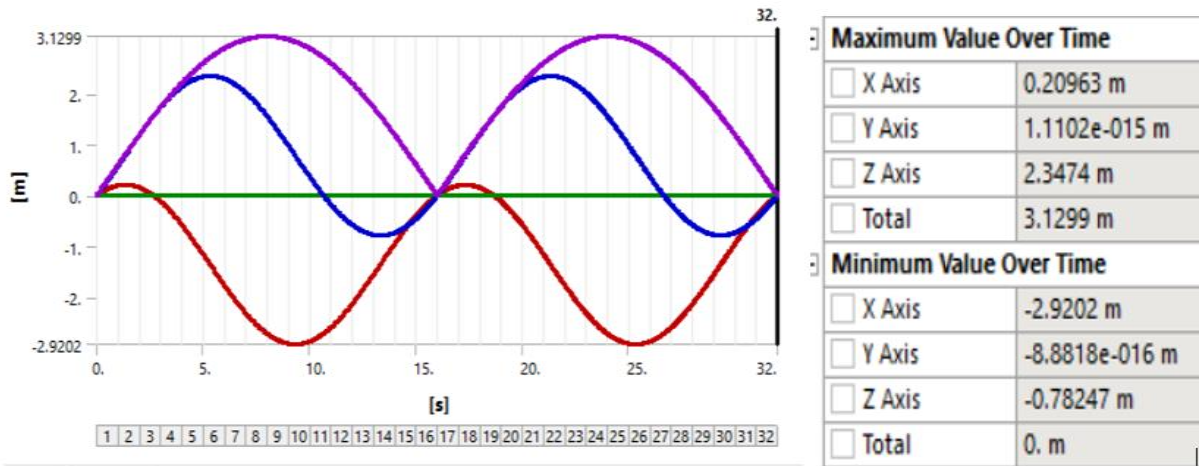


Figure 79: Position analysis of mitad per two cycle revolution (Time Scale 1:12)

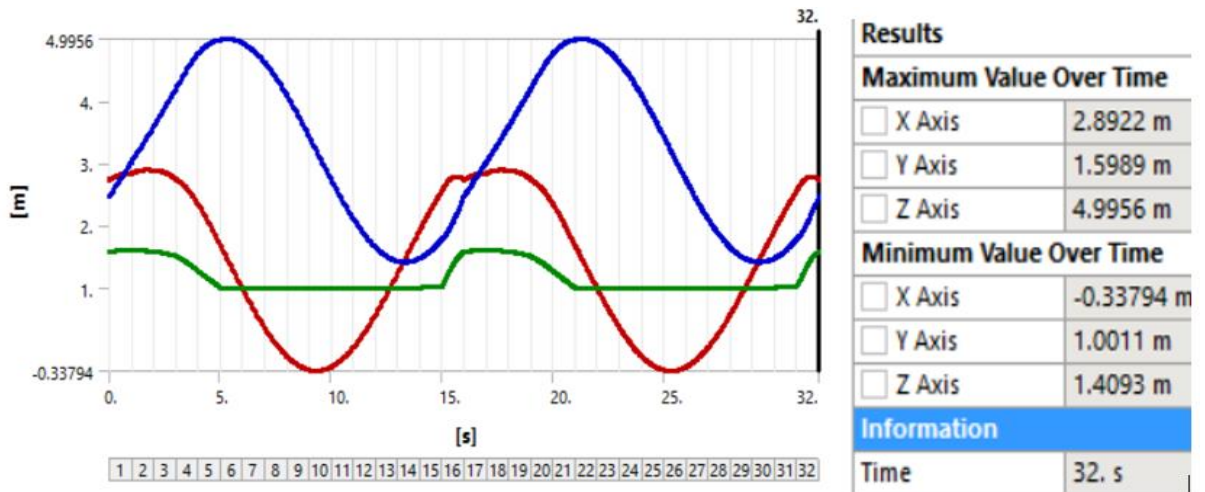


Figure 80: Total Position analysis of cover opening and closing mechanism

Note: The cover is opened to the y-axis according to the software simulation and the IBM rotates about z –axis and injera extracting mechanism works along x-axis. Look the Fig. 79 below about the x-y-z coordinates of the system.

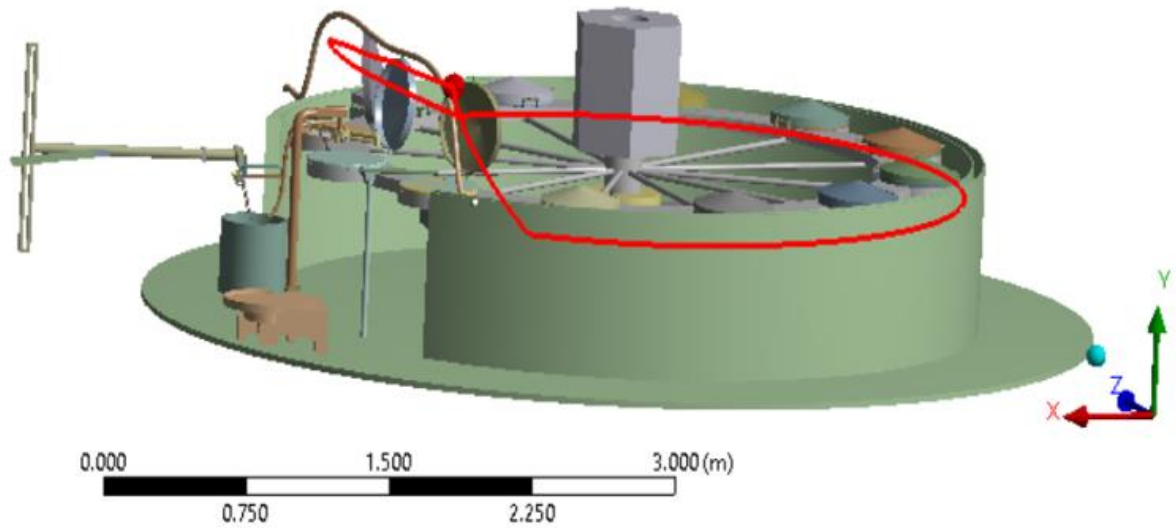


Figure 81: Injera baking machine integrated with injera extracting mechanism

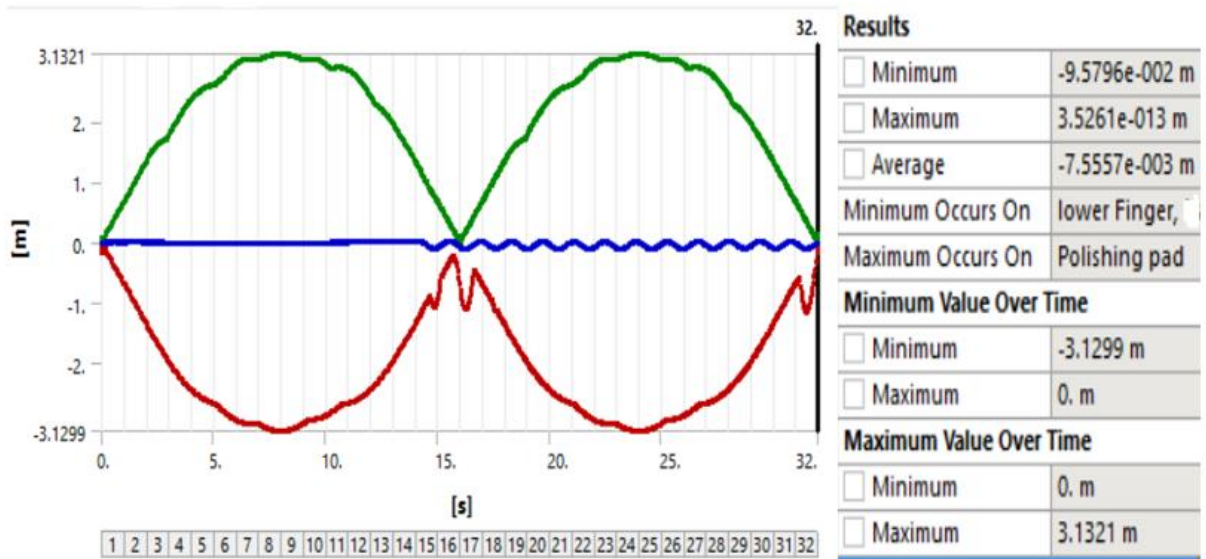


Figure 82: Directional position analysis of the system

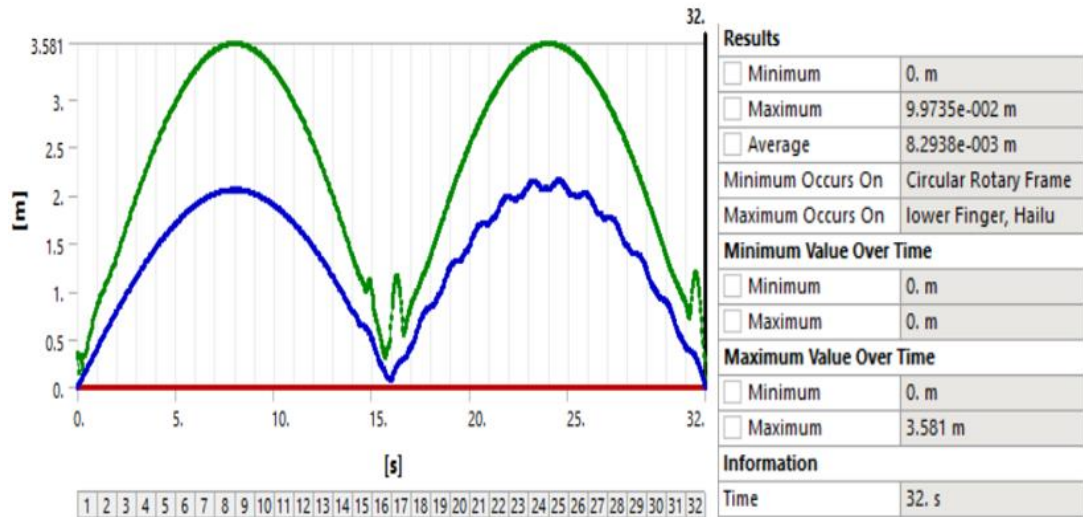


Figure 83: Total position analysis of the system

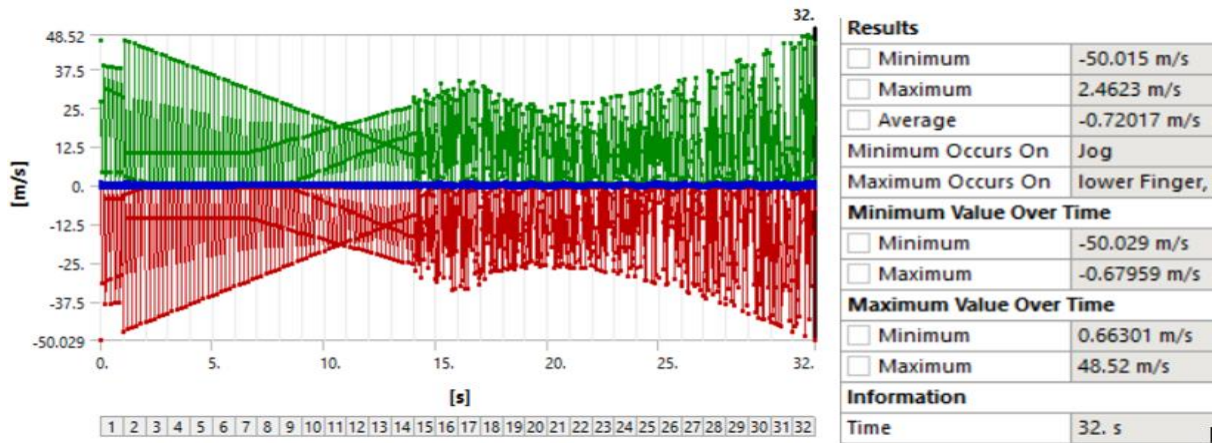


Figure 84: Directional velocity analysis of the integrated (IBM & IEM) system

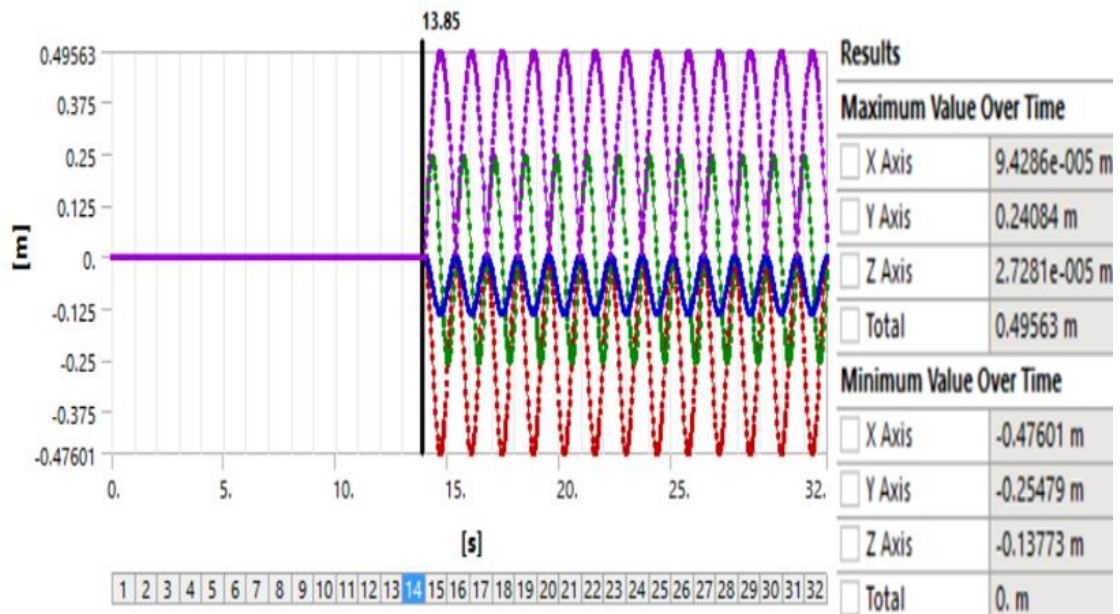


Figure 85: Position Analysis of link 2 of IEM integrated with IBM (Time scale 1:12)

The above graph in Fig. 83 illustrates that *injera* extracting mechanism starts moving from $\theta_2 = 0$ degree immediately as the baked *injera* carried mitad arrived to the extracting port and arrived to the port as the *injera* delivered mitad leaves the port. *Injera* extractor mechanism drops injera at 15 seconds. Check that the red line valley points and peak points are 12 per 30 seconds with considering the system has 12 mitads. This shows the extracting mechanism grasps at the peak point 12 times and drops 12 times at the peak point. The constant value from $t = 0$ seconds to 13.85 seconds shows that the baking time of the first *injera* and until that time the *injera* extracting mechanism will be at stationary at the commence round of *injera* baking process in this machine.